

MIT NUCLEAR REACTOR LABORATORY

AN MIT INTERDEPARTMENTAL CENTER

John A. Bernard
Director of Reactor Operations

Mail Stop: NW12-208a
138 Albany Street
Cambridge, MA 02139

Phone: 617 253-4202
Fax: 617 253-7300
Email: bernardj@mit.edu

February 22, 2008

U.S. Nuclear Regulatory Commission
Attn: Stephen Pierce, 012-G15
Research and Test Reactors Branch B
Division of Policy and Rulemaking
Office of Nuclear Reactor Regulation
Washington, DC 20555

Re: Request for Additional Information; License No. R-37; TAC No. MA 6084

Dear Mr. Pierce:

Enclosed is the information requested pursuant to the NRC letter of 30 November 2007:

- a) The redone Chapter 13 calculations are documented in a file memo dated 29 April, 2003 (copy enclosed.)
- b) The dose calculations were performed as part of a MS thesis, "Estimate of Radiation Release During Design Basis Accident," by Qing Li. A copy is enclosed.

Sincerely,

Lin-Wen Hu

John A. Bernard

I declare under penalty of perjury that the foregoing is true and correct to the best of our knowledge.

Executed 2-25-08
Date

Signature

cc: Senior Project Manager (without enclosures)
Document Control Room (without enclosures)

JAB/koc

Enclosures

AD20

KRR

Appendix D

Additional Information for Response to Question 92(b)

**File Memo dated 29 April 03, "Loss of Primary
Flow Transient Analysis"**



NUCLEAR REACTOR LABORATORY

AN INTERDEPARTMENTAL CENTER OF
MASSACHUSETTS INSTITUTE OF TECHNOLOGY




LIN-WEN HU
Reactor Relicensing Engineer

138 Albany Street, Cambridge, MA 02139-4296
Telefax No. (617)253-7300
Telephone No. (617)258-5860
Email: lwhu@mit.edu

Activation Analysis
Coolant Chemistry
Nuclear Medicine
Reactor Engineering

MEMORANDUM

TO: MITR Files
FROM: Lin-Wen Hu 
DATE: April 29, 2003
RE: Loss of Primary Flow Transient Analysis (2)

1. The loss of primary flow transient analysis was originally performed using initial conditions of reactor power 6.1 MW, primary flow 2000 gpm, coolant outlet temperature of 55 °C, and coolant height at 10 ft (LOF case#1). This analysis was repeated using the LSSS as the initial conditions (LOF case#2). The LSSS for the MITR-III are: reactor power 7.4 MW, primary flow 1800 gpm, coolant outlet temperature 60 °C, and coolant height at 10 ft. The MULCH-II code was used for both analyses. All other assumptions are the same for both analyses.
2. Figures 1 and 2 are comparisons of the coolant outlet temperatures of the average and hot channels for the two cases. Note that the initial coolant temperatures are higher in Figure 2 because of the higher initial power (7.4 MW v.s. 6.1 MW) and lower initial flow rate (1800 gpm v.s. 2000 gpm). The peak hot channel outlet coolant temperatures, which occur around 1.5 s into the transient, are 105.2 °C for case#2 and 97.0 °C for case#1. Note that the coolant temperature then decreases rapidly in both cases because of reactor scram. Both analyses showed that the hot channel coolant outlet temperature would reach saturation after about 15 to 20 seconds. Figure 3 shows the calculated fuel temperatures at the average and hot channel outlet assuming the initial conditions of the LOF transient are LSSS. The calculated fuel temperatures are well below the cladding softening point of 450 °C.
3. Figure 4 is the calculated reactor decay power assuming equilibrium reactor power was at 7.4 MW before scram. The reactor decay heat at 16 seconds after reactor scram is about 325 kW. As shown in SAR section 4.6.6.3, the best-estimate dry-out condition is 468 kW.
4. The MULCH-II output file for LOF case#2 is attached to this memo.

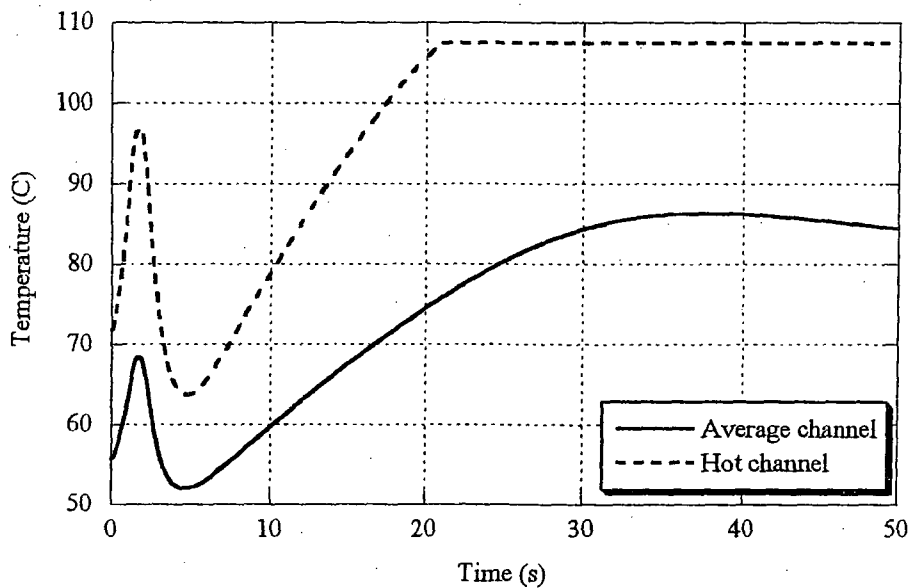


Figure 1. Coolant outlet temperatures of average and hot channels during a loss of primary flow transient. The initial conditions used for this analysis are reactor power at 6.1 MW, primary flow 2000 gpm, coolant outlet temperature 55 °C, and coolant height at 10 ft.

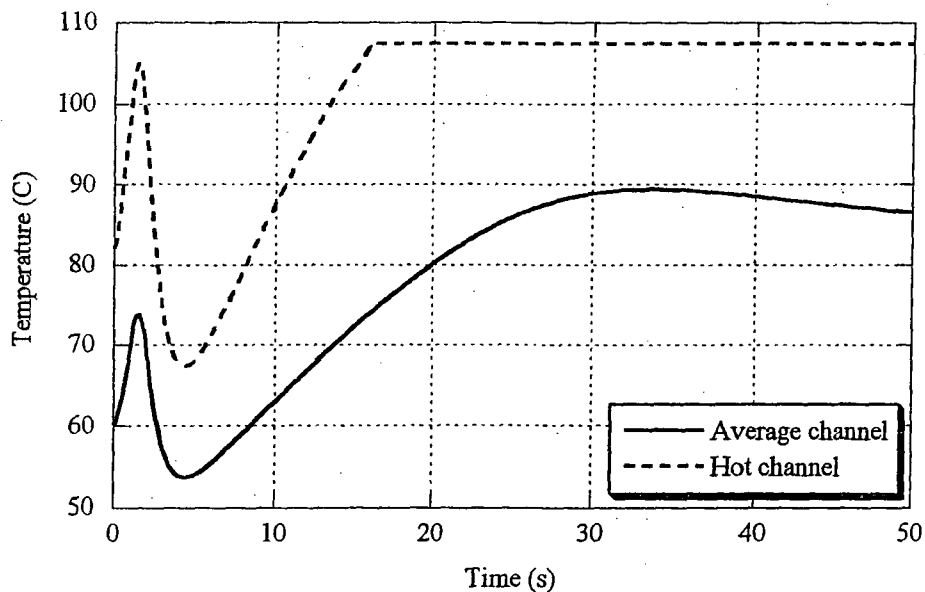


Figure 2. Coolant outlet temperatures of average and hot channels during a loss of primary flow transient. The initial conditions used for this analysis are reactor power at 7.4 MW, primary flow 1800 gpm, coolant outlet temperature 60 °C, and coolant height at 10 ft.

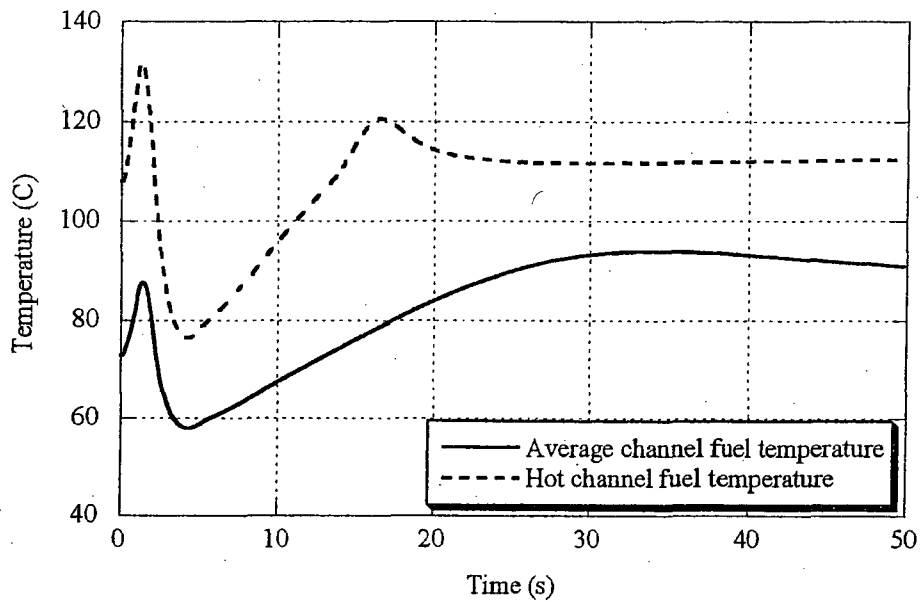


Figure 3. Fuel temperatures of average and hot channels at outlet during a loss of primary flow transient. The initial conditions used for this analysis are reactor power at 7.4 MW, primary flow 1800 gpm, coolant outlet temperature 60 °C, and coolant height at 10 ft.

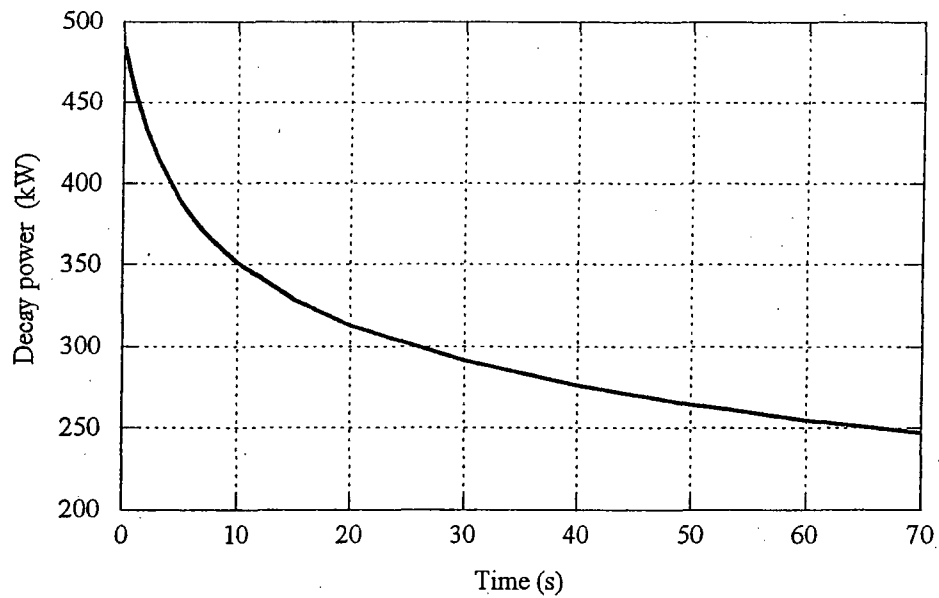


Figure 4 Reactor decay power calculated using DKPOWR assuming equilibrium power of 7.4 MW before reactor scram.

Multi-Channel Analysis Code, MULCH-II
MIT Nuclear Reactor Laboratory 7/15/1996

LOSS OF FLOW PREDICTION FOR MITR-III best estimate

Reactor Power (kw)= 7400.00 Cooling Tower Outlet Temp (C)= 13.00
Primary Flow (kg)= 111.00 Secondary Flow (kg)= 103.00 Cooling Tower Efficiency= .80
Reference Temp (C)= 50.00 Coolant height from air/water interface to top of flow guide (m)= 2.31

*** simulated case is --> LOSS OF PRIMARY FLOW ***
Steady-State operation before Shutdown for ***** hours
Time Step (s)=.100E+00 Total Simulation Time (s)= 50.00
Instrument Delay Time (s)= 1.00 80% Blade Insertion Time (s)= 1.00

Pump Coastdown Curve:
(exp(-1.870+ .410*t/10+ 2.950*exp(t/10)+ -.680*exp(-(t/10)^2))- .514)/(1.492- .514)

Loop Component Geometries:

I	Aflow(m^2)	Vol(m^3)	De(m)	dz(m)	Kform	Nchan
1	.320E-01	.427E+00	.203E+00	-7.08	4.58	1
2	.389E-04	.168E-03	.704E-02	.00	7.30	1770
3	.320E-01	.468E+00	.203E+00	6.97	2.17	1
4	.339E+00	.413E+00	.180E+00	-1.22	.00	1
5	.111E+00	.760E-01	.630E-01	-.69	.30	1
6	.440E-02	.160E-01	.220E+00	-.01	.18	1
7	.290E-01	.180E-01	.400E-01	-.61	.00	1
8	.125E-03	.824E-04	.219E-02	.66	2.05	345
9	.130E+00	.990E-01	.387E+00	.76	.00	1
10	.923E+00	.192E+01	.108E+01	1.22	.00	1
11	.320E-01	.427E+00	.203E+00	-7.08	4.58	1
12	.900E-04	.389E-03	.301E-02	.00	7.30	1770
13	.320E-01	.468E+00	.203E+00	6.97	2.17	1

Anti-siphon and Natural Convection Valve Geometries:

	Acont(m^2)	Aref(m^2)	Vball(m^3)	Rball(kg/m^3)	Kup	Kdown	NV
ASV	.178E-02	.384E-02	.1059E-03	2715.00	7.90	6.90	2
NCV	.271E-02	.811E-02	.2040E-03	2715.00	*****	*****	4

Fraction of coolant cooling the fueled region= .920
HX Fouling factor (C m^2/W)= .3500E-03

Fraction of energy deposited in fuel= .910 Coolant= .054 D2O= .021 Graphite= .015
Hot Channel Factor= 2.000

	bottom	2	3	4	5	6	7	8	9	10	11	top
Shape_avg	1.000	1.000	1.000	1.000	1.000	1.000	1.000	1.000	1.000	1.000	1.000	1.000
Shape_hot	1.000	1.000	1.000	1.000	1.000	1.000	1.000	1.000	1.000	1.000	1.000	1.000
Peak_avg	1.000	1.000	1.000	1.000	1.000	1.000	1.000	1.000	1.000	1.000	1.000	1.000
Peak_hot	1.000	1.000	1.000	1.000	1.000	1.000	1.000	1.000	1.000	1.000	1.000	1.000

Minimum flow distribution in flow channel= .8640

Engineering Factors for:

Reactor Power= 1.000 Hot Channel Flow Rate= 1.000
Heat Transfer Coef= 1.000 Hot Spot Heat flux= 1.000

Min CHF ratio= 1.500 Min DNB ratio= 1.500

----- END OF INPUT -----

----- START OF OUTPUT -----

DP_core= 41528.180000
DPratio1= -2.104542E-01

** steady-state temperatures for each components **

1	2	3	4	5	6	7	8	9	10	11	12	13
---	---	---	---	---	---	---	---	---	----	----	----	----

59.0 43.7 43.7 43.7 43.7 43.7 43.7 59.0 59.0 59.0 13.0 29.5 29.5

** steady-state temperatures for core region **
 Tw_hot=coolant temperature at the hot channel
 Tw_avg=coolant temperature at the average channel
 Tc_hot=clad temperature at the hot channel
 Tc_avg=clad temperature at the average channel
 Tf_hot=fuel temperature at the hot channel
 Tf_avg=fuel temperature at the average channel

	1	2	3	4	5	6	7	8	9	10	11	12
Tw_hot	43.7	47.5	51.4	55.2	59.1	63.0	66.8	70.7	74.5	78.4	82.2	82.2
Tw_avg	43.7	45.3	47.0	48.7	50.3	52.0	53.6	55.3	57.0	58.6	60.3	60.3
Tc_hot	43.8	68.7	71.8	75.1	78.2	81.6	85.1	88.6	92.2	95.8	99.4	82.4
Tc_avg	43.8	55.2	56.7	58.2	59.7	61.3	62.9	64.4	65.9	67.4	69.0	60.4
Tf_hot	43.7	77.0	80.2	83.4	86.8	90.1	93.6	97.1	100.7	104.2	107.9	82.2
Tf_avg	43.7	59.1	60.6	62.1	63.6	65.2	66.7	68.2	69.8	71.4	72.9	60.3
Qflux_h	.1000E-04	.3234E+06	.3234E+06	.3234E+06	.3234E+06	.3234E+06	.3234E+06	.3234E+06	.3234E+06	.3234E+06	.3234E+06	.3234E+06

** Cladding Temperature at ONB and CHF **

	1	2	3	4	5	6	7	8	9	10	11	12
TONB_hot	107.5	114.3	114.3	114.3	114.3	114.3	114.3	114.3	114.3	114.3	114.3	107.5
TONB_avg	107.5	112.4	112.4	112.4	112.4	112.4	112.4	112.4	112.4	112.4	112.4	107.5
CHFR	999.9	9.1	9.1	9.1	9.1	9.1	9.1	9.1	9.1	9.1	9.1	999.9

LSSS OK!

Safety Limits OK!

** LSSS and Safety Limits Index **

0: below limit 1: limit exceeded

	1	2	3	4	5	6	7	8	9	10	11	12
LSSS	0	0	0	0	0	0	0	0	0	0	0	0
SL	0	0	0	0	0	0	0	0	0	0	0	0

0.000000E+00 102.175500 0.000000E+00 0.000000E+00

Scram signal sent at: 1.000000E-01(s)

Blades 80% inserted at: 2.100000(s)

1.000000E-01	98.917020	0.000000E+00	0.000000E+00
2.000000E-01	92.767810	0.000000E+00	0.000000E+00
3.000000E-01	87.031840	0.000000E+00	0.000000E+00
4.000000E-01	81.677700	0.000000E+00	0.000000E+00
5.000000E-01	76.676730	0.000000E+00	0.000000E+00
6.000000E-01	72.002690	0.000000E+00	0.000000E+00
7.000000E-01	67.631540	0.000000E+00	0.000000E+00
8.000001E-01	63.541280	0.000000E+00	0.000000E+00
9.000001E-01	59.711720	0.000000E+00	0.000000E+00
1.000000	56.124330	0.000000E+00	0.000000E+00
1.100000	52.762060	0.000000E+00	0.000000E+00
1.200000	49.609260	0.000000E+00	0.000000E+00
1.300000	46.651530	0.000000E+00	0.000000E+00
1.400000	43.875560	0.000000E+00	0.000000E+00
1.500000	41.269100	0.000000E+00	0.000000E+00
1.600000	38.820880	0.000000E+00	0.000000E+00
1.700000	36.520440	0.000000E+00	0.000000E+00
1.800000	34.358120	0.000000E+00	0.000000E+00
1.900000	32.325000	0.000000E+00	0.000000E+00
2.000000	30.412800	0.000000E+00	0.000000E+00
2.100000	28.613860	0.000000E+00	0.000000E+00
2.200000	26.921060	0.000000E+00	0.000000E+00
2.300000	25.327790	0.000000E+00	0.000000E+00
2.400000	23.827910	0.000000E+00	0.000000E+00
2.500000	22.415700	0.000000E+00	0.000000E+00
2.600000	21.085840	0.000000E+00	0.000000E+00
2.700000	19.833370	0.000000E+00	0.000000E+00
2.799999	18.653680	0.000000E+00	0.000000E+00
2.899999	17.542420	0.000000E+00	0.000000E+00
2.999999	16.495570	0.000000E+00	0.000000E+00
3.099999	15.509360	0.000000E+00	0.000000E+00
3.199999	14.580240	0.000000E+00	0.000000E+00
3.299999	13.704900	0.000000E+00	0.000000E+00
3.399999	12.880240	0.000000E+00	0.000000E+00
3.499999	12.103330	0.000000E+00	0.000000E+00
3.599999	11.371440	0.000000E+00	0.000000E+00
3.699999	10.682000	0.000000E+00	0.000000E+00
3.799999	10.032570	0.000000E+00	0.000000E+00
3.899998	9.420874	0.000000E+00	0.000000E+00
3.999998	8.844763	0.000000E+00	0.000000E+00

4.099998	8.302208	0.000000E+00	1of	0.000000E+00
4.199998	7.015791	0.000000E+00		2.003114E-01
4.299998	6.504248	1.587088E-01		1.942458E-01
4.399998	5.977942	2.753256E-01		1.878818E-01
4.499998	5.510567	3.540489E-01		1.824389E-01
4.599998	5.095648	4.006996E-01		1.775728E-01
4.699998	4.726803	4.209365E-01		1.730859E-01
4.799998	4.398181	4.198132E-01		1.688775E-01
4.899998	4.104669	4.015948E-01		1.649104E-01
4.999998	3.841931	3.697387E-01		1.611942E-01
5.099998	3.606340	3.269660E-01		1.577492E-01
5.199997	3.394952	2.753318E-01		1.546045E-01
5.299997	3.205383	2.163307E-01		1.517894E-01
5.399997	3.035687	1.510319E-01		1.493479E-01
5.499997	2.884278	8.015008E-02		1.473253E-01
5.599997	2.749908	4.106613E-03		1.457715E-01
5.699997	2.631436	-7.659547E-02		1.445610E-01
5.799997	2.526958	-1.603023E-01		1.433120E-01
5.899997	2.434266	-2.452841E-01		1.419336E-01
5.999997	2.351322	-3.299991E-01		1.403838E-01
6.099997	2.276308	-4.131188E-01		1.386381E-01
6.199996	2.207646	-4.935606E-01		1.366928E-01
6.299996	2.144015	-5.704918E-01		1.345587E-01
6.399996	2.084339	-6.433241E-01		1.322558E-01
6.499996	2.027776	-7.116890E-01		1.298102E-01
6.599996	1.973688	-7.754114E-01		1.272496E-01
6.699996	1.921612	-8.344782E-01		1.246014E-01
6.799996	1.871231	-8.889959E-01		1.218944E-01
6.899996	1.822338	-9.391606E-01		1.191508E-01
6.999996	1.774816	-9.852273E-01		1.163909E-01
7.099996	1.728600	-1.027484		1.136317E-01
7.199996	1.683668	-1.066240		1.108836E-01
7.299995	1.640030	-1.101803		1.081580E-01
7.399995	1.597709	-1.134467		1.054642E-01
7.499995	1.556729	-1.164514		1.028053E-01
7.599995	1.517125	-1.192201		1.001875E-01
7.699995	1.478921	-1.217760		9.761380E-02
7.799995	1.442143	-1.241400		9.508589E-02
7.899995	1.406808	-1.263309		9.260777E-02
7.999995	1.372934	-1.283645		9.017731E-02
8.099995	1.340529	-1.302553		8.780032E-02
8.199995	1.309600	-1.320155		8.547834E-02
8.299995	1.280158	-1.336552		8.321528E-02
8.399996	1.252196	-1.351835		8.101422E-02
8.499996	1.225722	-1.366078		7.887962E-02
8.599997	1.200733	-1.379346		7.681540E-02
8.699997	1.177235	-1.391691		7.482932E-02
8.799997	1.196599	-1.388446		8.393250E-02
8.899998	1.192712	-1.381219		8.550014E-02
8.999998	1.187602	-1.375722		8.555257E-02
9.099998	1.184407	-1.372126		8.543236E-02
9.199999	1.182682	-1.370032		8.521260E-02
9.299999	1.182099	-1.369107		8.491838E-02
9.400000	1.182408	-1.369089		8.456647E-02
9.500000	1.183406	-1.369776		8.417004E-02
9.600000	1.184939	-1.371010		8.373737E-02
9.700001	1.186888	-1.372666		8.327780E-02
9.800001	1.189156	-1.374646		8.279454E-02
9.900002	1.191668	-1.376875		8.229468E-02
10.000000	1.194368	-1.379294		8.177859E-02
10.100000	1.197209	-1.381856		8.125336E-02
10.200000	1.200158	-1.384526		8.071849E-02
10.300000	1.203185	-1.387272		8.017738E-02
10.400000	1.206270	-1.390073		7.962916E-02
10.500000	1.209391	-1.392913		7.907599E-02
10.600000	1.212539	-1.395778		7.852047E-02
10.700000	1.215703	-1.398654		7.796098E-02
10.800000	1.218873	-1.401535		7.739930E-02
10.900010	1.222044	-1.404415		7.683378E-02
11.000010	1.225211	-1.407290		7.626760E-02
11.100010	1.228369	-1.410153		7.570115E-02
11.200010	1.231516	-1.413003		7.513127E-02
11.300010	1.234649	-1.415838		7.456143E-02
11.400010	1.237769	-1.418654		7.398985E-02
11.500010	1.240870	-1.421451		7.341693E-02
11.600010	1.243954	-1.424227		7.284595E-02
11.700010	1.247016	-1.426982		7.227081E-02
11.800010	1.250061	-1.429715		7.169686E-02
11.900010	1.253086	-1.432427		7.112198E-02

12.000010	1.256091	-1.435115	7.054621E-02
12.100010	1.259075	-1.437781	6.996840E-02
12.200010	1.262040	-1.440423	6.939100E-02
12.300010	1.264982	-1.443042	6.881388E-02
12.400010	1.267903	-1.445638	6.823530E-02
12.500010	1.270804	-1.448209	6.765780E-02
12.600010	1.273682	-1.450758	6.707720E-02
12.700010	1.276541	-1.453281	6.649942E-02
12.800010	1.279374	-1.455783	6.591803E-02
12.900010	1.282192	-1.458259	6.533635E-02
13.000010	1.284986	-1.460713	6.475499E-02
13.100010	1.287759	-1.463143	6.417334E-02
13.200010	1.290509	-1.465551	6.359024E-02
13.300010	1.293241	-1.467937	6.300624E-02
13.400010	1.295954	-1.470298	6.242431E-02
13.500020	1.298642	-1.472635	6.184042E-02
13.600020	1.301310	-1.474948	6.125543E-02
13.700020	1.303957	-1.477239	6.066981E-02
13.800020	1.306584	-1.479507	6.008346E-02
13.900020	1.309191	-1.481753	5.949731E-02
14.000020	1.311777	-1.483976	5.891071E-02
14.100020	1.314344	-1.486175	5.832172E-02
14.200020	1.316890	-1.488352	5.773330E-02
14.300020	1.319415	-1.490506	5.714568E-02
14.400020	1.321918	-1.492637	5.655696E-02
14.500020	1.324403	-1.494745	5.596639E-02
14.600020	1.326867	-1.496831	5.537626E-02
14.700020	1.329311	-1.498896	5.478402E-02
14.800020	1.331736	-1.500939	5.419026E-02
14.900020	1.334143	-1.502960	5.359902E-02
15.000020	1.336528	-1.504958	5.300551E-02
15.100020	1.338895	-1.506934	5.241111E-02
15.200020	1.341240	-1.508889	5.181507E-02
15.300020	1.343569	-1.510821	5.121904E-02
15.400020	1.345876	-1.512732	5.062192E-02
15.500020	1.348167	-1.514621	5.002357E-02
15.600020	1.350437	-1.516489	4.942461E-02
15.700020	1.352689	-1.518334	4.882572E-02
15.800020	1.354920	-1.520159	4.822573E-02
15.900020	1.357134	-1.521961	4.762429E-02
16.000020	1.359328	-1.523743	4.702012E-02
16.100030	1.361506	-1.525504	4.641682E-02
16.200030	1.363663	-1.527243	4.581314E-02
16.300030	1.365802	-1.528961	4.520664E-02
16.400030	1.367923	-1.530659	4.459845E-02
16.500030	1.370026	-1.532336	4.398996E-02
16.600030	1.372112	-1.533991	4.338052E-02
16.700030	1.374181	-1.535626	4.276973E-02
16.800030	1.376230	-1.537239	4.215769E-02
16.900030	1.378261	-1.538833	4.154232E-02
17.000030	1.380276	-1.540407	4.092557E-02
17.100030	1.382275	-1.541960	4.030832E-02
17.200030	1.384255	-1.543492	3.969054E-02
17.300030	1.386217	-1.545004	3.906859E-02
17.400030	1.388165	-1.546495	3.844668E-02
17.500030	1.390093	-1.547966	3.782198E-02
17.600030	1.392005	-1.549417	3.719531E-02
17.700030	1.393901	-1.550848	3.656527E-02
17.800030	1.395782	-1.552258	3.593502E-02
17.900030	1.397644	-1.553649	3.530069E-02
18.000030	1.399493	-1.555020	3.466428E-02
18.100030	1.401323	-1.556371	3.402504E-02
18.200030	1.403140	-1.557702	3.338385E-02
18.300030	1.404940	-1.559013	3.273974E-02
18.400030	1.406725	-1.560304	3.209186E-02
18.500030	1.408494	-1.561575	3.144047E-02
18.600030	1.410249	-1.562826	3.078729E-02
18.700040	1.411987	-1.564057	3.012876E-02
18.800040	1.413713	-1.565270	2.946629E-02
18.900040	1.415425	-1.566462	2.880011E-02
19.000040	1.417121	-1.567635	2.812902E-02
19.100040	1.418803	-1.568788	2.745483E-02
19.200040	1.420473	-1.569922	2.677305E-02
19.300040	1.422130	-1.571036	2.608772E-02
19.400040	1.423774	-1.572130	2.539635E-02
19.500040	1.425404	-1.573204	2.469829E-02
19.600040	1.427022	-1.574259	2.399493E-02
19.700040	1.428630	-1.575293	2.328474E-02
19.800040	1.430224	-1.576308	2.256517E-02

19.900040	1.431809	-1.577302	1of	2.183984E-02
20.000040	1.433381	-1.578276		2.110512E-02
20.100040	1.434944	-1.579229		2.036150E-02
20.200040	1.436497	-1.580162		1.960638E-02
20.300040	1.438040	-1.581075		1.884016E-02
20.400040	1.439577	-1.581966		1.806357E-02
20.500040	1.441105	-1.582836		1.727110E-02
20.600040	1.442629	-1.583684		1.646614E-02
20.700040	1.444145	-1.584510		1.564514E-02
20.800040	1.445657	-1.585314		1.480731E-02
20.900040	1.447165	-1.586094		1.395013E-02
21.000040	1.448669	-1.586850		1.307002E-02
21.100040	1.450178	-1.587582		1.216443E-02
21.200040	1.451686	-1.588288		1.123034E-02
21.300050	1.453200	-1.588966		1.026593E-02
21.400050	1.454720	-1.589617		9.263691E-03
21.500050	1.456253	-1.590237		8.220721E-03
21.600050	1.457798	-1.590823		7.126574E-03
21.700050	1.459365	-1.591373		5.975167E-03
21.800050	1.460959	-1.591881		4.752456E-03
21.900050	1.462589	-1.592344		3.442875E-03
22.000050	1.464268	-1.592751		2.025819E-03
22.100050	1.466011	-1.593090		4.705717E-04
22.200050	1.467837	-1.593352		-1.250510E-03
22.300050	1.469713	-1.593582		-3.058654E-03
22.400050	1.471583	-1.593843		-4.828255E-03
22.500050	1.473397	-1.594168		-6.474151E-03
22.600050	1.475123	-1.594566		-7.953397E-03
22.700050	1.476750	-1.595028		-9.257955E-03
22.800050	1.478272	-1.595539		-1.040088E-02
22.900050	1.479694	-1.596079		-1.140486E-02
23.000050	1.481027	-1.596635		-1.229586E-02
23.100050	1.482276	-1.597195		-1.309329E-02
23.200050	1.483453	-1.597750		-1.381631E-02
23.300050	1.484563	-1.598297		-1.447770E-02
23.400050	1.485618	-1.598832		-1.508596E-02
23.500050	1.486617	-1.599354		-1.565339E-02
23.600050	1.487573	-1.599862		-1.618138E-02
23.700050	1.488482	-1.600355		-1.667478E-02
23.800050	1.489351	-1.600834		-1.714033E-02
23.900050	1.490183	-1.601299		-1.758057E-02
24.000060	1.490983	-1.601751		-1.799627E-02
24.100060	1.491750	-1.602189		-1.839096E-02
24.200060	1.492485	-1.602615		-1.876486E-02
24.300060	1.493195	-1.603027		-1.912266E-02
24.400060	1.493877	-1.603429		-1.946339E-02
24.500060	1.494534	-1.603818		-1.978798E-02
24.600060	1.495167	-1.604197		-2.009743E-02
24.700060	1.495777	-1.604563		-2.039221E-02
24.800060	1.496364	-1.604919		-2.067434E-02
24.900060	1.496927	-1.605263		-2.094286E-02
25.000060	1.497473	-1.605596		-2.120037E-02
25.100060	1.497997	-1.605920		-2.144692E-02
25.200060	1.498500	-1.606233		-2.168299E-02
25.300060	1.498988	-1.606536		-2.190831E-02
25.400060	1.499457	-1.606829		-2.212310E-02
25.500060	1.499904	-1.607112		-2.232907E-02
25.600060	1.500337	-1.607385		-2.252585E-02
25.700060	1.500754	-1.607649		-2.271327E-02
25.800060	1.501151	-1.607903		-2.289182E-02
25.900060	1.501531	-1.608147		-2.306193E-02
26.000060	1.501898	-1.608381		-2.322299E-02
26.100060	1.502244	-1.608605		-2.337735E-02
26.200060	1.502578	-1.608822		-2.352508E-02
26.300060	1.502898	-1.609029		-2.366372E-02
26.400060	1.503202	-1.609227		-2.379479E-02
26.500060	1.503491	-1.609416		-2.392026E-02
26.600070	1.503766	-1.609597		-2.403887E-02
26.700070	1.504027	-1.609769		-2.414987E-02
26.800070	1.504273	-1.609932		-2.425598E-02
26.900070	1.504506	-1.610087		-2.435462E-02
27.000070	1.504727	-1.610233		-2.444609E-02
27.100070	1.504932	-1.610371		-2.453255E-02
27.200070	1.505127	-1.610499		-2.461181E-02
27.300070	1.505305	-1.610621		-2.468755E-02
27.400070	1.505474	-1.610734		-2.475617E-02
27.500070	1.505629	-1.610839		-2.481985E-02
27.600070	1.505772	-1.610937		-2.487769E-02
27.700070	1.505904	-1.611028		-2.493072E-02

27.800070	1.506024	-1.611110	-2.497788E-02
27.900070	1.506132	-1.611186	-2.502044E-02
28.000070	1.506229	-1.611253	-2.505745E-02
28.100070	1.506315	-1.611314	-2.508906E-02
28.200070	1.506389	-1.611367	-2.511787E-02
28.300070	1.506454	-1.611414	-2.514047E-02
28.400070	1.506507	-1.611454	-2.515927E-02
28.500070	1.506550	-1.611487	-2.517409E-02
28.600070	1.506584	-1.611513	-2.518300E-02
28.700070	1.506606	-1.611533	-2.518821E-02
28.800070	1.506619	-1.611546	-2.518821E-02
28.900070	1.506622	-1.611553	-2.518732E-02
29.000070	1.506617	-1.611554	-2.517909E-02
29.100070	1.506602	-1.611549	-2.516777E-02
29.200080	1.506579	-1.611537	-2.515061E-02
29.300080	1.506542	-1.611520	-2.513105E-02
29.400080	1.506498	-1.611497	-2.510715E-02
29.500080	1.506448	-1.611467	-2.507993E-02
29.600080	1.506386	-1.611433	-2.504946E-02
29.700080	1.506319	-1.611393	-2.501572E-02
29.800080	1.506242	-1.611347	-2.497600E-02
29.900080	1.506156	-1.611296	-2.493420E-02
30.000080	1.506062	-1.611240	-2.488744E-02
30.100080	1.505959	-1.611179	-2.483982E-02
30.200080	1.505851	-1.611113	-2.478710E-02
30.300080	1.505733	-1.611041	-2.473072E-02
30.400080	1.505608	-1.610965	-2.467160E-02
30.500080	1.505478	-1.610884	-2.460838E-02
30.600080	1.505336	-1.610799	-2.454247E-02
30.700080	1.505190	-1.610709	-2.447328E-02
30.800080	1.505036	-1.610615	-2.440239E-02
30.900080	1.504878	-1.610516	-2.432626E-02
31.000080	1.504709	-1.610414	-2.424818E-02
31.100080	1.504538	-1.610307	-2.416544E-02
31.200080	1.504356	-1.610195	-2.408019E-02
31.300080	1.504169	-1.610080	-2.399280E-02
31.400080	1.503978	-1.609961	-2.390226E-02
31.500080	1.503778	-1.609839	-2.380924E-02
31.600080	1.503573	-1.609712	-2.371334E-02
31.700080	1.503363	-1.609583	-2.361307E-02
31.800090	1.503147	-1.609450	-2.351165E-02
31.900090	1.502924	-1.609313	-2.340735E-02
32.000080	1.502697	-1.609174	-2.330017E-02
32.100080	1.502465	-1.609031	-2.318972E-02
32.200080	1.502226	-1.608886	-2.307670E-02
32.300080	1.501984	-1.608737	-2.296138E-02
32.400080	1.501735	-1.608585	-2.284381E-02
32.500080	1.501482	-1.608430	-2.272280E-02
32.600070	1.501224	-1.608273	-2.259913E-02
32.700070	1.500960	-1.608112	-2.247278E-02
32.800070	1.500691	-1.607949	-2.234402E-02
32.900070	1.500418	-1.607784	-2.221331E-02
33.000070	1.500142	-1.607616	-2.207980E-02
33.100070	1.499859	-1.607447	-2.194403E-02
33.200070	1.499575	-1.607274	-2.180535E-02
33.300060	1.499284	-1.607101	-2.166487E-02
33.400060	1.498991	-1.606925	-2.152194E-02
33.500060	1.498693	-1.606747	-2.137623E-02
33.600060	1.498392	-1.606567	-2.122924E-02
33.700060	1.498088	-1.606385	-2.107867E-02
33.800060	1.497776	-1.606202	-2.092541E-02
33.900050	1.497464	-1.606017	-2.077113E-02
34.000050	1.497146	-1.605831	-2.061507E-02
34.100050	1.496829	-1.605643	-2.045495E-02
34.200050	1.496504	-1.605453	-2.029348E-02
34.300050	1.496179	-1.605262	-2.012923E-02
34.400050	1.495848	-1.605070	-1.996345E-02
34.500050	1.495516	-1.604876	-1.979363E-02
34.600040	1.495178	-1.604682	-1.962218E-02
34.700040	1.494838	-1.604486	-1.944821E-02
34.800040	1.494495	-1.604289	-1.927311E-02
34.900040	1.494149	-1.604092	-1.909550E-02
35.000040	1.493800	-1.603893	-1.891546E-02
35.100040	1.493450	-1.603694	-1.873143E-02
35.200040	1.493094	-1.603493	-1.854666E-02
35.300030	1.492737	-1.603293	-1.835950E-02
35.400030	1.492376	-1.603092	-1.817018E-02
35.500030	1.492014	-1.602890	-1.797869E-02
35.600030	1.491651	-1.602688	-1.778410E-02

1of

35.700030	1.491284	-1.602486	-1.758801E-02
35.800030	1.490914	-1.602283	-1.738917E-02
35.900020	1.490543	-1.602079	-1.718676E-02
36.000020	1.490166	-1.601876	-1.698286E-02
36.100020	1.489789	-1.601672	-1.677777E-02
36.200020	1.489410	-1.601469	-1.656916E-02
36.300020	1.489028	-1.601266	-1.635811E-02
36.400020	1.488643	-1.601062	-1.614357E-02
36.500020	1.488257	-1.600859	-1.592861E-02
36.600010	1.487871	-1.600655	-1.570979E-02
36.700010	1.487479	-1.600453	-1.548832E-02
36.800010	1.487087	-1.600251	-1.526505E-02
36.900010	1.486693	-1.600049	-1.503813E-02
37.000010	1.486297	-1.599846	-1.480828E-02
37.100010	1.485896	-1.599645	-1.457653E-02
37.200000	1.485495	-1.599444	-1.434135E-02
37.300000	1.485093	-1.599244	-1.410384E-02
37.400000	1.484688	-1.599045	-1.386308E-02
37.500000	1.484280	-1.598847	-1.361850E-02
37.600000	1.483871	-1.598649	-1.337187E-02
37.700000	1.483460	-1.598452	-1.312200E-02
37.800000	1.483046	-1.598257	-1.286903E-02
37.899990	1.482632	-1.598062	-1.261239E-02
37.999990	1.482213	-1.597868	-1.235214E-02
38.099990	1.481793	-1.597676	-1.208714E-02
38.199990	1.481370	-1.597484	-1.182016E-02
38.299990	1.480946	-1.597295	-1.154899E-02
38.399990	1.480520	-1.597107	-1.127353E-02
38.499980	1.480090	-1.596920	-1.099371E-02
38.599980	1.479658	-1.596734	-1.070929E-02
38.699980	1.479224	-1.596551	-1.042129E-02
38.799980	1.478786	-1.596369	-1.012780E-02
38.899980	1.478345	-1.596189	-9.829902E-03
38.999980	1.477903	-1.596011	-9.527512E-03
39.099980	1.477458	-1.595835	-9.219238E-03
39.199970	1.477008	-1.595661	-8.905144E-03
39.299970	1.476556	-1.595490	-8.585324E-03
39.399970	1.476100	-1.595321	-8.259334E-03
39.499970	1.475641	-1.595155	-7.926368E-03
39.599970	1.475178	-1.594992	-7.586495E-03
39.699970	1.474711	-1.594831	-7.239194E-03
39.799960	1.474239	-1.594674	-6.883518E-03
39.899960	1.473762	-1.594520	-6.519997E-03
39.999960	1.473281	-1.594369	-6.146389E-03
40.099960	1.472792	-1.594223	-5.763267E-03
40.199960	1.472299	-1.594080	-5.370494E-03
40.299960	1.471800	-1.593943	-4.965522E-03
40.399960	1.471293	-1.593810	-4.547326E-03
40.499950	1.470778	-1.593683	-4.115441E-03
40.599950	1.470255	-1.593562	-3.668632E-03
40.699950	1.469722	-1.593446	-3.204937E-03
40.799950	1.469178	-1.593339	-2.723122E-03
40.899950	1.468624	-1.593238	-2.219493E-03
40.999950	1.468055	-1.593146	-1.692263E-03
41.099950	1.467471	-1.593066	-1.138750E-03
41.199940	1.466868	-1.592995	-5.522370E-04
41.299940	1.466243	-1.592940	6.712226E-05
41.399940	1.465601	-1.592897	7.237979E-04
41.499940	1.464942	-1.592854	1.396837E-03
41.599940	1.464278	-1.592807	2.070386E-03
41.699940	1.463618	-1.592750	2.729499E-03
41.799930	1.462969	-1.592680	3.365042E-03
41.899930	1.462334	-1.592594	3.970317E-03
41.999930	1.461716	-1.592496	4.542008E-03
42.099930	1.461119	-1.592385	5.079654E-03
42.199930	1.460543	-1.592263	5.583453E-03
42.299930	1.459989	-1.592134	6.055246E-03
42.399930	1.459456	-1.591996	6.498110E-03
42.499920	1.458941	-1.591854	6.913925E-03
42.599920	1.458446	-1.591709	7.306622E-03
42.699920	1.457968	-1.591560	7.677304E-03
42.799920	1.457505	-1.591409	8.028515E-03
42.899920	1.457058	-1.591256	8.363643E-03
42.999920	1.456622	-1.591104	8.683452E-03
43.099910	1.456201	-1.590952	8.989996E-03
43.199910	1.455789	-1.590800	9.284188E-03
43.299910	1.455388	-1.590647	9.567777E-03
43.399910	1.454996	-1.590496	9.841777E-03
43.499910	1.454613	-1.590344	1.010676E-02

1of

43.599910	1.454237	-1.590193	1.036406E-02
43.699910	1.453869	-1.590042	1.061368E-02
43.799900	1.453506	-1.589892	1.085660E-02
43.899900	1.453152	-1.589742	1.109205E-02
43.999900	1.452803	-1.589593	1.132236E-02
44.099900	1.452459	-1.589444	1.154736E-02
44.199900	1.452121	-1.589296	1.176662E-02
44.299900	1.451787	-1.589149	1.198145E-02
44.399890	1.451459	-1.589001	1.219188E-02
44.499890	1.451133	-1.588854	1.239764E-02
44.599890	1.450812	-1.588707	1.259945E-02
44.699890	1.450496	-1.588561	1.279690E-02
44.799890	1.450184	-1.588416	1.299107E-02
44.899890	1.449875	-1.588271	1.318214E-02
44.999890	1.449569	-1.588126	1.336916E-02
45.099880	1.449268	-1.587982	1.355402E-02
45.199880	1.448968	-1.587838	1.373451E-02
45.299880	1.448672	-1.587695	1.391179E-02
45.399880	1.448380	-1.587551	1.408693E-02
45.499880	1.448089	-1.587409	1.426012E-02
45.599880	1.447802	-1.587267	1.442968E-02
45.699870	1.447518	-1.587125	1.459639E-02
45.799870	1.447237	-1.586985	1.476063E-02
45.899870	1.446959	-1.586844	1.492265E-02
45.999870	1.446684	-1.586704	1.508252E-02
46.099870	1.446410	-1.586564	1.524117E-02
46.199870	1.446137	-1.586425	1.539599E-02
46.299870	1.445869	-1.586286	1.554886E-02
46.399860	1.445603	-1.586148	1.570006E-02
46.499860	1.445339	-1.586010	1.584881E-02
46.599860	1.445078	-1.585873	1.599582E-02
46.699860	1.444818	-1.585736	1.614152E-02
46.799860	1.444560	-1.585599	1.628525E-02
46.899860	1.444304	-1.585464	1.642615E-02
46.999860	1.444052	-1.585329	1.656556E-02
47.099850	1.443801	-1.585194	1.670424E-02
47.199850	1.443553	-1.585060	1.684051E-02
47.299850	1.443304	-1.584926	1.697551E-02
47.399850	1.443060	-1.584793	1.710829E-02
47.499850	1.442817	-1.584661	1.724035E-02
47.599850	1.442576	-1.584529	1.736999E-02
47.699840	1.442336	-1.584397	1.749717E-02
47.799840	1.442100	-1.584267	1.762479E-02
47.899840	1.441864	-1.584136	1.775018E-02
47.999840	1.441630	-1.584006	1.787424E-02
48.099840	1.441399	-1.583877	1.799701E-02
48.199840	1.441168	-1.583748	1.811897E-02
48.299840	1.440938	-1.583619	1.823897E-02
48.399830	1.440711	-1.583491	1.835712E-02
48.499830	1.440487	-1.583364	1.847461E-02
48.599830	1.440263	-1.583237	1.859141E-02
48.699830	1.440040	-1.583110	1.870685E-02
48.799830	1.439819	-1.582984	1.882121E-02
48.899830	1.439599	-1.582859	1.893365E-02
48.999820	1.439381	-1.582735	1.904452E-02
49.099820	1.439167	-1.582610	1.915560E-02
49.199820	1.438951	-1.582486	1.926526E-02
49.299820	1.438739	-1.582363	1.937333E-02
49.399820	1.438526	-1.582240	1.948095E-02
49.499820	1.438316	-1.582119	1.958690E-02
49.599820	1.438107	-1.581997	1.969198E-02
49.699810	1.437900	-1.581875	1.979690E-02
49.799810	1.437693	-1.581755	1.989900E-02

tof

LIU-WEN'S COPY

Estimate of Radiation Release for MIT Research Reactor During Design Basis Accident

by

Qing Li

Submitted to the Department of Nuclear Engineering
in partial fulfillment of the requirements for the degree of

Master of Science in Nuclear Engineering

at the

MASSACHUSETTS INSTITUTE OF TECHNOLOGY

May 1998

© Massachusetts Institute of Technology 1998. All rights reserved.

Author
Department of Nuclear Engineering
May 8, 1998

Certified by
John A. Bernard
Director, MIT Nuclear Reactor Laboratory
Thesis Supervisor

Certified by
Jacquelyn C. Yanch
Professor, Nuclear Engineering Department
Thesis Supervisor

Accepted by
Lawrence M. Lidsky
Chairman, Department Committee on Graduate Students

Estimate of Radiation Release for MIT Research Reactor During Design Basis Accident

by
Qing Li

Submitted to the Department of Nuclear Engineering
on May 8, 1998, in partial fulfillment of the
requirements for the degree of
Master of Science in Nuclear Engineering

Abstract

During a postulated design basis accident at the MIT Research Reactor (MITR), radioactive fission products may be released from melted fuel plates into the containment. To comply with regulations, the whole-body dose and thyroid dose at the boundary of the exclusion area as a result of this accident are determined.

The fractions of the fission products contained in the fuel that are released through the reactor coolant system (RCS) into the containment are determined based on current regulations, experimental tests, and results from TMI-2 accident.

After the fission products are released into the containment, a portion may be released to the outside through a containment crack or the stack. Also, the portion retained in the containment would contribute to the external gamma dose. The calculated dose due to atmospheric release depends on the source strength, the meteorological conditions, and the dispersion model. For containment crack release and stack release, different dispersion models are used according to pertinent regulatory guides. The gamma dose through penetration or scattering depends on the structure of the containment shielding and is determined analytically under appropriate approximations.

Because the MITR is considering upgrading its power level, results at power levels from 5 to 10 MW are determined. At 5, 6, 7, 8, 9, 10 MW, the whole body doses at the back fence (8 meters away from the MITR) are 0.644, 0.764, 0.885, 1.00, 1.13, 1.25 rem respectively; the thyroid doses at the back fence are 0.112, 0.135, 0.157, 0.179, 0.202, 0.225 rem respectively; the whole body doses at the front fence (21 meters away from the MITR) are 0.887, 1.06, 1.22, 1.39, 1.56, 1.72 rem respectively; and the thyroid doses at the front fence are 0.112, 0.134, 0.156, 0.179, 0.201, 0.224 rem respectively.

The results show that even under conservative assumptions, the released doses for power levels from 5 MW to 10 MW are well below the regulatory limit – 25 rem for whole body and 300 rem for thyroid.

Thesis Supervisor: John A. Bernard
Title: Director, MIT Nuclear Reactor Laboratory

Thesis Supervisor: Jacquelyn C. Yanch
Title: Professor, Nuclear Engineering Department

Acknowledgments

First, I would like to thank Dr. John A. Bernard for his overall guidance and assistance. I also want to thank Prof. Jacquelyn C. Yanch for her co-supervision of this work and Dr. Lin Wen Hu and Mr. Fred McWilliams for their great assistance.

Contents

1	Introduction	13
1.1	Description of MITR-II and Previous Work	13
1.2	Regulatory Limit on Dose Release	14
2	Development of the Containment Source Term	17
2.1	Fission Product Inventory	17
2.1.1	Fission Product Build-up in the Fuel	17
2.1.2	Build-up of Ar ⁴¹ in the Containment	18
2.1.3	Fission Product Inventory in the Melted Fuel	20
2.2	Release Fraction	20
2.2.1	Overview of Release Fraction	20
2.2.2	Release Magnitude from the Fuel to the RCS	22
2.2.3	RCS Retention	24
2.2.4	Summary of Release Fraction	28
2.3	Natural Depletion in Containment	29
3	Atmospheric Release	31
3.1	Introduction	31
3.2	Release from Pressure Relief System	31
3.2.1	Release Fraction Through the Stack Filter System	31
3.2.2	Release Rate	32
3.2.3	Atmospheric Dispersion Model	32
3.2.4	Dispersion Coefficient	34

3.2.5	Meteorological Data	34
3.2.6	Application of Dispersion Model	35
3.2.7	Total Activity Released	36
3.3	Release from Containment Leakage	42
3.3.1	Leakage Rate	42
3.3.2	Atmospheric Dispersion Model	42
3.3.3	Application of Diffusion Models	43
3.3.4	Total Activity Release	44
3.4	Adjustment of the Release Term Outside the Containment	44
3.5	External Gamma Dose from Plume	44
3.6	Beta Dose	47
3.7	Thyroid Dose	49
3.8	Summary	50
4	Direct Gamma Dose, Scattered Gamma Dose, and Gamma Dose Through the Truck Lock	56
4.1	General	56
4.2	Gamma Source Term	57
4.3	Direct Gamma Dose	58
4.3.1	Steel Shell Penetration Gamma Dose	59
4.3.2	Shadow Shield Penetration Gamma Dose	62
4.4	Scattered Gamma Dose	64
4.4.1	Air Scattering Gamma Dose	66
4.4.2	Steel Shell Scattering Dose	67
4.5	Radiation Penetration Through the Truck Lock	72
4.5.1	Concrete Scattered Dose	74
4.5.2	Steel Door Scattered Dose	75
4.5.3	Summary of Radiation Through the Truck Lock	76
5	Summary	78

A Tables	88
B Figures	99

List of Figures

3-1	Dependency of χ/Q on SigY for stack release under condition of wind-speed = 11.9 KTS, class D stability, $h_s = 46$ m.	37
3-2	Dependency of χ/Q on wind speed for stack release under condition of class D stability, $h_s = 46$ m. The solid line curve is for a wind speed of 11.9 KTS (6.125 m/s), the dash - dot line curve is for a wind speed of 30 KTS (15.44 m/s) and the dash - dash curve is for a wind speed of 3 KTS (1.544 m/s).	38
3-3	Dependency of χ/Q on stack height for stack release under condition of class D stability with a wind speed of 11.9 KTS. The solid line curve is for a stack height of 46 m, the dash - dot line curve is for a stack height of 46 m and the dash - dash curve is for a stack height of 46 m.	39
3-4	Dependency of χ/Q on SigZ for stack release under condition of wind-speed = 11.9 KTS, class D stability, $h_s = 46$ m.	40
3-5	χ/Q Distribution as a function of plume distance for each atmospheric condition from stack release.	41
3-6	χ/Q Distribution as a function of plume distance for each atmospheric condition from containment leakage using "conservative" calculation. A, B, C, D, E and F in the figure stand for the atmospheric stability classes.	45
3-7	χ/Q Distribution as a function of plume distance for each atmospheric condition from containment leakage using "exact" calculation. A, B, C, D, E and F in the figure stand for the atmospheric stabilities.	46

3-8	Two hour stack release showing beta-Dose, gamma dose and thyroid dose versus distance. Dotted line is thyroid dose, dot-dash line is gamma dose, and solid line is beta dose. C, D and E is the respective atmospheric stability.	51
3-9	Two hour containment leakage beta-dose, gamma dose and thyroid dose vs. distance using exact calculation.	52
3-10	Two hour containment leakage beta-dose, gamma dose and thyroid dose vs. distance using conservative calculation. Different lines in each plot are for different power levels.	53
3-11	Two hour containment leakage whole-body dose(rem) and thyroid dose(rem) vs. reactor power for "exact" model.	54
5-1	Exclusion area doses as a function of reactor power. The solid lines are for whole-body doses, and the solid-dash lines are for thyroid doses. The circle sign is for doses at 21 meters and the plus sign is for doses at 8 meters. Thyroid doses at 8 meters and at 21 meters are not distinguishable in the plot.	81
B-1	Meander factors for correction of Pasquill-Gifford sigma y values by atmospheric stability class. D, E, F, and G are the stability classes. .	100
B-2	Direct dose containment volume transformations	101

List of Tables

1.1	Exclusion Area Distance	15
2.1	Source Term Contributions	19
2.2	Release From the Core in the TMI-2 Accident	23
2.3	Fuel Release Fractions From Severe Fuel Damage Tests	24
2.4	Release Fraction From Core to RCS	25
2.5	Summary of Experiment Retention Fractions (% of Source)	25
2.6	NUGREG-1150 Expert Elicitation Median RCS Retention Factors	27
2.7	RCS Retention Factors	27
2.8	Release Fraction From Core to RCS	28
3.1	Formulas for σ_y and σ_z by Briggs (1973)	35
3.2	Wind-Speed for Each Stability Category (KTS) Averaged Over All Directions	36
3.3	Total containment leakage dose (rem) in two hours using "exact" at- mosphere dispersion model	50
3.4	Total Containment Leakage Dose (rem) in two hours Using "Conser- vative" Atmospheric Dispersion Model	55
4.1	Average Containment Volume Source Strength	58
4.2	Steel Dome Penetration Doses (rem) at 8 Meters	62
4.3	Steel Dome Penetration Doses (rem) at 21 Meters	63
4.4	Shadow Shield Penetration Doses (rem) at 8 Meters	65
4.5	Shadow Shield Penetration Doses (rem) at 21 Meters	65

4.6	Air Scattering Doses (rem) From Upper Source at 8 Meters	68
4.7	Air Scattering Doses (rem) From Upper Source at 21 Meters	69
4.8	Air Scattering Doses (rem) From Lower Source at 8 Meters	69
4.9	Air Scattering Doses (rem) From Lower Source at 21 Meters	69
4.10	Air Scattering Doses (rem) From All Sources at 8 Meters	70
4.11	Air Scattering Doses (rem) From All Sources at 21 Meters	71
4.12	Single Steel Scattering Doses (rem) 8 Meters vs. Source	73
4.13	Single Steel Scattering Doses (rem) 21 Meters vs. Source	73
4.14	Total Steel Scattering Doses (rem)	73
4.15	Direct Dose at the Concrete Wall	75
4.16	Concrete Albedo Dose (rem)	76
4.17	Steel Door Scattered Dose (rem)	77
5.1	Total Dose at 5 MW	80
5.2	Total Dose at 6 MW	82
5.3	Total Dose at 7 MW	82
5.4	Total Dose at 8 MW	82
5.5	Total Dose at 9 MW	83
5.6	Total Dose at 10 MW	83
A.1	Total Core Fission Product Inventory	89
A.2	Values of N_g^i/N_{235}^0 for Neutron-Capture Influenced Isotopes at $\phi_T = 4 \times 10^{13}$	90
A.3	Parameters for Calculating Atmospheric Doses by Isotope	91
A.4	Gamma Emission Energies by Isotope	93
A.5	Attenuation and Absorption Coefficients	95
A.6	Shield Thicknesses in Mean Free Paths	96
A.7	Point Isotopic Source Exposure Build-Up Factors for Iron (Steel) . . .	96
A.8	Coefficients of the Taylor Exposure Build-up Factor Formula	97
A.9	Values of the Functions $G(1,p,0,b'_2)$ and $G(1,p,0,b''_2)$	97
A.10	Air Scattering Input Parameters	98

A.11 Steel Scattering Input Parameters	98
--	----

Chapter 1

Introduction

1.1 Description of MITR-II and Previous Work

The MIT reactor is a tank-type research reactor that is cooled and moderated by light water and reflected by heavy water. It currently runs at a power of 5MW. It is fueled by [REDACTED] [REDACTED]

[REDACTED] This core design maximizes the neutron flux in the D₂O reflector region where numerous experimental beam ports are located. The core is contained within a light-water filled aluminum tank which is in turn contained within the D₂O reflector tank. The H₂O coolant is directed so as to flow down along the tank walls and then upwards through the fuel elements. Heat from the primary system is transferred by heat exchangers to the secondary system which dissipates it to the atmosphere through the cooling towers.

The reactor is located at the center of a gas tight cylindrical steel building equipped with a controlled pressure relief system. Access to the containment is through either a personnel or a truck air-lock. There is also a small personnel airlock which leads directly into the control room. All building penetrations are either sealed permanently or can be sealed rapidly by manual or automatic operation. The building is designed to withstand a maximum overpressure of 2 psi and normally operates at a slightly negative pressure.

The design basis accident is the maximum credible accident which could result in

the release of radiation from the reactor [1][2]. For MITR-II, the design basis accident is postulated as a coolant flow blockage in the fuel element which contains the hottest channel. This could occur, for example, as the result of some foreign material falling into the reactor during refueling. After the pumps are started, the material would be swept from the bottom of the tank up to the entrance of the fuel elements. Because of the size of the openings in the adapters at the end of each fuel element, no material passing through the adapter would be large enough to block more than five of the coolant channels. So, the maximum number of plates that could be overheated is four. It is conservative to assume that these four plates could melt completely and release their inventory of fission products to the coolant water. For a more detailed description of the MITR please refer to the MITR-II reactor systems manual.

The most recent previous work on this topic is a thesis by Mull [3]. In it, he calculated the dose from radiation release through building leakage and the truck lock and the dose due to direct and scattered gamma radiation during a design basis accident of the MITR-II at 5 MW. His values for release fractions were mainly based on WASH-1400 [4] and other information available then.

Although the purpose of this thesis is to calculate the same doses via the same release paths, great revisions are made in the release fractions based on current experimental and analytical studies and the results from the TMI-2 accident. Other revisions and additions included are:

- Radiation release through the pressure relief system to the stack.
- Build-up of Ar^{41} source term in the building due to the sealing of the containment in the accident.
- Radiation release at different reactor powers from 5MW up to 10MW.

1.2 Regulatory Limit on Dose Release

In CFR 100.11, the limit on dose release is stated as:

Table 1.1: Exclusion Area Distance

Sector Direction	Minimum Exclusion Area Distance X(m)
N	20.6
NNE	22.1
NE	18.7
ENE	18.7
E	17.1
ESE	10.3
SE	8.00
SSE	8.00
S	8.00
SSW	9.53
SW	13.0
WSW	24.0
W	24.0
WNW	24.8
NW	21.0
NNW	20.6

- Exclusion area of such size that an individual located at any point on its boundary for two hours immediately following onset of the postulated fission product release would not receive a total radiation dose to the whole body in excess of 25 rem or a total radiation dose in excess of 300 rem to the thyroid from Iodine.
- A low population zone of such size that an individual located at any point on its outer boundary who is exposed to the radioactive cloud resulting from the postulated fission product release during the entire period of its passage would not receive a total radiation dose to the whole body in excess of 25 rem or a total radiation dose in excess of 300 rem to the thyroid from iodine exposure.

To comply with the above regulation, we first have to define the exclusion area for the MITR. The exclusion area around the reactor was divided into 16 sectors of 45 degrees each, centered on each wind direction. The shortest distance between the reactor containment shell and the exclusion area boundary within each sector has been designated as the sector distance, X. These values are listed in Table 1.1.

The back fence is defined at a distance of 8 meters and the front fence is defined at 21 meters (the Albany St. fence).

Chapter 2

Development of the Containment Source Term

2.1 Fission Product Inventory

2.1.1 Fission Product Build-up in the Fuel

Because current regulations on source term estimation require a simultaneous release assumption, the fission product inventory in the fuel at the time of the accident is assumed to be equal to the maximum value of equilibrium fission products during the two hour release period. This is a conservative assumption.

Based on the volatility, quantity produced, half-life and degree of biological effectiveness, the fission product isotopes are selected from a suggested list in Thompson and Beckerley and from those used in the Reactor Safety Study, WASH-1400[4]. The resulting fission product isotopes are listed in Appendix A.1[3].

The saturation activities of the fission product isotopes can be calculated by both an analytical and a computational method. For the analytical method, the saturation activity, Q_s^i in Curies, due to the presence of N_s^i , is

$$Q_s^i = \frac{N_s^i \lambda_i}{3.7 \times 10^{10}} \quad (2.1)$$

where N_s^i is the saturation number of nuclei of isotope i , Q_s^i is the saturation activity due to the presence of N_s^i (Ci), and λ_i is the decay constant for isotope i (s^{-1}).

One megawatt equals 3.2×10^{16} fissions/s if one assumes that 195 MeV of energy per fission is recoverable, so,

$$Q_s^i = \frac{Y_i P (3.2 \times 10^{16})}{3.7 \times 10^{10}} = 8.65 \times 10^5 P Y_i \quad (2.2)$$

where P is the reactor power (MW), and Y_i is the fission product yield for isotope i (atoms/fission).

For the computational method, the saturation activity, Q_s^i in Curies, due to the presence of N_s^i , is

$$Q_s^i = \frac{1.49 \times 10^{27} \lambda_i P (N_s^i / N_{235}^0)}{\phi_T} \quad (2.3)$$

where N_s^i / N_{235}^0 is the saturated number of fission product atoms produced per initial atom of U^{235} , and ϕ_T is the thermal neutron flux (neutrons/cm² · s). The N_s^i / N_{235}^0 values found from literature[5] at $\phi_T = 4 \times 10^{13}$ are listed in Appendix A.2.

For both methods, the saturation activity is proportional to the reactor power. For more details of the derivation of the equations, please see reference[3].

The resulting saturation activity of each isotope at 5, 6, 7, 8, 9 and 10 MW are listed in Appendix A.1.

2.1.2 Build-up of Ar^{41} in the Containment

Argon-41 is produced by irradiating air, nearly one percent(0.93%) of which consists of Ar^{40} , with thermal neutrons. Ar^{40} has a neutron cross section of 0.65 barns and can produce Ar^{41} , which is a gamma and beta emitter, through a neutron capture reaction. The half-life of the Ar^{41} is 1.83 hour. Because the MIT reactor is designed for research, air inherently gets into the areas of significant neutron flux (in and around the core, the flux is in the order of $10^{13} - 10^{14}$ neutrons/cm² · s) [6]. Air could be expected to get into experimental ports, instrument ports, irradiation facilities, the lead shutter region, and the fission converter area.

Table 2.1: Source Term Contributions

Source	Air Flow rate (ft ³ /min)	Sample Ar ⁴¹ Conc. (μ Ci/ml)	Source Term (μ Ci Ar ⁴¹ /min)
Pipe tunnel	11.8 \pm 1.8	2.28 \pm 0.01($\times 10^{-2}$)	7.63 \pm 1.2($\times 10^3$)
Core purge	5.75 \pm 0.30	6.80 \pm 0.04($\times 10^{-3}$)	1.11 \pm 0.06($\times 10^3$)
Pneumatic tubes	81.9 \pm 4.1	1.85 \pm 0.03($\times 10^{-4}$)	0.430 \pm 0.02($\times 10^3$)
Basement hot cell	739 \pm 37	3.57 \pm 0.12($\times 10^{-5}$)	0.747 \pm 0.05($\times 10^3$)
Reactor floor hot cell	450 \pm 23	1.19 \pm 0.30($\times 10^{-6}$)	0.015 \pm 0.004($\times 10^3$)
Primary chemistry	834 \pm 42	1.37 \pm 0.04($\times 10^{-6}$)	0.032 \pm 0.002($\times 10^3$)
Medical room	587 \pm 29	2.12 \pm 0.05($\times 10^{-6}$)	0.035 \pm 0.002($\times 10^3$)
Main Ventilation	2708 \pm 135	1.04 \pm 0.03($\times 10^{-6}$)	0.080 \pm 0.005($\times 10^3$)
Total Input	5417 \pm 151	2.98 \pm 0.01($\times 10^{-2}$)	10.08 \pm 1.2($\times 10^3$)

During typical operating conditions, the ventilation system exhausts air through the stack to prevent the build up of an Ar⁴¹ source term. In reference [6], the output rate of Ar⁴¹ was measured thoroughly in all the possible source-term producing areas. The results are presented in Table 2.1. The total release rate from all sources for MITR II at 5MW at normal operating conditions is $S = 10.08E3 \mu\text{Ci}/\text{min}$ [6]. The average containment concentration was $2.18E-8 \mu\text{Ci}/\text{ml}$ (measured in 1984).

During an accident, the containment is sealed and the ventilation system is secured. The Ar⁴¹ already generated in those source places may be released to the containment and result in a build-up of Ar⁴¹ in the containment.

The total volume of those source places is 5% of the containment volume. The concentration of Ar⁴¹ in the containment after sealing would be $2.98 \times 10^{-2} \times 5\% = 1.49 \times 10^{-3} \mu\text{Ci}/\text{ml}$ for power level at 5MW. Compared with the Ar⁴¹ containment concentration of $2.18 \times 10^{-8} \mu\text{Ci}/\text{ml}$ at operation condition, it is much higher.

Measurements showed that the source producing rate is proportional to the power. Thus, the Ar⁴¹ concentration for power levels other than 5MW can be determined based on the data at 5MW. The Ar⁴¹ concentrations for power levels of 6MW, 7MW, 8MW, 9MW and 10 MW would be 1.79, 2.09, 2.38, 2.68 and $1.98 \times 10^{-3} \mu\text{Ci}/\text{ml}$ respectively. Compared to other fission products released from the fuel, this concentration is much lower (by an order of 5 to 7), thus the dose contribution of Ar⁴¹ at

the exclusion area is negligible.

2.1.3 Fission Product Inventory in the Melted Fuel

In the previous sections the saturated core inventory of fission product activities was determined. But not all of this fission product inventory can be released. Only a small portion of that contained in the four fuel plates that are assumed to melt could be released. If the core contains [REDACTED] and the [REDACTED], then the fraction of the total saturated core inventory which is contained in the four fuel plates, F_s , could be determined to be:

$$F_s = \frac{[REDACTED]}{[REDACTED]} = 0.0176 \quad (2.4)$$

Therefore, a maximum of 1.76% of each Q_i^j is available for release from the melted core.

2.2 Release Fraction

2.2.1 Overview of Release Fraction

The Reactor Safety Study (WASH-1400), was the first systematic attempt to provide realistic estimates of public risk from potential accidents in commercial nuclear power plants. Based on WASH-1400, the total release fraction from the fuel to the containment is the fraction from the fuel to the primary coolant system(RCS) F_f times the fraction from the RCS to the containment F_p and the release is instantaneous. Based on the information available then, the release fractions were chosen as shown below in Mull's thesis:

- Fraction of release from fuel to primary coolant system F_f ,
 - 100% of the noble gases(Kr, Xe)
 - 100% of the halogens(I, Br)
 - 70% of the Tellurium

30% of the alkali metals (Cs, Rb)
1% of the remaining fission products

- Fraction of the release from primary coolant system to containment F_p ,
100% of the noble gases
10% of all other isotopes

Following the publication of WASH-1400 and the accident at Three Mile Island Unit 2 (TMI-2), work was initiated to review the predictive method for calculating fission product release and transport. The results of this review are contained in NUREG-0772 [7]. That review resulted in several conclusions that represented significant departures from the WASH-1400 assumptions including the suggestion that cesium iodide (CsI) will be the predominant iodine chemical form under most postulated light water reactor (LWR) accident conditions.

Updated fission product source term methods were developed under the sponsorship of NRC and the nuclear industry. As a result, the Source Term Code Package (STCP) was developed as an integration tool for source term evaluation. NUREG-1150 [8] documents a Probabilistic Risk Assessment (PRA) study of five U.S. commercial nuclear power plants by using the STCP. A limited number of source term calculations were done for selected plant accident scenarios. The second draft of the study was published in April, 1989 and presents an update, extension, and improvement upon the 1975 risk study, WASH-1400[4]. Thus, NUREG-1150 reflects current NRC thinking regarding the source term. But the results are not directly applicable to MITR, because the results are very sensitive to the specification of the plant's design and accident scenarios. Another important document was prepared by the Department of Energy (DOE) which sponsored the Advanced Reactor Severe Accident Program in support of the Utility/Electric Power Research Institute (EPRI) advanced light water reactor (ALWR) program [9]. In this document, a physically-based source term backed by experimental and analytical results is provided and is in agreement with that from NUREG-1150 under similar conditions.

Based on the above documents, the results from the TMI-2 accident, and available experimental results, the release fractions have been re-determined here for the MITR.

In both references [8] and [9], the release progression is divided into an in-vessel release phase, and an ex-vessel phase [8, 9]. The "in-vessel release phase" of a severe accident refers to that period of time during which the reactor core is damaged and begins to melt, but is still retained within the RCS [8]. The "ex-vessel release phase" refers to that period of time after vessel penetration, in which the molten material and most of the remaining radioactive materials would transfer to the containment. However, for the MITR-II, the core temperature is much lower. Therefore, the core will be retained in the vessel during the whole period. All the releases are due to in-vessel release. Detailed deduction of the release fraction is given in the following sections.

2.2.2 Release Magnitude from the Fuel to the RCS

As discussed previously, we assumed four plates in the core melt in the maximum severe case. The radioactive materials contained in these four plates will be released into the primary coolant system and lead to release to the containment. In this section, fission product release from the melted fuel to the RCS is estimated and justifications for these releases are provided.

Noble Gases, Iodine, and Cesium

Analysis of fission product releases from the TMI-2 accident [10, 11, 12, 13] and from the severe fuel damage experiments [14, 15, 16, 17, 18, 19, 20, 21] indicate that the releases of iodine, and cesium are approximately equal and are closely related to the fraction of the fuel that becomes molten in the accident sequence. In the TMI-2 accident, about 45% of the core was molten and the releases of iodine, and cesium were in the neighborhood of 55%.

Measurements of residual fission products in previously molten fuel indicate that up to about 10% of the original cesium inventory and somewhat less of the iodine can

Table 2.2: Release From the Core in the TMI-2 Accident

Isotope	Fraction of Core Inventory Released
I	0.55
Cs	0.55
Te	0.06
Sr	0.001
Ru	0.005
Sb	0.016
Ce	0.0001

be retained by the formation of chemical species that are stable at high temperatures and/or geometries having low surface-to-volume ratios (see References [11] and [22]). On the basis of these results, releases of 90% of the iodine and cesium from molten fuel are proposed. No residual fission gases were found in molten fuel debris from TMI-2 (see reference [10]), so a 100% release of noble gas from molten fuel is proposed.

Tellurium

Considerable study has resulted in the understanding that tellurium is released from the fuel at about the same rate as noble gases, iodine, and cesium, but is largely retained by the surrounding metallic zircaloy cladding and is then released during oxidation of the cladding [23, 24]. Tellurium has a chemical affinity for metallic zircaloy and most other metals such as aluminum. The results of the tellurium release from TMI-2 accident and severe fuel damage tests are listed in Table 2.2 and 2.3.

Oxidation of the cladding has the effect of increasing the concentration (and therefore the chemical activity) of tellurium in the remaining metallic cladding, thereby increasing the partial pressure of tellurium. A value of 0.23 for in-vessel tellurium release from the fuel is assumed for use [9].

Semi-Volatiles and Low Volatiles

The release of strontium, barium, antimony, and ruthenium have been found to be quite low as demonstrated in Tables 2.2 and 2.3 and are bounded by a value of 1%.

Table 2.3: Fuel Release Fractions From Severe Fuel Damage Tests

Element/Exp.Cond.	SFD-ST	SFD1-1	SFD1-3	SFD1-4
I	0.51	0.12	0.18	0.26
Cs	0.32	0.09	0.18	0.44-0.56
Te	0.40	0.01	0.01-0.09	0.03
Sr	0.00002		0.00024	0.0088
Ba	0.011	0.006	0.004	0.008
Sb			0.00019	0.0013
Ru	0.0003	0.0002	0.00003	0.00007
Ce	0.000002	0.00009	0.00008	0.00013
Actinides			< 0.0001	< 0.00001
Zr Oxidized (%)	75	26	22	32
Fuel Melted (%)	15	16	18	18

Cerium, lanthanum, and actinides are oxides with very low volatilities which are dissolved in the fuel matrix and thus are released to a very small extent (<0.01%) (see reference [20]).

Conclusion

The proposed releases from fuel to the RCS are listed in Table 2.4. All numbers are fractions of the original core fission product inventory. They are based on experience gained in the analysis of core melt progression experiments and the TMI-2 accident.

For the MIT reactor, the release fractions are expected to be lower. The core of MITR is made of a cermet fuel that is more efficient in retaining fission products.

2.2.3 RCS Retention

After the fission products are released from the fuel into the RCS, substantial quantities of fission products may be deposited in the RCS correspondingly reducing the source term to containment.

The NRC and the commercial nuclear industry have developed computer codes to predict the extent of deposition in the RCS for various accident sequences and have undertaken experiments to validate their calculational methods. Detailed analysis

Table 2.4: Release Fraction From Core to RCS

Element	Releases From Fuel to RCS
Noble Gases (NG)	1.0
I	0.9
Cs	0.9
Te	0.23
Sr	0.01
Ba	0.01
Ru	0.01
La	0.0001
Ce	0.0001
Other	0.0001

Table 2.5: Summary of Experiment Retention Fractions (% of Source)

Test	Species	Deposition Close to Fuel	Total Piping Deposition
LACE LA3A	CsOH/MnO=.21	26	77
LA3B	CsOH/MnO=.13	15	51
LA3C	CsOH/MnO=.61	46	83
LA1	CsOH/MnO=.43	—	99
Marviken	—	—	74
SFD 1-4	Iodine	10	95
	Cesium	30	95
LOFT FP-2	Iodine	66	70
	Cesium	60	71

using these codes and supporting experimental evidence from tests, indicate that iodine, cesium and the less volatile radionuclides will condense on or interact with other structural materials released from the damaged core to generate aerosols[9].

Experimental Results on RCS Retention

Experimental evidence of aerosol retention processes in the RCS is provided by the LACE[25, 26] and Marviken[27] aerosol transport tests as well as by the SFD 1-4 test (see reference [18]) and the LOFT FP-2 test [28]. Table 2.5 summarizes the measured deposition results [9].

Additional evidence of fission product retention during severe accidents is provided by the TMI-2 accident evaluation. Water pathways that existed throughout the duration of the accident retained nearly 100% of the iodine, cesium and other aerosols generated during the accident.

Analytical Results on RCS Retention

In support of NUREG-1150, the NRC's TRAP-MELT code (one of the modules of the Source Term Code Package (STCP)) estimates the amount of RCS retention that can be expected for a variety of accident sequences in modern, operating PWRs and BWRs[29]. The predicted retention factors for aerosols in the RCS range from approximately 15% to 85%. The lowest values are associated with large, hot-leg pipe break accidents in PWRs and low-to-intermediate pressure sequences in BWRs in which core uncover occurs early. Because the design of the MITR-II is different from most of the operating plants evaluated in NUREG-1150, the probability of large primary pipe breaks is very low. Hence, the low values of RCS retention associated with large break Loss of Coolant Accident (LOCA) are not applicable to the MITR-II.

The version of TRAP-MELT used in the Source Term Package is recognized to underpredict aerosol retention within the RCS because of unmodeled phenomena[9]. An uncertainty analysis (MAAP) was conducted as part of NUREG-1150 in which the range of the RCS retention fraction was determined by polling source term experts. Table 2.6 shows the resulting median values for RCS retention for different scenarios. The cases considered by the expert panel are defined as [8]:

- PWR-1: System setpoint pressure (2500 psia); release through a cycling Over-pressure Relief Valve (PORV).
- PWR-2: High pressure (600 to 2000 psia); release through a very small break or pump seal LOCA.
- PWR-3: Intermediate pressure (200 to 600 psia); release through a break of approximately two inches diameter.

Table 2.6: NUGREG-1150 Expert Elicitation Median RCS Retention Factors

Cases	Conditions	Iodine	Cesium	Low Volatility Aerosol
PWR 1	Setpoint Pressure	91	96	97
PWR 2/3	High and Intermediate Pressure	59	71	76
PWR 4	Low Pressure	48	60	66
BWR 1	High Pressure, Early Melt	91	97	97
BWR 2	Low Pressure, Early Melt	59	70	74
BWR 3	High Pressure, Delayed Melt	72	75	92

Table 2.7: RCS Retention Factors	
Aerosol Chemical Species	Retention factor
Iodine	0.7
All Other	0.7

- PWR-4: Low pressure (below 200 psia); release through a large break.
- BWR-1: High pressure fast station blackout.
- BWR-2: Low pressure fast station blackout.
- BWR-3: High pressure ATWS sequences.

The RCS retention values are higher than the TRAP-MELT predictions and thus appear to have corrected the underpredictions.

Conclusions for RCS Retention

The RCS retention for CsI is on the order of 70% for both PWRs and BWRs according to the STCP and MAAP calculations[9]. Experimental results from Marviken, SFD, LOFT, and LACE also support such a high retention. So, we assume a retention of 70% for iodine and 70% for all other aerosols. The RCS retentions are summarized in Table 2.7

Because the kinetics and the mechanism of the interaction of the volatile fission products with the RCS gases and on solid structures are complicated and not well

evaporation

*how did these particulates
get into containment
from the coolant?*

Table 2.8: Release Fraction From Core to RCS					
Element	F_s	F_f	F_p	F_F	F_R^i
NG	0.0176	1.0	1.0	1.0	0.0176
I, Br	0.0176	0.9	0.30	0.27	0.0047
Cs	0.0176	0.9	0.30	0.27	0.0047
Te	0.0176	0.23	0.30	0.07	0.0012
Sr, Ba	0.0176	0.01	0.30	0.003	0.0001
Ru	0.0176	0.01	0.30	0.003	0.0001
La	0.0176	0.0001	0.30	0.00003	0.000001
Ce	0.0176	0.0001	0.30	0.00003	0.000001
Other	0.0176	0.0001	0.30	0.00003	0.000001

known, and because of the stochastic nature of the process, it is difficult to identify an accurate prediction of the RCS retention rate. Our choice is a 70% retention of iodine. Thus, a 30% release is conservative compared to the 10% release Mull used. In the TMI-2 accident, nearly 100% retention of iodine was achieved. The primary coolant system of MITR is at low temperature and atmospheric pressure. Therefore, leakage from RCS to the containment is also expected to be lower than that in nuclear power reactors. Thus, our assumption provides a big margin.

2.2.4 Summary of Release Fraction

We use the notation of F_s to represent the fraction of fission products contained in the melted fuel that is available for release, F_f to represent the release fraction from fuel to RCS, and F_p to represent the release fraction from RCS to the containment. Hence $F_p = 1 - \text{RCS retention factor}$. The total fraction of fission product inventory in melted fuel released into the containment is $F_F = F_f \times F_p$. The total fraction of the fission product in the whole core released into the containment is $F_R^i = F_F \times F_s$. These values are summarized in Table 2.8.

2.3 Natural Depletion in Containment

The chemical form of radionuclide releases to the containment would be: The noble gases are gaseous form; iodine is 97% particulate, 2.85% elemental, and 0.15% organic; the remaining nuclides are particulate [9]. This is based on recent experimental data including that from the SFD tests, LOFT, and STEP tests, TMI-2 post accident examination, and the ACE tests as well as an extensive review of the potential chemical reactions in the RCS and containment.

Because the MITR has no containment spray or other engineered safety features to reduce the quantity of fission products in the containment atmosphere, depletion of the radioactive isotopes released to the containment can occur only through natural processes. These include agglomeration, sedimentation, hygroscopicity and diffusio-phoresis. The noble gases are not expected to undergo any of these depletion process thus have a 100% release fraction.

Agglomeration is the process by which the size distribution of airborne particulate tends to shift with time to larger sizes until an equilibrium condition is reached. This process affects the other depletion processes. Sedimentation is deposition due to gravitation. Hygroscopicity is a removal process due to the affinity of the released product for water. As discussed before, Cs and I will enter the containment in the chemical form of CsOH and CsI, both of which are hygroscopic. In an atmosphere near saturation, these substances would be absorbed by water by a large ratio. Diffusiophoresis occurs when steam condenses on a surface, the aerosol particles will migrate with the water vapor moving to the surface and be deposited.

From simulation results[9], the activity in the containment is varying with time. It steadily increases as more fission products are released from the melted core to the containment until it reaches a maximum. Then it drops because of the natural depletion processes described above and leakage. The drop is fast, about a 99% drop of the mass of suspended aerosols in 10000 seconds for BWRs, mainly due to the hygroscopicity effects. Because current regulations require a simultaneous release assumption, we assume the containment activity is at its maximum from the

beginning. Under this assumption, we should also include the natural depletion from the beginning. For a two hour period, we assume the depletion to be 70% for iodine and cesium and 10% for the others.

The fraction of fission products released to the containment which remain airborne in the containment atmosphere will be designated as F_c .

- 100% of the noble gases
- 30% of the I, Cs
- 90% of others

Chapter 3

Atmospheric Release

3.1 Introduction

There are two ways for the isotopes in the containment to be released to the outside. One is through a crack in the containment, which is called containment leakage. The other is through the pressure relief system – stack, which is called stack release. Both are discussed below.

3.2 Release from Pressure Relief System

3.2.1 Release Fraction Through the Stack Filter System

During abnormal conditions, the plenum monitors would trip the exhaust dampers thereby sealing the building automatically. The building could also be sealed manually from the control room. In such a situation, changes in atmospheric pressure and temperature may cause the internal building pressure to rise. If the building pressure should approach its design set-point of 2.0 psig, a safe effective relief can be achieved by use of the pressure relief system which can filter the exhaust air and discharge it to the base of the ventilation exhaust stack above the manually operated exhaust control damper. It was shown in the safety analysis of the system that the pressure relief system can be safely operated during a design basis accident.

The inside diameter of the stack is 0.4318 m at the exit point and the stack height is 46 m.

The building pressure relief exhaust line contains two high-efficiency absolute particulate air filters that are 99.9% efficient for particle sizes of 0.3 microns, and an activated charcoal filter that is 99% efficient for removal of elemental Iodine. The actual system flow would be determined by the difference between the internal building and atmospheric pressure which is assumed to be 2.0 psig. Experimental data show that flow at 2 psig overpressure is 355 cubic feet per minute (cfm) for filter 1 and 330 cfm for filter 2[30]. Thus, the average volumetric flow rate through the stack is $342.5 \text{ ft}^3 \cdot \text{min}^{-1}$.

The fractions penetrating the filters of the pressure relief system are:

- 100% of noble gases and Br.
- 5% of Iodine.
- 50% of all other isotopes.

The total fraction of the initial inventory that is released from the stack is:

$$F_{R,S}^i = F_S^i \cdot F_f^i \cdot F_p^i \cdot F_c^i \cdot F_{filter}^i \quad (3.1)$$

3.2.2 Release Rate

The release rate through the stack $\lambda_{S,L}^i$ is $342.5 \text{ ft}^3 \cdot \text{min}^{-1}$, or $0.1616 \text{ m}^3 \cdot \text{s}^{-1}$ or $3.42 \times 10^{-5} V \cdot \text{s}^{-1}$ (V is the volume of the containment. $V = 4.73 \times 10^3 \text{ m}^3$).

3.2.3 Atmospheric Dispersion Model

Atmospheric dispersion of a pollutant is primarily dependent on (1) meteorological conditions such as ambient temperature, wind speed, time of day, insulation and cloud cover (atmospheric stability), and (2) pollutant stack emission parameters such as gas velocity and temperature. The stability of the atmosphere is determined by the atmospheric thermal gradient, which is called the lapse rate. Neutral stability exists

for a temperature gradient of $-1^{\circ}\text{C}/100$ meters, or a temperature decrease of 1°C for every 100 meters of vertical ascent. Unstable conditions with lapse rates greater than $-1^{\circ}\text{C}/100$ m add to the buoyancy of an emission, and stable conditions (lapse rates less than $-1^{\circ}\text{C}/100$ m) tend to inhibit vertical motion of the pollutant gases (plume). Dispersion from an elevated source(stack) is effected by the mixing and dilution of polluted gases with the atmosphere.

For a stack release, the maximum ground-level concentration in a sector may occur beyond the exclusion area boundary distance. Therefore, for stack releases, the atmospheric relative concentration (χ/Q) values are calculated at various distances.

The basic equation for atmospheric diffusion from an elevated release is [31]:

$$\chi/Q = \frac{1}{\pi \bar{U}_h \sigma_y \sigma_z} \exp\left[-\frac{h_e^2}{2\sigma_z^2}\right] \quad (3.2)$$

where:

χ : ground level concentration (Ci/m³)

Q : pollutant exit rate (Ci/s)

\bar{U}_h : mean wind-speed at the release height, in m/s. (In this calculation, the wind-speed at 10-meter level is used.)

h_e : effective stack height, in m;

σ_y : lateral plume dispersion coefficient, in m;

σ_z : vertical plume dispersion coefficient, in m;

$$h_e = h_s + h_{pr} - h_t - c \quad (3.3)$$

h_s : stack height, in m;

h_{pr} : rise of the plume above the release point, in m;

h_t : maximum terrain height (above the stack base) between the release point and the point for which the calculation is made (≥ 0), in m;

c : when vertical exit velocity is less than 1.5 times the horizontal wind-speed, cor-

rection for down-wash, in m;

$$c = 3(1.5 - W_0/\bar{U}_h)D \quad (3.4)$$

$$h_{pr} = \frac{1.6(F^{1/3})(3.5W)^{2/3}}{\bar{U}_h} \quad (3.5)$$

$$F = 2.45W_0D^2\left(\frac{T_s - T_a}{T_s}\right) \quad (3.6)$$

$$W = 14F^{5/8} \quad (3.7)$$

W_0 : vertical exit velocity of the plume, in m/s;

D : inside diameter of the stack, in m;

T_s : stack temperature in K;

T_a : air temperature in K;

3.2.4 Dispersion Coefficient

Values of dispersion coefficients, which depend on the downwind distance and the atmospheric stability category, can be determined from the Pasquill curves [32] (a set of diffusion coefficient curves versus plume travel distance). In most references, the dispersion coefficients are given as a set of curves over the range of 10^2 to 10^5 meters. It is impossible to extrapolate accurately to the range of the MITR's exclusion area distance, 8 to 25 meters. One alternative is to use the interpolation formulas for σ_y and σ_z developed by Briggs which fit the Pasquill curves[4], see Table 3.1.

3.2.5 Meteorological Data

The meteorological data needed for χ/Q calculation include wind-speed, wind direction, and a measure of atmospheric stability. The meteorological data used in this thesis were recorded at the Boston Station, MA 240BS 93-95. The wind speed data are expressed in the unit of knots (KTS) and one KTS equals 1853 meters/hour. The annual average wind-speed for each stability category in the Boston area is listed in Table 3.2. We can see that class D is the most frequent stability condition, accounting

Table 3.1: Formulas for σ_y and σ_z by Briggs (1973)

Pasquill stability category	$\sigma(x)_y$	$\sigma(x)_z$
A	$0.22x(1 + 0.0001x)^{-1/2}$	$0.20x$
B	$0.16x(1 + 0.0001x)^{-1/2}$	$0.12x$
C	$0.11x(1 + 0.0001x)^{-1/2}$	$0.08x(1 + 0.0002x)^{-1/2}$
D	$0.08x(1 + 0.0001x)^{-1/2}$	$0.06x(1 + 0.0015x)^{-1/2}$
E	$0.06x(1 + 0.0001x)^{-1/2}$	$0.03x(1 + 0.0003x)^{-1}$
F	$0.14x(1 + 0.0001x)^{-1/2}$	$0.016x(1 + 0.0003x)^{-1}$

for 73.9423% of the total events.

3.2.6 Application of Dispersion Model

We introduced the dispersion model in the previous section. Now, we will discuss the resulting χ/Q value and its dependence on the input parameters based on the model.

First, from equation 3-5, we can see that χ/Q is proportional to the inverse of σ_y and the mean wind-speed. This is also shown in Figures 3-1 and 3-2 for class D stability. The effective stack height, h_s , is in the exponential term. Because the flow rate from the stack during an accident is low, we can assume that the effective height equals the stack height (see also Figure 3-3). The buoyant effect of the plume is negligible. The most significant parameter that affects the final χ/Q value is σ_z which is included in both the exponential term and the magnitude term, and thus affects both the shape of the χ/Q distribution and its magnitude. This is shown clearly in Figure 3-4. Because σ_z depends on the atmospheric stability, the distribution of χ/Q also depends on the atmospheric stability. The more unstable an atmospheric condition, the more a pollutant will be deposited in a shorter range with a higher concentration. In contrast, a more stable atmosphere would disperse the pollutant over a wider range and thus result in a lower concentration. From the meteorological data, we can see that in the Boston area, the C,D and E categories account for most of the atmosphere cases.

Table 3.2: Wind-Speed for Each Stability Category (KTS) Averaged Over All Directions

	A	B	C	D	E	F
N	0.0	5.4	7.7	10.3	7.2	4.8
NNE	0.0	6.1	8.2	11.0	6.3	4.5
NE	0.0	5.0	8.4	12.4	6.0	3.8
ENE	5.0	6.3	9.6	11.8	6.5	3.8
E	5.0	6.6	9.8	10.4	6.8	3.8
ESE	5.0	6.2	9.6	10.8	6.9	3.8
SE	4.5	7.1	8.4	9.4	6.3	4.1
SSE	5.0	5.8	7.3	9.0	6.3	4.4
S	1.0	5.0	8.5	10.6	6.6	4.8
SSW	4.5	5.6	9.1	12.1	7.4	5.1
SW	5.0	6.6	9.9	12.0	7.9	5.1
WSW	0.0	6.5	9.7	12.0	8.1	5.3
W	5.0	6.7	9.7	13.2	8.4	5.0
WNW	3.0	6.7	9.0	13.4	8.4	5.0
NW	5.0	6.1	10.0	13.2	8.3	5.0
NNW	4.0	6.5	9.0	12.5	8.2	4.6
avg.	3.8	6.4	9.2	11.9	7.7	4.6
relative freq.(%)	0.00823	1.8254	8.3007	73.9423	12.0338	3.8154

The distribution of the χ/Q is plotted in figure 3-5 for the six stabilities and the probability of each distribution equals the relative frequency of each stability in Table 3.2.

3.2.7 Total Activity Released

Over the two hour release period, the total activity released in Ci from the stack for each isotope is:

$$Q_{t,S}^i = \int_0^{7200} F_{R,S}^i Q_S^i \lambda_L^S e^{-(\lambda_L^S + \lambda_L^G + \lambda_i)t} dt \quad (3.8)$$

$$Q_{t,S}^i = F_{R,S}^i Q_S^i \lambda_L^S \frac{1 - e^{-7200(\lambda_L^S + \lambda_L^G + \lambda_i)}}{\lambda_L^S + \lambda_L^G + \lambda_i} \quad (3.9)$$

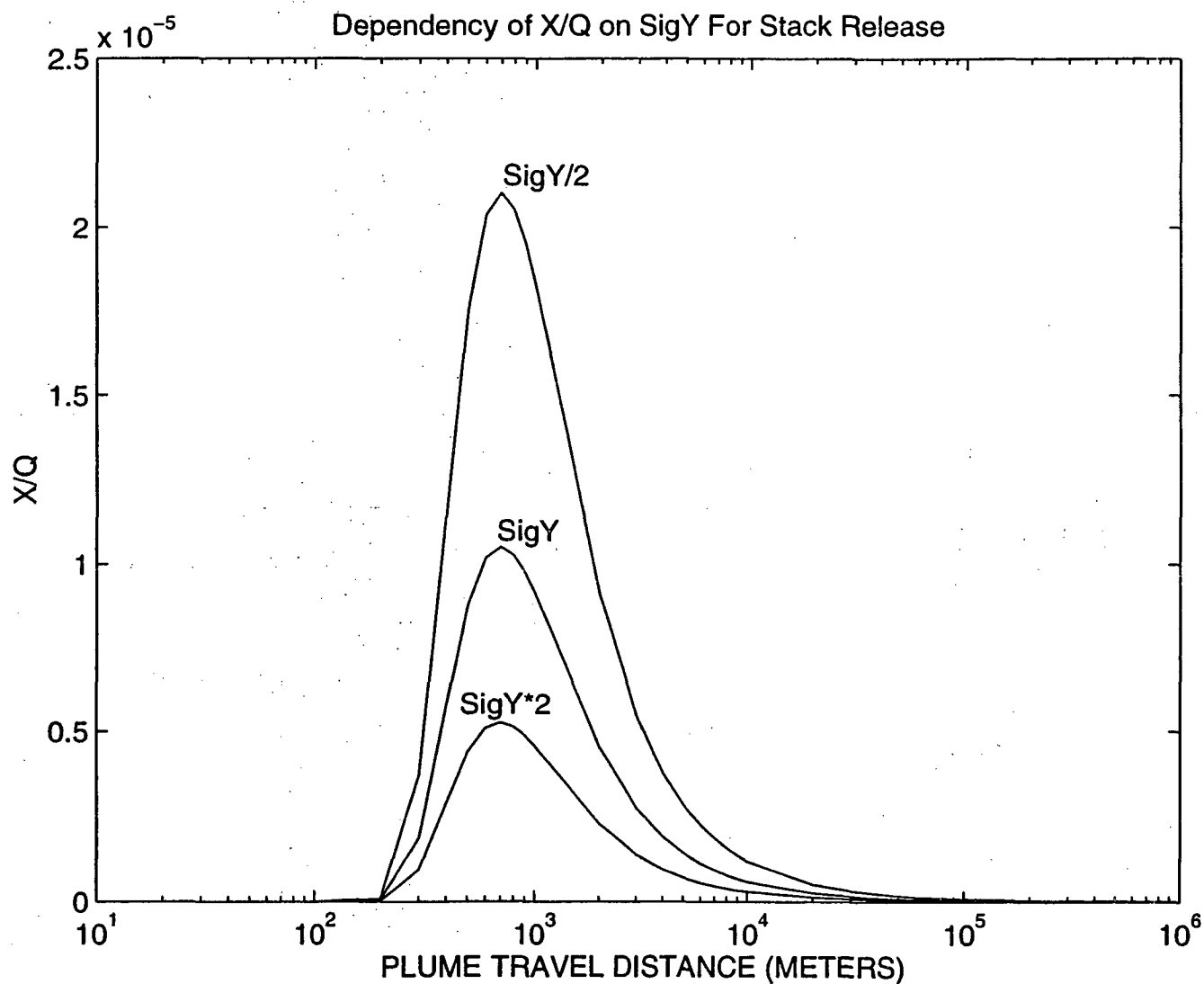


Figure 3-1: Dependency of χ/Q on SigY for stack release under condition of wind-speed = 11.9 KTS, class D stability, $h_s = 46$ m.

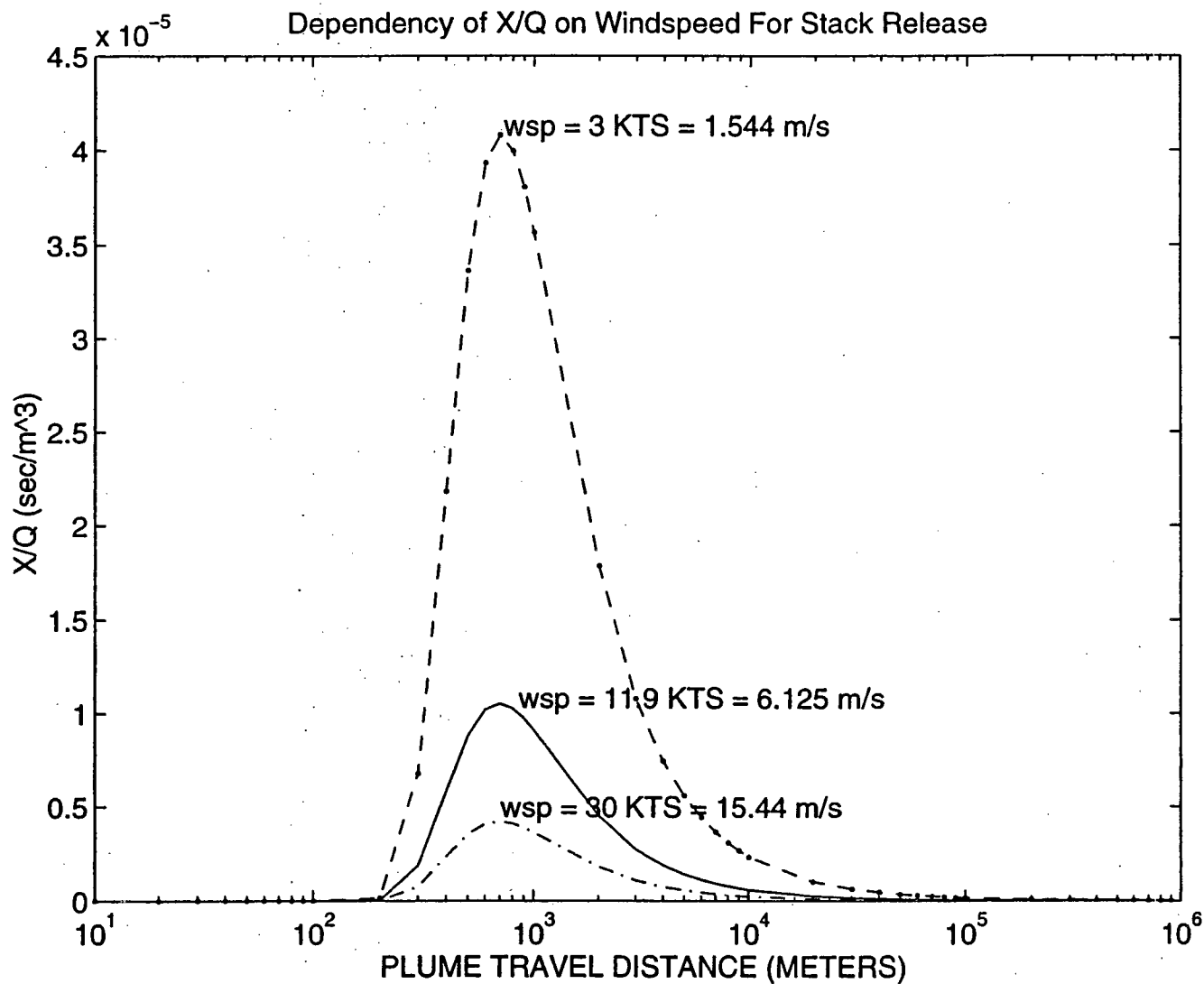


Figure 3-2: Dependency of χ/Q on wind speed for stack release under condition of class D stability, $h_s = 46$ m. The solid line curve is for a wind speed of 11.9 KTS (6.125 m/s), the dash - dot line curve is for a wind speed of 30 KTS (15.44 m/s) and the dash - dash curve is for a wind speed of 3 KTS (1.544 m/s).

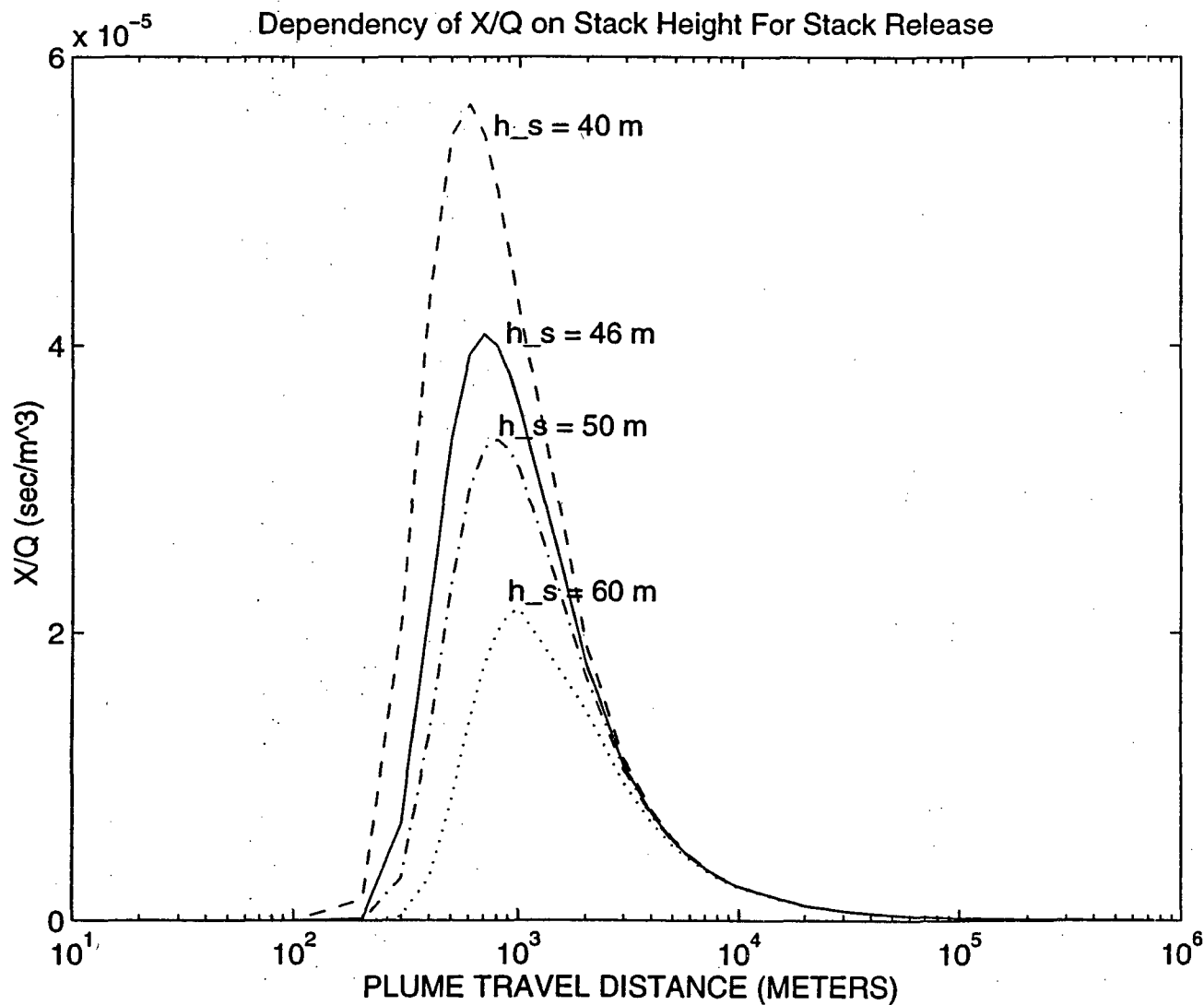


Figure 3-3: Dependency of χ/Q on stack height for stack release under condition of class D stability with a wind speed of 11.9 KTS. The solid line curve is for a stack height of 46 m, the dash - dot line curve is for a stack height of 46 m and the dash - dash curve is for a stack height of 46 m.

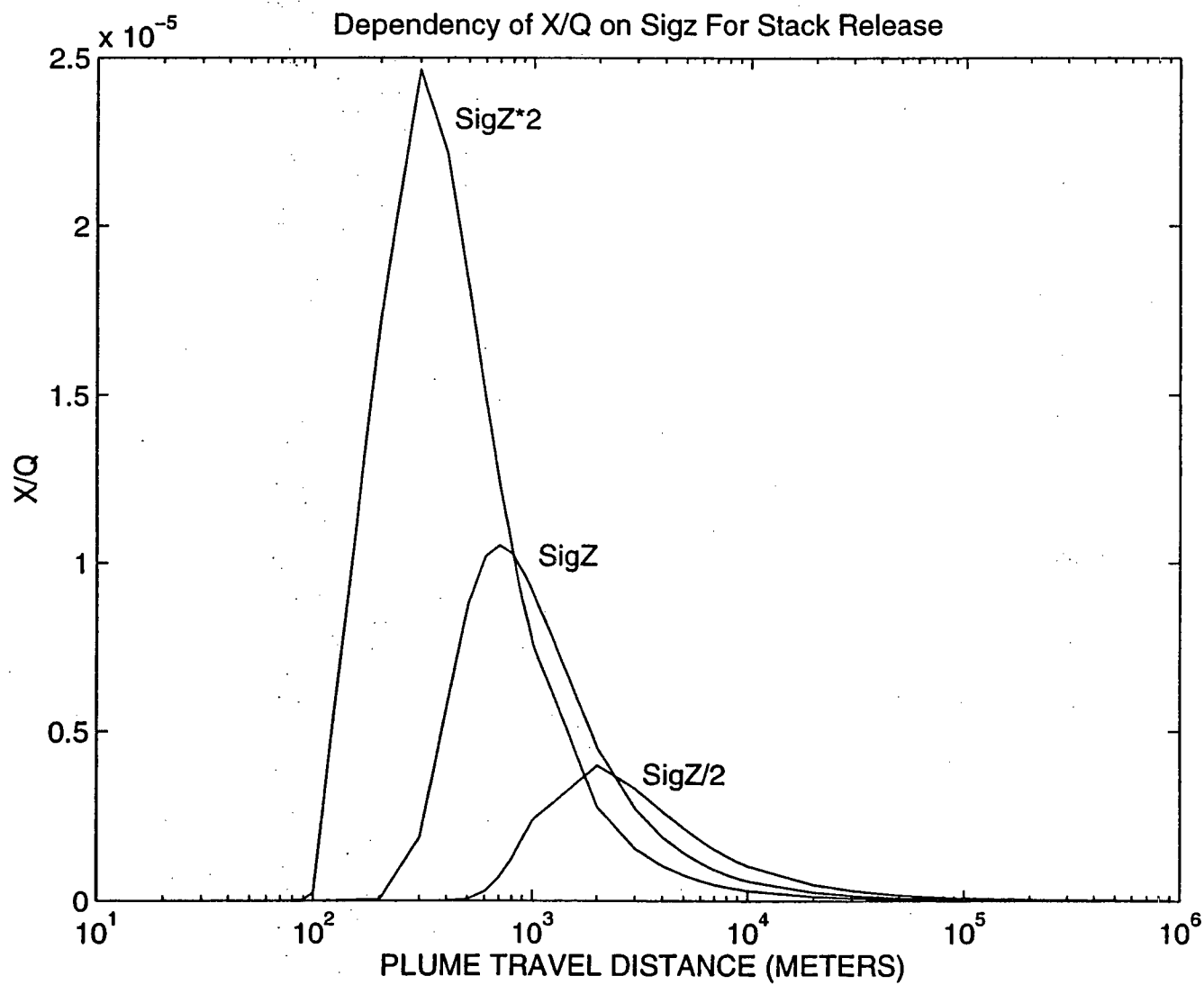


Figure 3-4: Dependency of χ/Q on $\text{Sig}Z$ for stack release under condition of windspeed = 11.9 KTS, class D stability, $h_e = 46$ m.

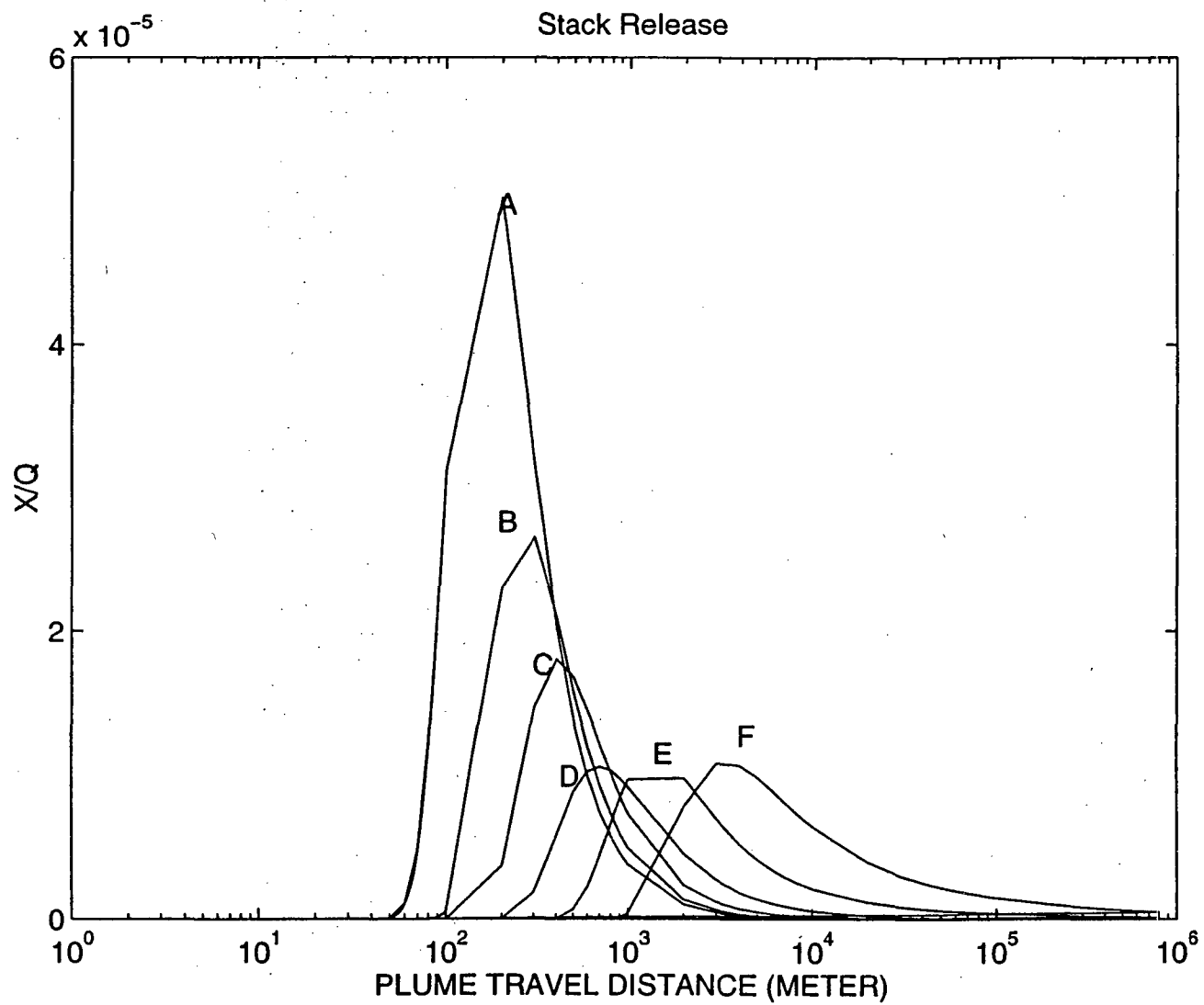


Figure 3-5: χ/Q Distribution as a function of plume distance for each atmospheric condition from stack release.

3.3 Release from Containment Leakage

3.3.1 Leakage Rate

The reactor building is designed to withstand internal pressure of 2.0 psig greater than atmospheric. If the building pressure should approach its design setpoint of 2.0 psig, a safe, effective relief can be achieved by use of the pressure relief system which can filter the exhaust air and discharge it to the ventilation exhaust stack.

The maximum permissible leakage rate is 1% of the building volume per day per psi of building overpressure. An integral air leakage test of the reactor building containment is performed annually with a maximum time of 18 months between tests to ensure above criteria.

When an accident happens, the containment building is assumed to reach its setpoint pressure of 2.0 psig simultaneously. The leakage rate of the building is assumed at its maximum permissible value of 1%. With the above conservative assumptions, the leakage rate, λ_L^G , is

$$\lambda_L^G = 0.02V/\text{day} = 2.3 \times 10^{-7}V/\text{s} \quad (3.10)$$

where V is the volume of containment ($4.73 \times 10^3 \text{ m}^3$).

3.3.2 Atmospheric Dispersion Model

For neutral (D) or stable (E,F, or G) atmospheric stability conditions when the wind-speed at the 10-meter level is less than 6 meters per second, meandering of the horizontal plume may be considered. χ/Q values may be determined by using following equations[31]:

$$\chi/Q = \frac{1}{\bar{U}_{10}(\pi\sigma_y\sigma_z + A/2)} \quad (3.11)$$

$$\chi/Q = \frac{1}{\bar{U}_{10}(3\pi\sigma_y\sigma_z)} \quad (3.12)$$

$$\chi/Q = \frac{1}{\bar{U}_{10}\pi\Sigma_y\sigma_z} \quad (3.13)$$

where χ/Q is relative concentration, in s/m^3 ,

π is 3.1415926,

\bar{U}_{10} is wind-speed at 10meters above plant grade, in m/s ,

σ_y is lateral plume spread, in m ,

σ_z is vertical plume spread, in m ,

Σ_y is lateral plume spread with meandering and building wake effects, in m . For distances of 800 meters or less, $\Sigma_y = M\sigma_y$ where M is determined from Appendix B-1; for distances greater than 800 meters, $\Sigma_y = (M - 1)\sigma_{y800\text{m}} + \sigma_y$, and

A is the smallest vertical-plane cross-sectional area of the reactor building, in m^2 .

The larger value from equation 3.11 and equation 3.12 should then be compared with the value from equation 3.13 and the lower value should be selected as χ/Q .

During all other meteorological conditions, plume meandering should not be considered. The appropriate χ/Q value is the higher value from equation 3.11 and 3.12.

These procedures for calculating χ/Q are conservative. The reason that the higher value of equation 3.11 and 3.12 is chosen is because the NRC specifies that the reduction of χ/Q due to the wake effect can be no more than a factor of three. We call the values derived from these procedures "conservative" values and those from equation 3.11 "exact" values. The resulting doses obtained by using these two methods will be compared.

3.3.3 Application of Diffusion Models

In Figure 3-6 the resulting χ/Q from the "conservative" calculation is shown for each stability class and in Figure 3-7 the resulting χ/Q from the "exact" calculation is shown for each stability class. The difference is obvious. For our case, where the plume distances are small (smaller than 100 meters), the wake effect from the containment building would be strong. Thus it would be justifiable to use the "exact" equation instead of the "conservative" method.

Figure 3-7 shows that only in class A stability would the χ/Q value exceed that in class F stability. Class A has frequency of occurrence of less than 1%. Therefore, calculation of the dose for class F stability would give a conservative estimate of the dose with frequency greater than 99%.

3.3.4 Total Activity Release

Over the two hour release period, the total activity released in Ci from the stack for each isotope is:

$$Q_{t,G}^i = \int_0^{7200} F_{R,S}^i Q_S^i \lambda_L^G e^{-(\lambda_L^S + \lambda_L^G + \lambda_i)t} dt \quad (3.14)$$

$$Q_{t,G}^i = F_{R,S}^i Q_S^i \lambda_L^G \frac{1 - e^{-7200(\lambda_L^S + \lambda_L^G + \lambda_i)}}{\lambda_L^S + \lambda_L^G + \lambda_i} \quad (3.15)$$

3.4 Adjustment of the Release Term Outside the Containment

Reduction due to decay, ground deposition, and precipitation scavenging of the fission products after leaving the containment can be conservatively neglected.

3.5 External Gamma Dose from Plume

It is assumed that the plume is infinitely large in calculating the external doses. This assumption simplifies the computations and gives conservative results. Consider a hemispherical uniform cloud with infinite radius located above ground level, containing a radionuclide with a concentration of χ Ci/m³, emitting gamma rays with an average energy of \bar{E} MeV. The exposure rate (R/s) to the center point is[33]:

$$\gamma^X = 0.262 \bar{E} \chi \quad (3.16)$$

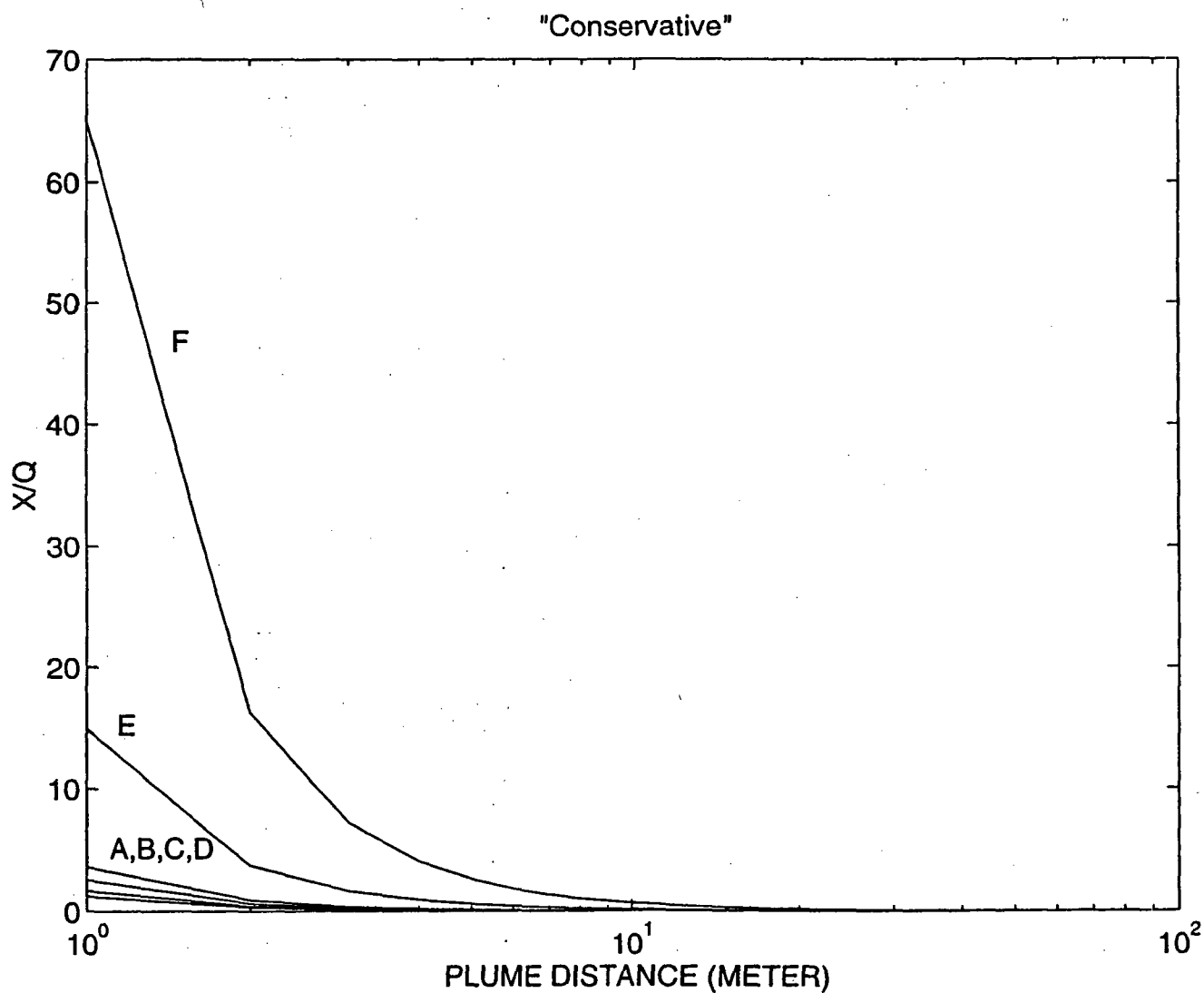


Figure 3-6: χ/Q Distribution as a function of plume distance for each atmospheric condition from containment leakage using "conservative" calculation. A, B, C, D, E and F in the figure stand for the atmospheric stability classes.

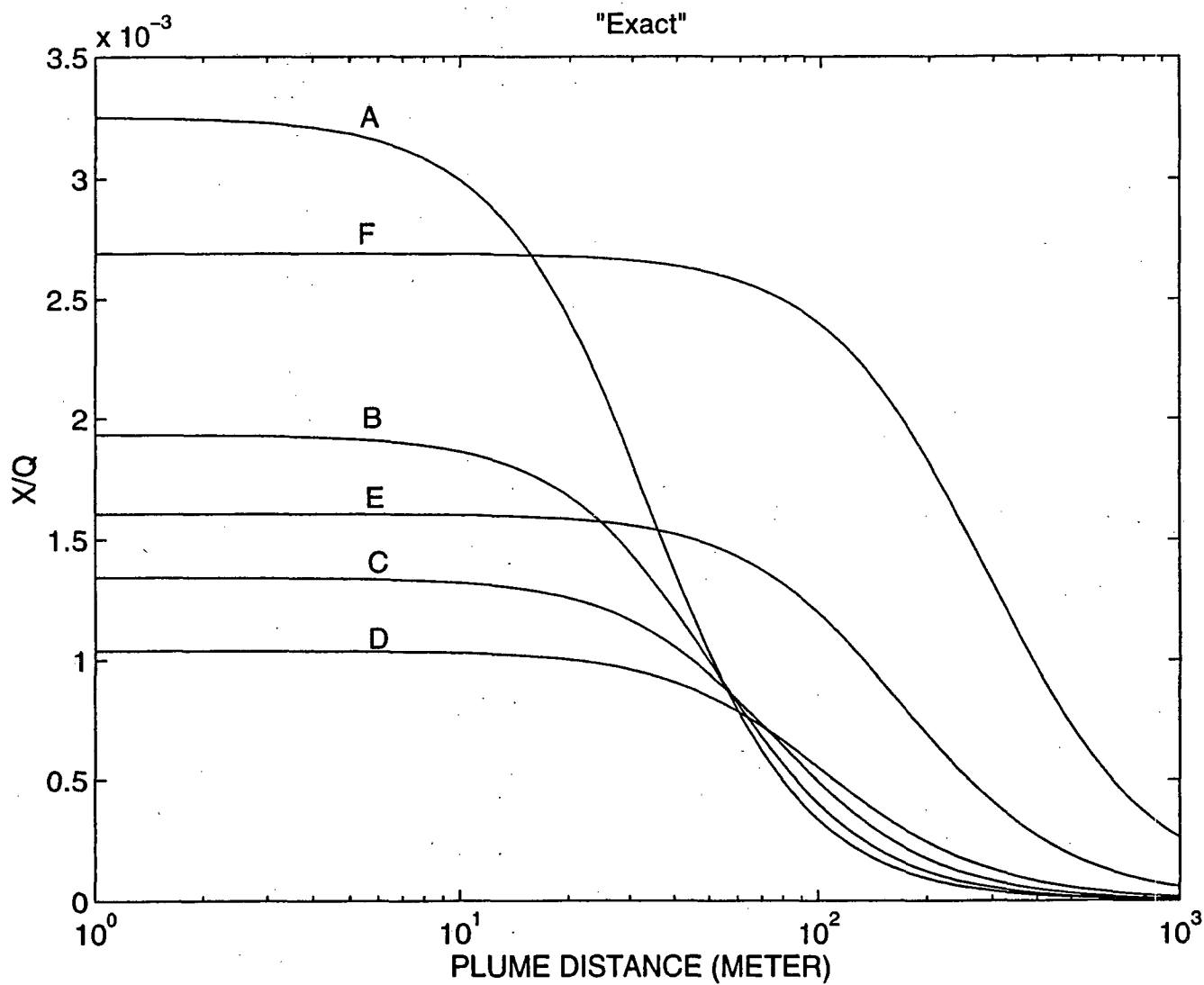


Figure 3-7: χ/Q Distribution as a function of plume distance for each atmospheric condition from containment leakage using "exact" calculation. A, B, C, D, E and F in the figure stand for the atmospheric stabilities.

Thus the total exposure in roentgen due to isotope i is :

$$\gamma_i^X = 0.262 \bar{E}_\gamma^i Q_T^i (\chi/Q) \quad (3.17)$$

The \bar{E}_γ^i are obtained by evaluating the gamma energy spectrum of each isotope. To obtain the dose equivalent, γ_i^X must be multiplied by the f-factor, which converts the roentgen to dose in tissue, and by the quality factor, which converts rad to rem. Both of the factors are approximately unity, so that

$$\gamma_i^H = 0.262 \bar{E}_\gamma^i Q_T^i (\chi/Q) \text{ rem} \quad (3.18)$$

Another method was developed by using computer-generated conversion factors [4]:

$$\gamma_i^H = C_\gamma^i Q_T^i (\chi/Q) \quad (3.19)$$

where C_γ^i is photon dose conversion factor for immersion in contaminated air due to isotope i, in rem per Ci-s/m³.

For those isotopes whose C_γ^i are not available, equation 3.17 is used to determine the gamma dose. All the parameters used in the calculation of the gamma dose are listed in Appendix A.3.

The estimated total gamma exposure distribution with distance due to all isotopes from containment leakage (from "exact" model) is illustrated in Fig 3-9 and from stack release is illustrated in Fig 3-8. In the stack release, only the results for 10 MW are plotted and the stabilities of classes C, D and E, the total frequency of which are around 94%. For comparison, the "conservative" values from containment releases are illustrated in Fig. 3-10.

3.6 Beta Dose

The dose rate in air from an infinite uniform cloud of beta radiation is determined from [33]:

$$\beta^D = \frac{87.5}{100} \times 0.262 \bar{E}_\beta \chi = 0.229 \bar{E}_\beta \chi \text{ rad/s} \quad (3.20)$$

where,

β^D : Beta dose rate (rad/s)

\bar{E}_β : Average beta energy per disintegration (MeV/dis)

χ : Concentration of beta-emitting isotope (Ci/m³).

The dose equivalent rate in tissue is then given by

$$\beta^H = 0.229 \bar{E}_\beta \chi \times f(d, E_{\max}) \text{ rem/s} \quad (3.21)$$

where f is an experimentally determined function of d , the distance into the tissue, and E_{\max} , the maximum energy of the emitted β rays. The dose rate is largest at the surface of the skin, where $f = 1$, and decreases rapidly with distance into the tissue. To be conservative, the external dose due to the β plume is computed with $f = 1$. The total beta dose equivalent in rem in two hours is :

$$\beta^H = 0.229 \bar{E}_\beta \int \chi(t) dt \quad (3.22)$$

The χ (in Ci/m³) can be related to the previously determined χ/Q value by the relationship

$$\chi(t) = (\chi/Q) Q(t) \quad (3.23)$$

which when integrated yields :

$$\int \chi(t) dt = (\chi/Q) \int Q(t) dt = (\chi/Q) Q_T \quad (3.24)$$

The total beta dose equivalent(in rem) received due to isotope i is therefore:

$$\beta_i^H = 0.23 \bar{E}_\beta^i Q_T^i (\chi/Q) \quad (3.25)$$

The value of \bar{E}_β^i equals one-third the value of the maximum beta energy for isotope

i and are listed in Appendix A.3.

The estimated two hour total beta dose equivalent distribution with distance due to all isotopes from containment leakage (using the "exact" model) is illustrated in Fig 3-9 and from stack release is illustrated in Fig 3-8. In the stack release, only the results for 10 MW are plotted and the stabilities include classes C, D and E, the total frequency of which are around 94%. The "conservative" values from containment releases are illustrated in Fig. 3-10 for comparison.

3.7 Thyroid Dose

The thyroid dose equivalent is calculated according to WASH-1400[4]:

$$T_i^H = B_r C_T^i Q_T^i (\chi/Q) \quad (3.26)$$

where

T_i^H : Dose to thyroid from isotope i (rads),

B_r : Breathing rate (m^3/s),

C_T^i : Thyroid inhalation conversion factor for isotope i (rem per Ci inhaled) in 0-2 days. The values are listed in Appendix A.3.

Isotopes of interest which are not included in WASH-1400 were checked against ICRP Report #2 [34] and found to have no contribution to the thyroid dose. The standard breathing rate for the calculation of internal dose is $3.47 \times 10^{-4} m^3/s$ [31].

The estimated total thyroid dose distribution with distance due to all isotopes from containment leakage(from the "exact" model) is illustrated in Fig 3-9 and from stack release is illustrated in Fig 3-8. In the stack release, the results for 10 MW are plotted for stability classes C, D and E, the total frequency of which is around 94%. For comparison, the "conservative" values from containment release are illustrated in Fig. 3-10

Table 3.3: Total containment leakage dose (rem) in two hours using “exact” atmosphere dispersion model

Power(MW)	Beta Dose(rem)	Gamma Dose(rem)	Thyroid Dose(rem)
Dose at 8 m			
5.0	0.0054	0.0084	0.1121
6.0	0.0065	0.0101	0.1346
7.0	0.0076	0.0118	0.1570
8.0	0.0087	0.0135	0.1794
9.0	0.0098	0.0152	0.2018
10.0	0.0109	0.0168	0.2246
Dose at 21 m			
5.0	0.0054	0.0084	0.1116
6.0	0.0065	0.0101	0.1339
7.0	0.0076	0.0117	0.1562
8.0	0.0086	0.0134	0.1786
9.0	0.0097	0.0151	0.2009
10.0	0.0108	0.0168	0.2235

3.8 Summary

The beta, gamma, and thyroid doses at the front and back fence for MITR at power levels of 5MW up to 10 MW are listed in Tables 3.3 and 3.4. The former were obtained using the “exact” atmospheric dispersion model and the latter by using the “conservative” atmospheric dispersion model. Even in the latter, the doses are well within the limitation of 25 rem for whole body dose and 300 rem for thyroid dose. Because of the short distance of the exclusion area, the wake effect of the atmospheric dispersion should be dominant, and hence the “exact” values are more reasonable for MITR.

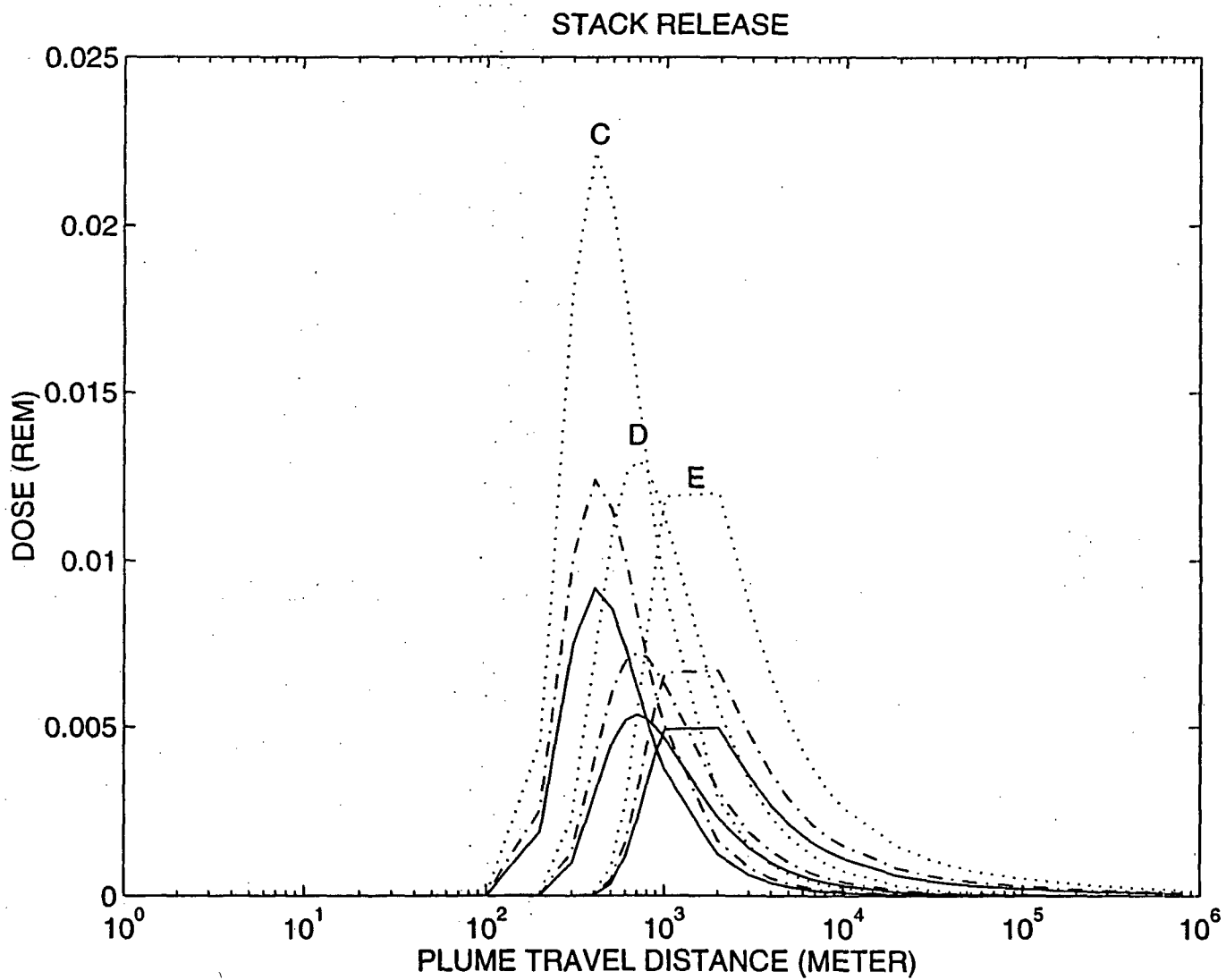


Figure 3-8: Two hour stack release showing beta-Dose, gamma dose and thyroid dose versus distance. Dotted line is thyroid dose, dot-dash line is gamma dose, and solid line is beta dose. C, D and E is the respective atmospheric stability.

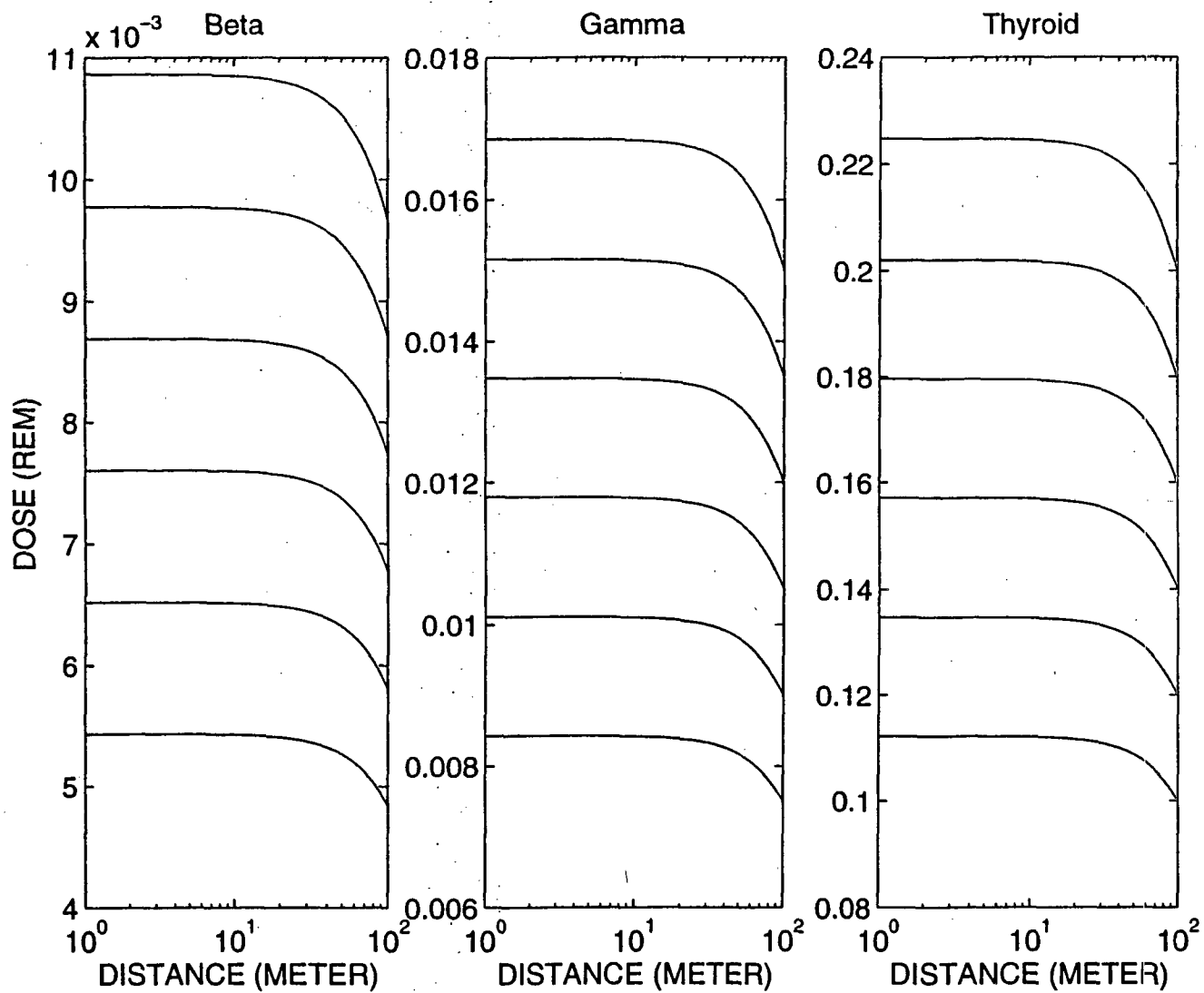


Figure 3-9: Two hour containment leakage beta-dose, gamma dose and thyroid dose vs. distance using exact calculation.

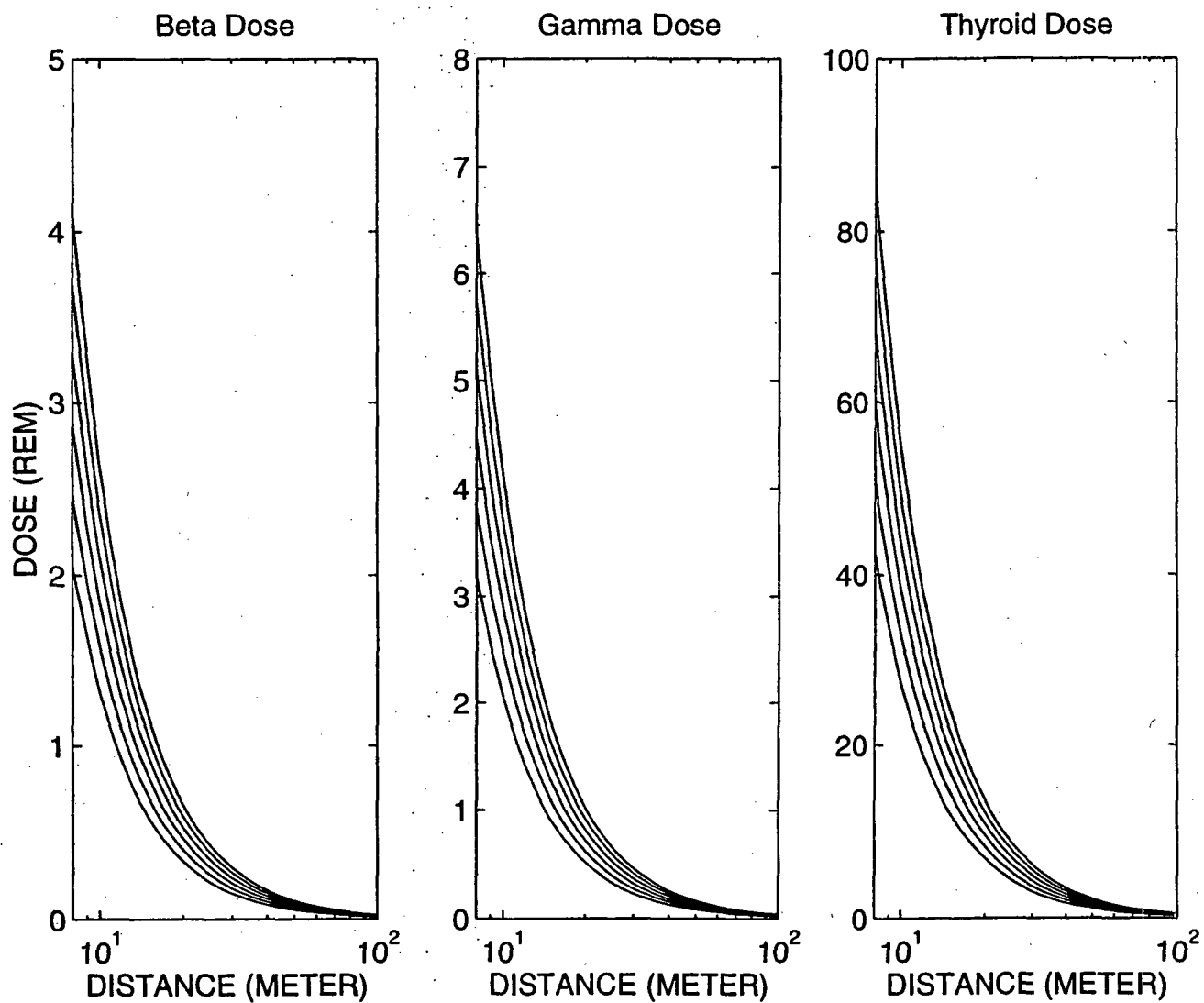


Figure 3-10: Two hour containment leakage beta-dose, gamma dose and thyroid dose vs. distance using conservative calculation. Different lines in each plot are for different power levels.

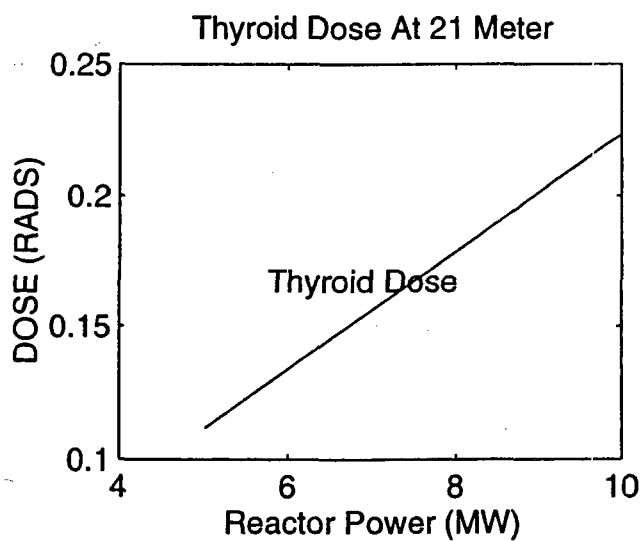
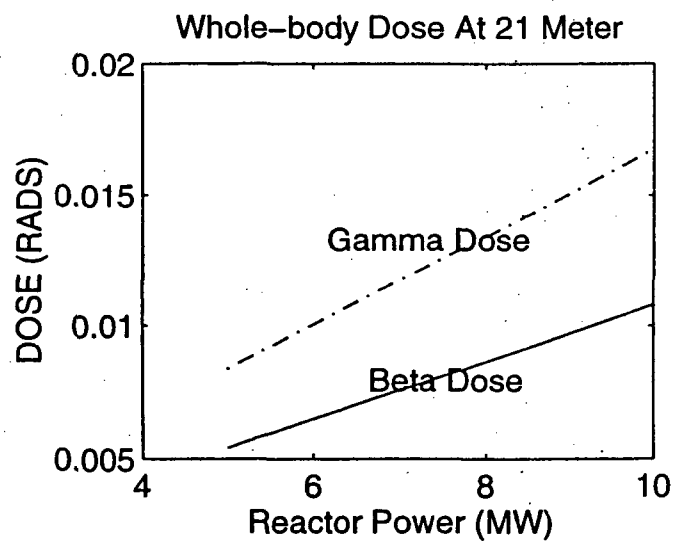
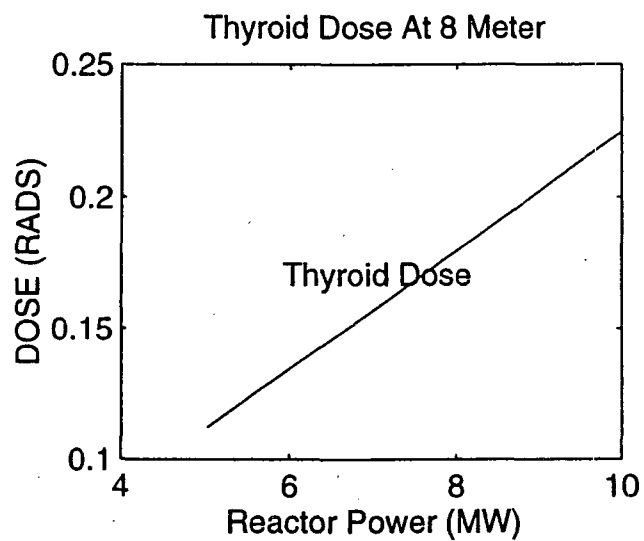
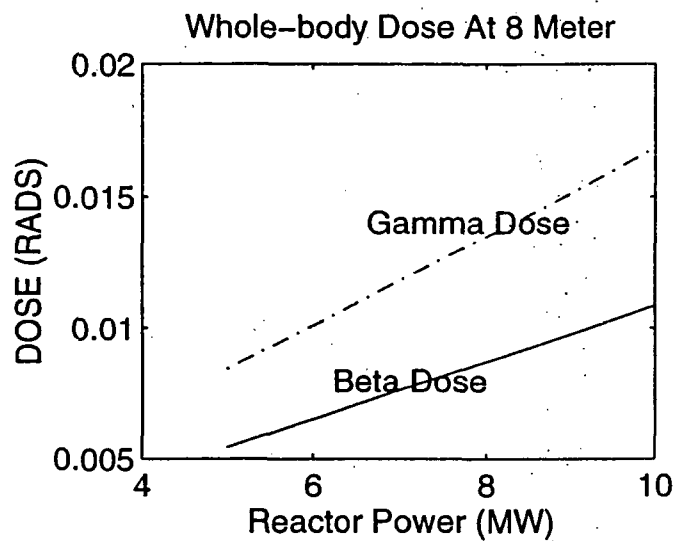


Figure 3-11: Two hour containment leakage whole-body dose(rem) and thyroid dose(rem) vs. reactor power for "exact" model.

Table 3.4: Total Containment Leakage Dose (rem) in two hours Using "Conservative" Atmospheric Dispersion Model

Power(MW)	Beta Dose(rem)	Gamma Dose(rem)	Thyroid Dose(rem)
Dose at 8 m			
5.0	2.0559	3.1888	42.4761
6.0	2.4670	3.8265	50.9713
7.0	2.8782	4.4643	59.4665
8.0	3.2894	5.1020	67.9617
9.0	3.7006	5.7398	76.4570
10.0	4.1117	6.3778	85.0591
Dose at 21 m			
5.0	0.2997	0.4649	6.1923
6.0	0.3597	0.5578	7.4308
7.0	0.4196	0.6508	8.6693
8.0	0.4795	0.7438	9.9077
9.0	0.5395	0.8368	11.1462
10.0	0.5994	0.9298	12.4002

Chapter 4

Direct Gamma Dose, Scattered Gamma Dose, and Gamma Dose Through the Truck Lock

4.1 General

Those isotopes that do not leak from the containment will constitute a source of gamma radiation. The gamma dose at the exclusion boundary from the isotopes retained within the containment building includes the penetration or direct gamma dose, the scattered gamma dose, and the gamma dose through the truck lock.

The containment building shield consists of two parts. One is the sides which are shielded by concrete and steel. The other is the dome which is shielded only by steel. This would result in two sets of dose for both the direct gamma dose and the scattered dose.

The methods used in this chapter are the same as those used by Mull[3]. A brief summary of the methods and the results calculated from the methods are provided.

4.2 Gamma Source Term

Those isotopes that are deposited in the containment and those that remain airborne in the containment would contribute to the direct and scattered gamma dose.

The initial quantity of fission product i airborne in the containment is equal to $F_s^i F_R^i Q_s^i$. This will be reduced over time due to leakage and decay. The quantity which deposits inside the containment is equal to $F_s^i F_R^i (1 - F_c^i) Q_s^i$ or $\frac{1 - F_c^i}{F_c^i} F_R^i Q_s^i$. This would be reduced over time due to decay only.

The time-dependent containment inventory of fission product i for direct and scattered gamma dose is therefore:

$$Q_c^i(t) = F_R^i Q_s^i [e^{-(\lambda_L + \lambda_i)t} + (\frac{1}{F_c^i} - 1)e^{-\lambda_i t}] \quad (4.1)$$

where Q_c^i is in Curies.

The total number of decay emissions from isotope i over the two hour period is given by:

$$Q_{cT}^i(t) = (3.7 \times 10^{10}) \int_0^{7200} Q_c^i(t) dt \quad (4.2)$$

which, after integration, gives

$$Q_{cT}^i(t) = (3.7 \times 10^{10}) F_R^i Q_s^i \left[\frac{1 - e^{-(\lambda_L + \lambda_i)7200}}{\lambda_L + \lambda_i} + (\frac{1}{F_c^i} - 1) \frac{1 - e^{-\lambda_i 7200}}{\lambda_i} \right] \quad (4.3)$$

The energy and abundance of each isotope's gamma decay spectrum are also shown in Table A.5. For convenience, photons have been grouped into discrete energies following a logarithmic scale, with individual photons being allocated to the closest energy.

The total number of emissions of each energy is then equal to the product of the number of emissions, Q_{cT}^i , for each isotope and the photon abundance for that isotope at that energy, summed over all isotopes. The resulting total number of gamma emissions for each energy is divided by the containment volume and duration

Table 4.1: Average Containment Volume Source Strength

E (MeV)	Average Volume Source Strength (Photons/cm ³ - s)					
	5 MW	6MW	7MW	8MW	9MW	10MW
0.03	3.06E+02	3.67E+02	4.29E+02	4.90E+02	5.51E+02	6.12E+02
0.04	1.65E-02	1.98E-02	2.31E-02	2.64E-02	2.97E-02	3.30E-02
0.05	1.92E+02	2.30E+02	2.68E+02	3.06E+02	3.45E+02	3.84E+02
0.06	1.39E+02	1.67E+02	1.95E+02	2.23E+02	2.51E+02	2.79E+02
0.08	1.11E+04	1.34E+04	1.56E+04	1.78E+04	2.01E+04	2.23E+04
0.10	5.67E+00	6.80E+00	7.94E+00	9.07E+00	1.02E+01	1.14E+01
0.15	6.93E+03	8.32E+03	9.71E+03	1.11E+04	1.25E+04	1.39E+04
0.20	6.39E+03	7.67E+03	8.94E+03	1.02E+04	1.15E+04	1.28E+04
0.30	7.47E+03	8.97E+03	1.05E+04	1.20E+04	1.34E+04	1.49E+04
0.40	1.65E+04	1.78E+04	1.91E+04	2.04E+04	2.17E+04	2.30E+04
0.50	1.08E+04	1.30E+04	1.52E+04	1.73E+04	1.95E+04	2.17E+04
0.60	2.33E+04	2.79E+04	3.26E+04	3.72E+04	4.19E+04	4.66E+04
0.80	3.55E+04	4.26E+04	4.97E+04	5.68E+04	6.39E+04	7.10E+04
1.00	4.31E+03	5.18E+03	6.04E+03	6.90E+03	7.77E+03	8.63E+03
1.50	6.81E+03	8.17E+03	9.53E+03	1.09E+04	1.23E+04	1.36E+04
2.00	1.04E+04	1.25E+04	1.45E+04	1.66E+04	1.87E+04	2.08E+04
3.00	1.07E+03	1.28E+03	1.50E+03	1.71E+03	1.93E+03	2.14E+03
4.00	3.35E+01	4.02E+01	4.69E+01	5.36E+01	6.03E+01	6.69E+01

of release to obtain the time-averaged total containment volumetric strength, S_{VT} . Values of S_{VT} for each energy E are listed in Table 4.1.

4.3 Direct Gamma Dose

In order to calculate the direct gamma dose at a given point on the ground outside the containment, the containment is divided into two parts (see Appendix B-2). Part one is all locations from which gamma rays will reach the target point through the steel dome. The corresponding volume is designated as V_1 . Part two is all locations from which gamma rays will have to penetrate the concrete shielding to reach the target point. This part's volume is designated as V_2 . The values of V_1 and V_2 are determined for the back fence (8 m) and the front fence (21 m) as[3]:

$$V_1(8) = 0.01V$$

$$V_1(21) = 0.05V$$

$$V_2(8) = 0.99V$$

$$V_2(21) = 0.95V$$

4.3.1 Steel Shell Penetration Gamma Dose

For simplicity, we make two approximations here. First, the radioactive isotopes are distributed uniformly in the containment. Second, the volume V_1 is approximated to be a sphere. Then, the spherical volume source of constant strength S_V (photons/cm³-s) can be approximated by a disk of the same radius (R_1) having a surface source strength

$$S_A = \frac{4}{3}R_1S_V \quad (4.4)$$

located at a self-absorption distance z [35]. If it is assumed that the containment atmosphere is primarily air, then self-absorption will be small and it is conservative to assume $z = 0$.

The unscattered flux at a point lying behind a parallel shielding slab from this disk source is (in photons/cm²-s)[36]:

$$\phi_\gamma = \frac{BS_{A1}}{2} \int_{b_1}^{b_1 \sec \theta_1} \frac{e^{-t}}{t} dt \quad (4.5)$$

By introducing the E_n functions defined by the integral:

$$E_n(x) = x^{n-1} \int_x^\infty \frac{e^{-t}}{t^n} dt \quad (4.6)$$

the flux can be expressed as:

$$\phi_\gamma = \frac{BS_{A1}}{2} [E_1(b_1) - E_1(b_1 \sec \theta_1)] \quad (4.7)$$

where

ϕ_γ = photon flux (photons/cm²-s)

B = buildup factor

S_{A_1} = surface source strength for volume V_1 and energy E (photons/cm² - s)

$b_1 = \mu_{ST} T_{ST}$ (number of mean free paths in the steel shield)

μ_{ST} = linear attenuation coefficient for steel (cm⁻¹)

T_{ST} = steel thickness (cm)

For the derivation of above equations, please see reference [3][35]. Substituting the S_A , the flux becomes

$$\phi_\gamma = \frac{2}{3} BR_1 S_{V_1} [E_1(b_1) - E_1(b_1 \sec \theta_1)] \quad (4.8)$$

Buildup and attenuation in the air will be neglected. Both effects are small and tend to cancel each other. Values of μ_{ST} and subsequent values of b_1 are shown in Appendices A.5 and A.6.

The dose at P is determined using the conversion factor C_D :

$$Dose = C_D \phi_\gamma \quad (4.9)$$

where

$$C_D = \frac{(1 \text{ rem/rad})(E \text{ MeV/photon})(1.6 \times 10^{-6} \text{ ergs/MeV})(\mu_a \text{ cm}^2/\text{g})(7200 \text{ s})}{100 \text{ ergs/g - rad}} \quad (4.10)$$

which reduces to

$$C_D = 1.15 \times 10^{-4} E \mu_a \quad (4.11)$$

where μ_a is true energy absorption coefficient in air (cm²/g). Substituting C_D and ϕ_γ into Eq. 4.9, the dose (in rem) becomes

$$Dose = 7.67 \times 10^{-5} E \mu_a BR_1 S_{V_1} [E_1(b_1) - E_1(b_1 \sec \theta_1)] \quad (4.12)$$

For computational purposes it is convenient to express the buildup factor as a mathematical function. One of the most useful forms is the sum of exponentials[37], namely:

$$B = Ae^{-\alpha_1 \mu T} + (1 - A)e^{-\alpha_2 \mu T} \quad (4.13)$$

in which A , α_1 , and α_2 are functions of energy. Values of A , α_1 , and α_2 are listed in Appendix A.8. Substituting the expression for B into the equation for $E_1(b)$ and integrating, the result is

$$E_1(b_1) = AE_1(b'_1) + (1 - A)E_1(b''_1) \quad (4.14)$$

where

$$b'_1 = (1 + \alpha_1)b_1$$

$$b''_1 = (1 + \alpha_2)b_1$$

For $\delta \ll 1$ and $b > 0$, below relation would hold [37]:

$$E_1(b) - E_1[b(1 + \delta)] = \delta e^{-b} \quad (4.15)$$

Let $(1 + \delta) = \sec\theta$, the final result would be[3]:

$$D = 7.67 \times 10^{-5} E \mu_a R_1 S_{V_1} [A(\sec\theta_1 - 1)e^{-b'_1} + (1 - A)(\sec\theta_1 - 1)e^{-b''_1}] \quad (4.16)$$

Assuming the fission products are uniformly distributed in the containment, the volume relations lead to the source strength relations:

$$S_{V_1}(8) = 0.01 S_{V_T}$$

$$S_{V_1}(21) = 0.05 S_{V_T}$$

The scattering geometry parameters are:

$$8 \text{ m} : \theta_1 = 0.179 \text{ radians; } R_1 = 2.25 \times 10^2 \text{ cm,}$$

$$21 \text{ m} : \theta_1 = 0.169 \text{ radians; } R_1 = 3.90 \times 10^2 \text{ cm.}$$

The resulting doses are listed in Tables 4.2 and 4.3. For $E < 0.5$ MeV, where the Taylor coefficients are not available, appropriate tabulated point buildup factor data are used (Appendix A.6). The dose can be determined approximately by:

$$Dose = 7.67 \times 10^{-5} E \mu_a R_1 S_{V_1} B(\sec\theta_1 - 1)e^{-b'_1} \quad (4.17)$$

Table 4.2: Steel Dome Penetration Doses (rem) at 8 Meters

E (MeV)	5 MW	6MW	7MW	8MW	9MW	10MW
0.10	8.41E-09	1.01E-08	1.18E-08	1.35E-08	1.51E-08	1.69E-08
0.15	3.81E-05	4.58E-05	5.34E-05	6.10E-05	6.87E-05	7.64E-05
0.20	6.92E-05	8.30E-05	9.69E-05	1.11E-04	1.25E-04	1.38E-04
0.30	1.32E-04	1.59E-04	1.85E-04	2.12E-04	2.38E-04	2.64E-04
0.40	4.19E-04	4.51E-04	4.84E-04	5.17E-04	5.50E-04	5.83E-04
0.50	4.02E-04	4.82E-04	5.63E-04	6.43E-04	7.23E-04	8.04E-04
0.60	1.04E-03	1.25E-03	1.46E-03	1.67E-03	1.88E-03	2.09E-03
0.80	2.10E-03	2.52E-03	2.94E-03	3.36E-03	3.78E-03	4.19E-03
1.00	3.09E-04	3.71E-04	4.33E-04	4.95E-04	5.56E-04	6.18E-04
1.50	6.69E-04	8.02E-04	9.36E-04	1.07E-03	1.20E-03	1.34E-03
2.00	1.24E-03	1.49E-03	1.74E-03	1.99E-03	2.24E-03	2.48E-03
3.00	1.68E-04	2.02E-04	2.35E-04	2.69E-04	3.03E-04	3.36E-04
4.00	6.40E-06	7.69E-06	8.97E-06	1.02E-05	1.15E-05	1.28E-05
Total	6.60E-03	7.87E-03	9.13E-03	1.04E-02	1.17E-02	1.29E-02

Doses for $E < 0.10$ have not been determined because buildup factor data for steel in this energy range is not available and the increasing attenuation at lower energies makes the dose at these energies negligible.

4.3.2 Shadow Shield Penetration Gamma Dose

The dose due to isotopes in V_2 can be obtained by approximating the source as a right circular cylinder volume source with a radius of R_2 and a height of h_2 shielded by a slab shield of thickness of b_2 .

For this situation the flux at point P is given by [37]:

$$\phi_\gamma = \frac{BR_2S_{V_2}}{2\pi} G(k, p, \mu_s R_2, b_2) \quad (4.18)$$

where:

$$k = \frac{h_2}{R_2}$$

$$p = \frac{s}{R_2} \text{ (must be } \geq 1.25\text{)}$$

μ_s = linear attenuation coefficient in the source medium (cm^{-1})

$b_2 = \mu_c T_c + \mu_{ST} T_{ST}$ = total shadow shield thickness in mean free paths

Table 4.3: Steel Dome Penetration Doses (rem) at 21 Meters

E (MeV)	5 MW	6MW	7MW	8MW	9MW	10MW
0.10	6.49E-08	7.78E-08	9.08E-08	1.04E-07	1.17E-07	1.30E-07
0.15	2.94E-04	3.53E-04	4.12E-04	4.71E-04	5.30E-04	5.89E-04
0.20	5.34E-04	6.40E-04	7.47E-04	8.54E-04	9.61E-04	1.07E-03
0.30	1.02E-03	1.22E-03	1.43E-03	1.63E-03	1.84E-03	2.04E-03
0.40	3.23E-03	3.48E-03	3.74E-03	3.99E-03	4.24E-03	4.50E-03
0.50	3.10E-03	3.72E-03	4.34E-03	4.96E-03	5.58E-03	6.20E-03
0.60	8.05E-03	9.67E-03	1.13E-02	1.29E-02	1.45E-02	1.61E-02
0.80	1.62E-02	1.94E-02	2.27E-02	2.59E-02	2.91E-02	3.24E-02
1.00	2.38E-03	2.86E-03	3.34E-03	3.81E-03	4.29E-03	4.77E-03
1.50	5.16E-03	6.19E-03	7.22E-03	8.25E-03	9.28E-03	1.03E-02
2.00	9.58E-03	1.15E-02	1.34E-02	1.53E-02	1.72E-02	1.92E-02
3.00	1.30E-03	1.56E-03	1.82E-03	2.08E-03	2.33E-03	2.59E-03
4.00	4.94E-05	5.93E-05	6.92E-05	7.90E-05	8.89E-05	9.87E-05
Total	5.09E-02	6.07E-02	7.05E-02	8.02E-02	9.00E-02	9.98E-02

G = attenuation function

Then the dose is given by multiplying the flux by a conversion factor C_D :

$$Dose = \frac{1.15 \times 10^{-4} E \mu_a B R_2 S_{V_2}}{2\pi} G(k, p, \mu_s R_2, b_2) \quad (4.19)$$

There is no tabulated buildup factor for a laminated shield. To find the exact buildup factor for a laminated shield, complicated numerical methods have to be used to solve the Boltzmann transport equation, with appropriate boundary conditions. However, it is found that the buildup factor is largely determined by the total number of mean free paths and is characteristic of the material in the outmost region if that is at least two or three mean free path in thickness. If the outmost single region is not thick, the buildup factor for the materials constituting the outmost two or three mean free paths can be chosen. From Appendix A.6, one can see that below an energy of 0.1MeV the buildup factor of steel should be used and above an energy of 0.1MeV the buildup factor of concrete should be used.

Incorporating the buildup factor in the Taylor form into the G function, the dose

becomes[3]:

$$Dose = \frac{1.15 \times 10^{-4} E \mu_a R_2 S_{V_2}}{2\pi} [AG(k, p, \mu_s R_2, b'_2) + (1 - A)G(k, p, \mu_s R_2, b''_2)] \quad (4.20)$$

where

$$b'_2 = (1 + \alpha_1)b_2$$

$b''_2 = (1 + \alpha_2)b_2$ Values of the Taylor coefficients for concrete are listed in Appendix A.8. The respective volumes for target points at 8 meters and 21 meters are

$$V_2(8) = 4.68 \times 10^3 \text{ m}^3$$

$$V_2(21) = 4.49 \times 10^3 \text{ m}^3$$

For convenience, k is set equal to one. This eliminates one set of interpolations in the G function tables and is not too far from the actual containment h/R ratio. Given that $k = 1$, and therefore $R_2 = h_2$, the radii can be solved for using[3]:

$$V_2 = \pi R_2^2 h_2$$

to yield

$$R_2(8) = 11.4 \text{ m}$$

$$R_2(21) = 11.3 \text{ m}$$

Because s is the total distance from the center of V_2 to P and the thickness of the shadow shield is 0.61 m (2 ft) the variable p can be determined to be[3]:

$$p(8) = (11.4 + 0.61 + 8)/(11.4) = 1.75$$

$$p(21) = (11.3 + 0.61 + 21)/11.3 = 2.90$$

Because self-absorption is neglected $\mu_s R_2 = 0$. Values of b'_2 and b''_2 are listed in Appendix A.9 along with the corresponding G function values.

The resulting doses are listed in Table 4.4 and 4.5

4.4 Scattered Gamma Dose

The gamma rays going upwards would be possibly scattered back to the ground by the steel dome or by the air. This scattered radiation is also called skyshine.

Table 4.4: Shadow Shield Penetration Doses (rem) at 8 Meters

E (MeV)	5 MW	6MW	7MW	8MW	9MW	10MW
0.10	6.04E-15	7.24E-15	8.45E-15	9.66E-15	1.09E-14	1.21E-14
0.15	6.86E-09	8.23E-09	9.60E-09	1.10E-08	1.23E-08	1.37E-08
0.20	1.33E-07	1.60E-07	1.87E-07	2.13E-07	2.40E-07	2.67E-07
0.30	2.87E-06	3.45E-06	4.02E-06	4.59E-06	5.17E-06	5.74E-06
0.40	3.48E-05	3.76E-05	4.03E-05	4.31E-05	4.58E-05	4.85E-05
0.50	7.70E-04	9.24E-04	1.08E-03	1.23E-03	1.39E-03	1.54E-03
0.60	3.18E-04	3.81E-04	4.45E-04	5.08E-04	5.72E-04	6.35E-04
0.80	2.02E-03	2.42E-03	2.83E-03	3.23E-03	3.64E-03	4.04E-03
1.00	8.36E-04	1.00E-03	1.17E-03	1.34E-03	1.51E-03	1.67E-03
1.50	6.59E-03	7.91E-03	9.23E-03	1.05E-02	1.19E-02	1.32E-02
2.00	2.59E-02	3.11E-02	3.63E-02	4.14E-02	4.66E-02	5.18E-02
3.00	1.11E-02	1.33E-02	1.55E-02	1.77E-02	2.00E-02	2.22E-02
4.00	5.16E-04	6.19E-04	7.22E-04	8.26E-04	9.29E-04	1.03E-03
Total	4.81E-02	5.77E-02	6.73E-02	7.69E-02	8.65E-02	9.61E-02

Table 4.5: Shadow Shield Penetration Doses (rem) at 21 Meters

E (MeV)	5 MW	6MW	7MW	8MW	9MW	10MW
0.10	3.37E-15	4.04E-15	4.72E-15	5.39E-15	6.06E-15	6.76E-15
0.15	5.00E-09	6.00E-09	7.00E-09	8.00E-09	9.00E-09	1.00E-08
0.20	9.66E-08	1.16E-07	1.35E-07	1.54E-07	1.74E-07	1.93E-07
0.30	2.00E-06	2.40E-06	2.79E-06	3.19E-06	3.59E-06	3.99E-06
0.40	2.39E-05	2.58E-05	2.77E-05	2.96E-05	3.15E-05	3.33E-05
0.50	5.32E-04	6.38E-04	7.45E-04	8.51E-04	9.57E-04	1.06E-03
0.60	1.83E-04	2.19E-04	2.56E-04	2.92E-04	3.29E-04	3.66E-04
0.80	1.34E-03	1.61E-03	1.88E-03	2.15E-03	2.42E-03	2.68E-03
1.00	3.14E-04	3.77E-04	4.39E-04	5.02E-04	5.65E-04	6.28E-04
1.50	3.10E-03	3.72E-03	4.34E-03	4.96E-03	5.58E-03	6.19E-03
2.00	1.25E-02	1.50E-02	1.75E-02	2.00E-02	2.25E-02	2.50E-02
3.00	4.77E-03	5.73E-03	6.68E-03	7.64E-03	8.59E-03	9.54E-03
4.00	2.78E-04	3.34E-04	3.89E-04	4.45E-04	5.01E-04	5.56E-04
Total	2.31E-02	2.77E-02	3.23E-02	3.69E-02	4.15E-02	4.61E-02

Because forward scattering is favored for high energy photons, the effect of sources located at different positions within the containment will be different. Thus the containment volume will be divided into two regions. One is the dome portion (V_u) above the shadow shield, where the photons only need to be scattered through small angles. The other is the portion below the shadow shield (V_l), where the photons need to be scattered through large angles. Volume V_l will be further subdivided into three portions with different heights. For each volume portion, the source is assumed to be a point source with the total activity of that part of volume located at the center of the volume.

The relationships between the volumes are:

$$V_u = 0.3 V,$$

$$V_l = 0.7 V.$$

4.4.1 Air Scattering Gamma Dose

The air scattering two hour dose (in rem) from sources for each energy group in V_u is[3]:

$$Dose = \frac{1.15E - 04 S_u N E \bar{\mu}_a e^{-b_1}}{4x} \int_{\psi_0}^{\pi-\phi_0} d\psi \int_{\phi_0}^{\pi-\psi} d\phi \frac{d\sigma_s}{d\Omega} (\theta = \psi + \phi) \quad (4.21)$$

Similarly, the air scattering two hour dose from a source in V_l is :

$$Dose = \frac{1.15E - 04 S_l N E \bar{\mu}_a e^{-b_1}}{12\pi x} \int_{\psi_0}^{\pi-\phi_0} \omega(\psi) d\psi \int_{\phi_0}^{\pi-\psi} d\phi \frac{d\sigma_s}{d\Omega} (\theta = \psi + \phi) \quad (4.22)$$

where:

N: electron density in air at STP (3.6×10^{20} electron/cm³),

E: incident photon energy, in MeV,

$\bar{\mu}_a$: approximate photon absorption coefficient of air for photon energy E, in cm²/g,

b_1 : steel thickness in number of mean free path,

ϕ_0 : initial value of ϕ , in radians,

ψ_0 : initial value of ψ , in radians,

$\frac{d\sigma_s}{d\Omega}$: Klein-Nishina differential scattering energy cross section, in $\text{cm}^2/\text{steradian}$,

given by:

$$\frac{d\sigma_s}{d\Omega} = \frac{r_e^2}{2} \left(\frac{E'}{E} \right)^3 \left(\frac{E}{E'} + \frac{E'}{E} - \sin^2\theta \right) \quad (4.23)$$

where r_e : classical radius of the electron = 2.818×10^{-13} cm,

E' : scattered photon energy, in MeV. The quantities E and E' have the relationship:

$$\frac{E'}{E} = \frac{1}{1 + \frac{E}{0.511}(1 - \cos\theta)} \quad (4.24)$$

The above equation was evaluated for each energy group using the numerical program package MapleTM. The resulting air scattering doses from the upper source at 8 meters for each power level are listed in Table 4.6, and those at 21 meters are listed in Table 4.7. The resulting air scattering doses from the lower source at 8 meters for each power level are listed in Table 4.8, and those at 21 meters are listed in Table 4.9. The resulting air scattering doses from all sources at 8 meters for each power level are listed in Table 4.10, and those at 21 meters are listed in Table 4.11. We can see that although the upper portion has a smaller volume and therefore a smaller total radiation source strength, they contribute more to the total air scattered dose.

4.4.2 Steel Shell Scattering Dose

The dose due to a single scattering of a photon with the steel wall can be approximated as[3]:

Table 4.6: Air Scattering Doses (rem) From Upper Source at 8 Meters

E (MeV)	5 MW	6MW	7MW	8MW	9MW	10MW
0.03	2.43E-28	2.92E-28	3.40E-28	3.89E-28	4.37E-28	4.86E-28
0.04	5.19E-19	6.23E-19	7.27E-19	8.31E-19	9.35E-19	1.04E-18
0.05	8.39E-10	1.01E-09	1.18E-09	1.34E-09	1.51E-09	1.68E-09
0.06	6.98E-08	8.38E-08	9.77E-08	1.12E-07	1.26E-07	1.40E-07
0.08	3.21E-04	3.85E-04	4.50E-04	5.14E-04	5.78E-04	6.42E-04
0.10	6.43E-07	7.72E-07	9.01E-07	1.03E-06	1.16E-06	1.29E-06
0.15	2.85E-03	3.42E-03	3.99E-03	4.56E-03	5.13E-03	5.71E-03
0.20	4.09E-03	4.91E-03	5.73E-03	6.55E-03	7.36E-03	8.19E-03
0.30	6.59E-03	7.91E-03	9.23E-03	1.05E-02	1.19E-02	1.32E-02
0.40	1.64E-02	1.77E-02	1.89E-02	2.02E-02	2.15E-02	2.28E-02
0.50	1.13E-02	1.36E-02	1.58E-02	1.81E-02	2.03E-02	2.26E-02
0.60	2.45E-02	2.94E-02	3.42E-02	3.91E-02	4.40E-02	4.89E-02
0.80	3.74E-02	4.49E-02	5.23E-02	5.98E-02	6.73E-02	7.47E-02
1.00	4.25E-03	5.10E-03	5.95E-03	6.80E-03	7.66E-03	8.51E-03
1.50	6.02E-03	7.22E-03	8.42E-03	9.63E-03	1.08E-02	1.20E-02
2.00	8.14E-03	9.77E-03	1.14E-02	1.30E-02	1.46E-02	1.63E-02
3.00	7.54E-04	9.04E-04	1.06E-03	1.21E-03	1.36E-03	1.51E-03
4.00	1.61E-05	1.93E-05	2.25E-05	2.57E-05	2.89E-05	3.21E-05
Total	1.23E-01	1.45E-01	1.68E-01	1.90E-01	2.13E-01	2.35E-01

Table 4.7: Air Scattering Doses (rem) From Upper Source at 21 Meters

E (MeV)	5 MW	6MW	7MW	8MW	9MW	10MW
0.03	2.26E-28	2.72E-28	3.17E-28	3.62E-28	4.07E-28	4.53E-28
0.04	4.86E-19	5.84E-19	6.81E-19	7.78E-19	8.75E-19	9.73E-19
0.05	7.92E-10	9.51E-10	1.11E-09	1.27E-09	1.43E-09	1.59E-09
0.06	6.64E-08	7.97E-08	9.30E-08	1.06E-07	1.20E-07	1.33E-07
0.08	3.10E-04	3.72E-04	4.34E-04	4.96E-04	5.58E-04	6.20E-04
0.10	6.28E-07	7.53E-07	8.79E-07	1.00E-06	1.13E-06	1.26E-06
0.15	2.88E-03	3.46E-03	4.03E-03	4.61E-03	5.19E-03	5.77E-03
0.20	4.26E-03	5.11E-03	5.97E-03	6.82E-03	7.67E-03	8.53E-03
0.30	7.27E-03	8.72E-03	1.02E-02	1.16E-02	1.31E-02	1.45E-02
0.40	1.90E-02	2.05E-02	2.19E-02	2.34E-02	2.49E-02	2.64E-02
0.50	1.36E-02	1.63E-02	1.91E-02	2.18E-02	2.45E-02	2.72E-02
0.60	3.08E-02	3.69E-02	4.31E-02	4.92E-02	5.54E-02	6.15E-02
0.80	4.95E-02	5.94E-02	6.93E-02	7.92E-02	8.90E-02	9.89E-02
1.00	6.19E-03	7.43E-03	8.67E-03	9.91E-03	1.11E-02	1.24E-02
1.50	1.01E-02	1.22E-02	1.42E-02	1.62E-02	1.82E-02	2.03E-02
2.00	1.54E-02	1.85E-02	2.15E-02	2.46E-02	2.77E-02	3.08E-02
3.00	1.50E-03	1.80E-03	2.10E-03	2.39E-03	2.69E-03	2.99E-03
4.00	4.25E-05	5.10E-05	5.95E-05	6.80E-05	7.66E-05	8.50E-05
Total	1.61E-01	1.91E-01	2.20E-01	2.50E-01	2.80E-01	3.10E-01

Table 4.8: Air Scattering Doses (rem) From Lower Source at 8 Meters

Source Point	5 MW	6MW	7MW	8MW	9MW	10MW
S ₁	5.14E-02	6.08E-02	7.02E-02	7.96E-02	8.90E-02	9.84E-02
S ₂	2.91E-02	3.44E-02	3.97E-02	4.50E-02	5.04E-02	5.57E-02
S ₃	1.78E-02	2.10E-02	2.43E-02	2.75E-02	3.08E-02	3.40E-02
Total	9.83E-02	1.16E-01	1.34E-01	1.52E-01	1.70E-01	1.88E-01

Table 4.9: Air Scattering Doses (rem) From Lower Source at 21 Meters

Source Point	5 MW	6MW	7MW	8MW	9MW	10MW
S ₁	5.69E-02	6.74E-02	7.78E-02	8.83E-02	9.87E-02	1.09E-01
S ₂	3.09E-02	3.65E-02	4.22E-02	4.78E-02	5.35E-02	5.91E-02
S ₂	1.86E-02	2.20E-02	2.55E-02	2.89E-02	3.23E-02	3.57E-02
Total	1.06E-01	1.62E-01	1.46E-01	1.65E-01	1.85E-01	2.04E-01

Table 4.10: Air Scattering Doses (rem) From All Sources at 8 Meters

E (MeV)	5 MW	6MW	7MW	8MW	9MW	10MW
0.03	4.92E-28	5.91E-28	6.89E-28	7.88E-28	8.86E-28	9.85E-28
0.04	1.05E-18	1.26E-18	1.47E-18	1.68E-18	1.89E-18	2.10E-18
0.05	1.69E-09	2.03E-09	2.36E-09	2.70E-09	3.04E-09	3.39E-09
0.06	1.40E-07	1.68E-07	1.96E-07	2.24E-07	2.52E-07	2.80E-07
0.08	6.40E-04	7.68E-04	8.95E-04	1.02E-03	1.15E-03	1.28E-03
0.10	1.27E-06	1.53E-06	1.78E-06	2.03E-06	2.29E-06	2.55E-06
0.15	5.56E-03	6.68E-03	7.79E-03	8.90E-03	1.00E-02	1.11E-02
0.20	7.87E-03	9.44E-03	1.10E-02	1.26E-02	1.42E-02	1.57E-02
0.30	1.25E-02	1.50E-02	1.75E-02	1.99E-02	2.24E-02	2.49E-02
0.40	3.04E-02	3.28E-02	3.52E-02	3.76E-02	4.00E-02	4.24E-02
0.50	2.06E-02	2.47E-02	2.88E-02	3.30E-02	3.71E-02	4.12E-02
0.60	4.42E-02	5.30E-02	6.18E-02	7.07E-02	7.95E-02	8.84E-02
0.80	6.59E-02	7.91E-02	9.23E-02	1.05E-01	1.19E-01	1.32E-01
1.00	7.52E-03	9.03E-03	1.05E-02	1.20E-02	1.35E-02	1.51E-02
1.50	1.04E-02	1.25E-02	1.46E-02	1.67E-02	1.88E-02	2.09E-02
2.00	1.40E-02	1.68E-02	1.96E-02	2.24E-02	2.52E-02	2.80E-02
3.00	1.22E-03	1.47E-03	1.71E-03	1.96E-03	2.20E-03	2.45E-03
4.00	2.80E-05	3.36E-05	3.92E-05	4.48E-05	5.04E-05	5.60E-05
Total	2.21E-01	2.61E-01	3.02E-01	3.42E-01	3.83E-01	4.23E-01

Table 4.11: Air Scattering Doses (rem) From All Sources at 21 Meters

E (MeV)	5 MW	6MW	7MW	8MW	9MW	10MW
0.03	4.56E-28	5.47E-28	6.38E-28	7.29E-28	8.20E-28	9.11E-28
0.04	9.75E-19	1.17E-18	1.36E-18	1.56E-18	1.75E-18	1.95E-18
0.05	1.58E-09	1.90E-09	2.21E-09	2.53E-09	2.85E-09	3.17E-09
0.06	1.32E-07	1.58E-07	1.85E-07	2.11E-07	2.37E-07	2.64E-07
0.08	6.10E-04	7.32E-04	8.54E-04	9.76E-04	1.10E-03	1.22E-03
0.10	1.22E-06	1.47E-06	1.71E-06	1.96E-06	2.20E-06	2.45E-06
0.15	5.51E-03	6.61E-03	7.71E-03	8.81E-03	9.91E-03	1.10E-02
0.20	7.98E-03	9.57E-03	1.12E-02	1.28E-02	1.44E-02	1.60E-02
0.30	1.32E-02	1.58E-02	1.85E-02	2.11E-02	2.38E-02	2.64E-02
0.40	3.35E-02	3.62E-02	3.88E-02	4.15E-02	4.41E-02	4.67E-02
0.50	2.34E-02	2.81E-02	3.28E-02	3.75E-02	4.22E-02	4.69E-02
0.60	5.20E-02	6.24E-02	7.28E-02	8.32E-02	9.36E-02	1.04E-01
0.80	8.09E-02	9.71E-02	1.13E-01	1.30E-01	1.46E-01	1.62E-01
1.00	9.92E-03	1.19E-02	1.39E-02	1.59E-02	1.79E-02	1.99E-02
1.50	1.54E-02	1.85E-02	2.16E-02	2.47E-02	2.77E-02	3.08E-02
2.00	2.25E-02	2.70E-02	3.15E-02	3.59E-02	4.04E-02	4.49E-02
3.00	2.11E-03	2.53E-03	2.95E-03	3.37E-03	3.79E-03	4.21E-03
4.00	5.87E-05	7.04E-05	8.22E-05	9.39E-05	1.06E-04	1.17E-04
Total	2.67E-01	3.17E-01	3.66E-01	4.15E-01	4.65E-01	5.14E-01

$$Dose = \frac{1.15 \times 10^{-4} S N_{ST} V_{ST} E \bar{\mu}_a e^{-b_1}}{4\pi r_1^2 r_2^2 (\psi_2 - \psi_1)(\phi_2 - \phi_1)} \int_{\psi_1}^{\psi_2} d\psi \int_{\phi_1}^{\phi_2} d\phi \frac{d\sigma_s}{d\Omega}(\theta = \psi + \phi) \quad (4.25)$$

where:

N_{ST} : the electron density in steel in STP, 2.19×10^{24} electron/ cm^3 ,

V_{ST} : the volume of the steel in the dome:

$V_{ST}(8) = 8.19 \times 10^5 \text{ cm}^3$,

$V_{ST}(21) = 2.91 \times 10^6 \text{ cm}^3$,

The dose due to double scattering of a photon with the the steel wall can be approximated as:

$$Dose = \frac{1.15 \times 10^{-4} S N_{ST}^2 V_{ST} V'_{ST} E \bar{\mu}_a e^{-b_1}}{4\pi r_1^2 r_2^2 x_2^2 (\psi_2 - \psi_1)(\phi_2 - \phi_1)} \int_{\psi_1}^{\psi_2} d\psi \int_{\phi_1}^{\phi_2} d\phi \frac{d\sigma_s}{d\Omega}(\theta) \frac{d\sigma_s}{d\Omega}(\theta') \quad (4.26)$$

where V'_{ST} is the volume of steel between the two scattering points, and θ' is the second scattering angle. The effect of the double scattering has been estimated by evaluating equation 4.26 for the three energies ($E = 0.4, 0.8$ and 2.0 MeV) which contribute the most to the total double steel scattering dose. The results indicate that the total steel scattering dose should be increased by a factor of 1.20 at 8 meters and by a factor of 1.02 at 21 meters[3].

The single steel scattering doses (rem) at 8 meters and at 21 meters versus source are listed in Tables 4.12 and 4.13. The total steel scattering doses after including the double steel scattering effect are listed in Table 4.14.

4.5 Radiation Penetration Through the Truck Lock

The truck lock is a rectangular steel tube 8 meters long closed at



Table 4.12: Single Steel Scattering Doses (rem) 8 Meters vs. Source

Source Point	5 MW	6MW	7MW	8MW	9MW	10MW
Upper	1.95E-01	2.32E-01	2.68E-01	3.05E-01	3.42E-01	3.78E-01
Point 1	5.30E-02	6.29E-02	7.27E-02	8.26E-02	9.25E-02	1.02E-01
Point 2	2.98E-02	3.53E-02	4.08E-02	4.64E-02	5.19E-02	5.74E-02
Point 3	1.73E-02	2.05E-02	2.37E-02	2.68E-02	3.00E-02	3.32E-02
Total	2.95E-01	3.50E-01	4.06E-01	4.61E-01	5.16E-01	5.71E-01

Table 4.13: Single Steel Scattering Doses (rem) 21 Meters vs. Source

Source Point	5 MW	6MW	7MW	8MW	9MW	10MW
Upper	3.83E-01	4.55E-01	5.28E-01	6.00E-01	6.73E-01	7.45E-01
Point 1	8.39E-02	9.97E-02	1.15E-01	1.31E-01	1.47E-01	1.62E-01
Point 2	3.49E-02	4.14E-02	4.79E-02	5.43E-02	6.08E-02	6.73E-02
Point 3	2.02E-02	2.39E-02	2.76E-02	3.14E-02	3.51E-02	3.88E-02
Total	5.22E-01	6.20E-01	7.19E-01	8.17E-01	9.16E-01	1.01E+00

Table 4.14: Total Steel Scattering Doses (rem)

Target	5 MW	6MW	7MW	8MW	9MW	10MW
8m	3.54E-01	4.21E-01	4.87E-01	5.53E-01	6.19E-01	6.86E-01
21m	5.32E-01	6.33E-01	7.33E-01	8.34E-01	9.34E-01	1.03E-00

The radiation reaching the lock will be treated as a point source located at the center of the inner surface of the inner door. The source strength for the truck lock penetration is the total source strength in the containment times a geometry factor. The resulting source strength is $S_T = 7.12 \times 10^{-3} S_c$ photon/s, where S_c is the total source strength of the containment.

4.5.1 Concrete Scattered Dose

Unattenuated Dose at the Concrete Wall

The dose on the concrete wall before penetration is determined as:

$$D_0 = \frac{1.15 \times 10^{-4} B S_T E \mu_a}{2\pi x^2} e^{-\Sigma \mu T} \quad (4.27)$$

where

B: point buildup factor for steel,

$\Sigma \mu T$: number of mean free paths through the two doors,

x : distance to the wall, in cm.

The values of the corresponding doses on the concrete wall are listed in Table 4.15.

Concrete Albedo Dose

The concrete albedo dose is that due to the back scattering of photons from the surface of the truck lock side walls. It is found that the northern boundary would receive the maximum dose. This dose can be arrived at[3]:

$$Dose = 8.23 \times 10^{-2} D_0 \frac{C_1 \frac{d\sigma_s}{d\Omega}(\theta, E) \times 10^{26} + C_2}{1 + \cos\theta_0 \sec\theta_r} \quad (4.28)$$

where C_1 , C_2 are energy and material dependent constants,

D_0 : incident dose, in rem, and

θ_r : reflection angle, in radians,

The resulting concrete albedo doses at the northern boundary are listed in Table

Table 4.15: Direct Dose at the Concrete Wall

E (MeV)	5 MW	6MW	7MW	8MW	9MW	10MW
0.10	8.84E-09	1.06E-08	1.24E-08	1.41E-08	1.59E-08	1.77E-08
0.15	3.57E-04	4.28E-04	4.99E-04	5.71E-04	6.42E-04	7.14E-04
0.20	1.08E-03	1.30E-03	1.51E-03	1.73E-03	1.95E-03	2.16E-03
0.30	3.31E-03	3.98E-03	4.64E-03	5.30E-03	5.96E-03	6.63E-03
0.40	1.26E-02	1.36E-02	1.46E-02	1.56E-02	1.66E-02	1.76E-02
0.50	1.07E-02	1.29E-02	1.50E-02	1.72E-02	1.93E-02	2.15E-02
0.60	2.93E-02	3.52E-02	4.11E-02	4.69E-02	5.28E-02	5.87E-02
0.80	6.27E-02	7.52E-02	8.78E-02	1.00E-01	1.13E-01	1.25E-01
1.00	9.65E-03	1.16E-02	1.35E-02	1.54E-02	1.74E-02	1.93E-02
1.50	2.28E-02	2.73E-02	3.19E-02	3.65E-02	4.10E-02	4.56E-02
2.00	4.43E-02	5.31E-02	6.20E-02	7.08E-02	7.97E-02	8.85E-02
3.00	5.89E-03	7.07E-03	8.25E-03	9.43E-03	1.06E-02	1.18E-02
4.00	2.23E-04	2.68E-04	3.12E-04	3.57E-04	4.02E-04	4.46E-04
Total	2.03E-01	2.42E-01	2.81E-01	3.20E-01	3.59E-01	3.98E-01

4.16.

4.5.2 XXXXXXXXXX Scattered Dose

The second way that gamma radiation can reach the exclusion area through the truck lock is by scattering on the XXXXXXXXXX. The same equation used in the previous chapter can be used here:

$$Dose = \frac{1.15 \times 10^{-4} S_T N_{ST} V_{ST} E \bar{\mu}_a e^{-\Sigma \mu T}}{4\pi r_1^2 r_2^2 (\psi_2 - \psi_1)(\phi_2 - \phi_1)} \int_{\psi_1}^{\psi_2} d\psi \int_{\phi_1}^{\phi_2} d\phi \frac{d\sigma_s}{d\Omega}(\theta) \quad (4.29)$$

where $S_T = 7.12 \times 10^{-3} S_c$ photons/s, and $N_{ST} = 2.19 \times 10^{24}$ electrons/cm³. The location along the boundary that receives the maximum dose is defined by the parameters:

$$r_1 = 9.14 \times 10^2 \text{ cm},$$

$$r_2 = 2.82 \times 10^3 \text{ cm},$$

$$\phi_1 = 0.140 \text{ radians}$$

$$\phi_2 = 0.209 \text{ radians}$$

$$\psi_1 = 0.436 \text{ radians}$$

Table 4.16: Concrete Albedo Dose (rem)

E (MeV)	5 MW	6MW	7MW	8MW	9MW	10MW
0.10	2.84E-11	3.41E-11	3.97E-11	4.54E-11	5.11E-11	5.69E-11
0.15	8.95E-07	1.07E-06	1.25E-06	1.43E-06	1.61E-06	1.79E-06
0.20	2.27E-06	2.72E-06	3.18E-06	3.63E-06	4.09E-06	4.54E-06
0.30	5.45E-06	6.55E-06	7.64E-06	8.73E-06	9.82E-06	1.09E-05
0.40	1.71E-05	1.85E-05	1.98E-05	2.12E-05	2.25E-05	2.39E-05
0.50	1.28E-05	1.54E-05	1.79E-05	2.05E-05	2.31E-05	2.56E-05
0.60	3.14E-05	3.77E-05	4.39E-05	5.02E-05	5.65E-05	6.28E-05
0.80	5.57E-05	6.69E-05	7.80E-05	8.92E-05	1.00E-04	1.11E-04
1.00	7.47E-06	8.96E-06	1.05E-05	1.19E-05	1.34E-05	1.49E-05
1.50	1.39E-05	1.67E-05	1.94E-05	2.22E-05	2.50E-05	2.78E-05
2.00	2.26E-05	2.71E-05	3.16E-05	3.61E-05	4.06E-05	4.52E-05
3.00	2.33E-06	2.79E-06	3.26E-06	3.73E-06	4.19E-06	4.66E-06
4.00	7.53E-08	9.04E-08	1.05E-07	1.20E-07	1.36E-07	1.50E-07
Total	1.72E-04	2.04E-04	2.37E-04	2.69E-04	3.01E-04	3.34E-04

$\psi_1 = 0.768$ radians.

The volume of the [REDACTED] door was determined to be [REDACTED]. An attenuation of [REDACTED] was used, and the buildup and attenuation due to the air were neglected. The resulting maximum dose are listed in Table 4.17.

4.5.3 Summary of Radiation Through the Truck Lock

Comparison of the truck lock penetration doses with those from direct and scattered gamma doses show that it is much smaller (on an order of 3) and thus can be neglected.

Table 4.17: XXXXXXXXXX Scattered Dose (rem)

E (MeV)	5 MW	6MW	7MW	8MW	9MW	10MW
0.10	3.73E-11	4.48E-11	5.23E-11	5.98E-11	6.72E-11	7.49E-11
0.15	1.39E-06	1.66E-06	1.94E-06	2.22E-06	2.49E-06	2.77E-06
0.20	3.99E-06	4.79E-06	5.59E-06	6.39E-06	7.18E-06	7.99E-06
0.30	1.24E-05	1.49E-05	1.73E-05	1.98E-05	2.23E-05	2.48E-05
0.40	4.56E-05	4.92E-05	5.28E-05	5.64E-05	6.00E-05	6.36E-05
0.50	3.83E-05	4.60E-05	5.37E-05	6.14E-05	6.90E-05	7.67E-05
0.60	1.07E-04	1.28E-04	1.50E-04	1.71E-04	1.92E-04	2.14E-04
0.80	2.12E-04	2.54E-04	2.96E-04	3.39E-04	3.81E-04	4.23E-04
1.00	3.10E-05	3.72E-05	4.34E-05	4.96E-05	5.57E-05	6.19E-05
1.50	6.08E-05	7.30E-05	8.51E-05	9.73E-05	1.09E-04	1.22E-04
2.00	1.03E-04	1.24E-04	1.44E-04	1.65E-04	1.85E-04	2.06E-04
3.00	1.10E-05	1.33E-05	1.55E-05	1.77E-05	1.99E-05	2.21E-05
4.00	3.25E-07	3.90E-07	4.55E-07	5.20E-07	5.85E-07	6.50E-07
Total	6.27E-04	7.46E-04	8.66E-04	9.86E-04	1.11E-03	1.23E-03

Chapter 5

Summary

For the MIT research reactor, the design basis accident is the maximum credible accident. For a design basis accident, the worst case is that the four plates in the center of the fuel element with the hot channel melt completely. During such an accident the fission products contained in these four plates may be released into the RCS. The fission product activity in the fuel is assumed to be the maximum equilibrium value and was calculated deterministically. Argon-41 build up in the containment after isolation was also determined. Though the concentration in the containment would be five orders of magnitude higher than that in operating conditions, its activity was five to seven orders of magnitude lower than the activities of fission products from the fuel. The contribution of Ar-41 to the exclusion area dose was therefore neglected.

The fraction of the fission products that may be released from the melted fuel to the RCS are estimated as:

- 100% Noble Gases,
- 90% Cs and I,
- 23% Te,
- 1% Sr, Ba, and Ru,
- 0.01% La, Ce and others.

The release fractions from the RCS to the containment were estimated as:

- 30% for all elements

and the release fraction that remained airborne in the two hour period in the containment were estimated as:

- 100% Noble Gases,
- 30% Cs and I,
- 90% others.

All these values were estimated based on current NUREG documents, experimental test results, and the results of the TMI-2 accident. Allowance was also made for reasonable margins. But because of the stochastic nature of the release process and the limitation of understanding all the physical and chemical processes involved, there are some uncertainties associated with these estimates.

After the fission products are released into the containment, part of them may be released from the containment to the outside environment through a building crack or through the stack. These would lead to pollution of the atmosphere and contribute to the whole body and thyroid dose. The stack is more efficient in mixing the pollutant plume with fresh air. Thus, a stack release would result in a smaller dose at each given point, but the distribution would be over a wider range, from 100 meter to 100 kilometer. For the release from a building crack, two sets of calculational methods were tried. Each gave different results. One is called "exact", that calculated by following the exact procedure provided in NRC regulatory guide 1.145. But actually this method is not appropriate for the MITR because the MITR exclusion area distances are much smaller than those used in regulatory guide 1.145. By taking account of the short distances and thus a strong wake effect of the plume, we used a "exact" model and got a smaller dose compared to the "conservative" model.

For those isotopes that were not released from the containment, the resulting direct and scattered gamma doses were determined. The methods used were the same as those used by Mull [3]. The dose from the truck lock was negligible smaller compared to the direct and scattered gamma dose.

Table 5.1: Total Dose at 5 MW

Component of the Dose	Dose at 8m (Rem)	Dose at 21m (Rem)
Whole-body :		
Containment Leakage	1.38E-02	1.38E-02
Steel Dome Penetration	6.60E-03	5.09E-02
Shadow Shield Penetration	4.81E-02	2.31E-02
Air Scattering	2.21E-01	2.67E-01
Steel Scattering	3.54E-01	5.32E-01
Total	0.644	0.887
Thyroid:		
Containment Leakage	1.12E-01	1.12E-01

The whole body dose which includes gamma and beta dose and the thyroid doses from all sources at the front and back fences are listed below. In the whole body dose, the scattering gamma doses contribute the highest portions, one or two orders of magnitude greater than those from other sources. The results are listed in Tables 5.1 through 5.6. The exclusion area doses as a function of reactor power are plotted in Fig. 5-1. The whole-body dose at 21 meters is greater than that at 8 meters. The thyroid doses at both distances are almost equal.

The regulation gives a limitation of 300 rem for thyroid dose and 25 rem for whole-body dose. Our results show that the doses released in a postulated design basis accident of the MIT Research Reactor at a power level of 5 MW up to 10 MW are well below the limitation.

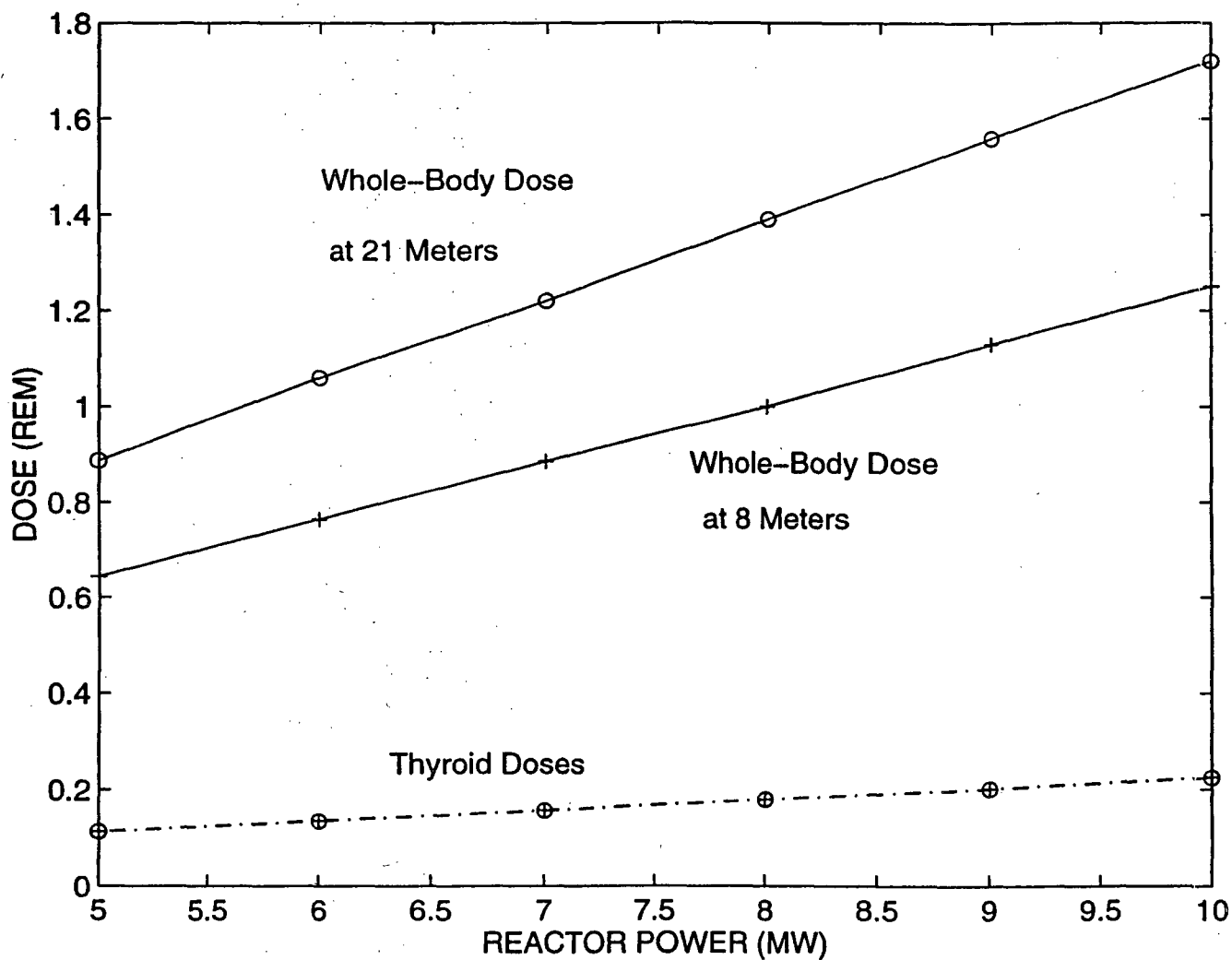


Figure 5-1: Exclusion area doses as a function of reactor power. The solid lines are for whole-body doses, and the solid-dash lines are for thyroid doses. The circle sign is for doses at 21 meters and the plus sign is for doses at 8 meters. Thyroid doses at 8 meters and at 21 meters are not distinguishable in the plot.

Table 5.2: Total Dose at 6 MW

Component of the Dose	Dose at 8m (Rem)	Dose at 21m (Rem)
Whole-body :		
Containment Leakage	1.66E-02	1.66E-02
Steel Dome Penetration	7.87E-03	6.07E-02
Shadow Shield Penetration	5.77E-02	2.77E-02
Air Scattering	2.61E-01	3.17E-01
Steel Scattering	4.21E-01	6.33E-01
Total	0.764	1.06
Thyroid:		
Containment Leakage	1.35E-01	1.34E-01

Table 5.3: Total Dose at 7 MW

Component of the Dose	Dose at 8m (Rem)	Dose at 21m (Rem)
Whole-body :		
Containment Leakage	1.94E-02	1.93E-02
Steel Dome Penetration	9.13E-03	7.05E-02
Shadow Shield Penetration	6.73E-02	3.23E-02
Air Scattering	3.02E-01	3.66E-01
Steel Scattering	4.87E-01	7.33E-01
Total	0.885	1.22
Thyroid:		
Containment Leakage	1.57E-01	1.56E-01

Table 5.4: Total Dose at 8 MW

Component of the Dose	Dose at 8m (Rem)	Dose at 21m (Rem)
Whole-body :		
Containment Leakage	2.22E-02	2.20E-02
Steel Dome Penetration	1.04E-02	8.02E-02
Shadow Shield Penetration	7.69E-02	3.69E-02
Air Scattering	3.42E-01	4.15E-01
Steel Scattering	5.53E-01	8.34E-01
Total	1.00	1.39
Thyroid:		
Containment Leakage	1.79E-01	1.79E-01

Table 5.5: Total Dose at 9 MW

Component of the Dose	Dose at 8m (Rem)	Dose at 21m (Rem)
Whole-body :		
Containment Leakage	2.50E-02	2.48E-02
Steel Dome Penetration	1.17E-02	9.00E-02
Shadow Shield Penetration	8.65E-02	4.15E-02
Air Scattering	3.83E-01	4.65E-01
Steel Scattering	6.19E-01	9.34E-01
Total	1.13	1.56
Thyroid:		
Containment Leakage	2.02E-01	2.01E-01

Table 5.6: Total Dose at 10 MW

Component of the Dose	Dose at 8m (Rem)	Dose at 21m (Rem)
Whole-body :		
Containment Leakage	2.77E-02	2.76E-02
Steel Dome Penetration	1.29E-02	9.98E-02
Shadow Shield Penetration	9.61E-02	4.61E-02
Air Scattering	4.23E-01	5.14E-01
Steel Scattering	6.86E-01	1.03E-00
Total	1.25	1.72
Thyroid:		
Containment Leakage	2.25E-01	2.24E-01

Bibliography

- [1] Safety analysis report for the MIT research reactor (MITR-II). *MITNE-115*, October 1970.
- [2] J. J. McCauley. A review of the MITR-II design basis accident. *MIT B.S. Thesis*, May 1982.
- [3] Robert Forrest Mull. Exclusion area radiation release during the MIT reactor design basis accident. *MIT Master's Thesis*, May 1983.
- [4] Reactor Safety Study. Calculations of reactor accident consequences. *WASH-1400*, October 1975.
- [5] J. O. Blomeke and M.F. Todd. Uranium-235 fission-product production as a function of thermal neutron flux, irradiation time, and decay time. *ORNL-2127*, I, August 1957.
- [6] John E. Deplitch. Reduction of argon-41 produced by the MITR II. *MIT M.S. Thesis*, June 1985.
- [7] Technical bases for estimating fission product behavior during LWR accident. *NUREG-0772*, 1981.
- [8] U.S. Nuclear Regulatory Commission. Severe accident risks: An assessment for five U.S nuclear power plants. *NUREG-1150*, June 1989.
- [9] The Advanced Reactor Severe Accident Program Source Term Group. Passive ALWR source term. February 1991.

- [10] D. W. Akers, E. L. Tolman, P. Kuan, and D. W. Golden. Three Mile Island unit 2 fission product inventory estimates. *Nuclear Technology*, (87), 1989.
- [11] D. W. Akers and R. K. McCardell. Fission product partitioning in core materials. *Nuclear Technology*, (87), 1989.
- [12] D. A. Petti, J. P. Adams, J. L. Anderson, and R. R. Hobbins. Analysis of fission product release behavior from the three mile island unit 2 core. *Nuclear Technology*, (87), August 1989.
- [13] R. R. Hobbins, A. W. Cronenberg, S. Langer, D. E. Owen, and D. W. Aker. Insights on severe accident chemistry from TMI-2. *Proceedings of the American Chemical Society Symposium on Chemical Phenomena Associated with Radioactivity Released During Severe Nuclear Plant Accidents*, June 1987.
- [14] R. R. Hobbins, D. J. Osetek, D. A. Petti, and D. L. Hagrman, editors. *Fission Product Release as a Function of Chemistry and Fuel Morphology*, International Seminar on Fission Product Transport Processes in Reactor Accidents, International Center for Heat and Mass Transfer, Dubrovnik, Yugoslavia, May 1989.
- [15] A. D. Knipe, S. A. Ploger, and D. J. Osetek. PBF severe fuel damage scoping test -test results report. Technical Report EG&G-2413, EG&G Idaho Rept. NUREG/CR-4683, March 1986.
- [16] Z. R. Martinson, D. A. Petti, and B. A. Cook. PBF severe fuel damage scoping test 1-1 test results report. Technical Report EG&G - 2463, EG&G Idaho Rept. NUREG/CR-4684, October 1986.
- [17] Z. R. Martinson, M. Gasparini, R. R. Hobbins, D. A. Petti, C. M. Allison, J. K. Hohorst, D. L. Hagrman, and K. Vinjamuri. PBF severe fuel damage scoping test 1-3 test results report. Technical Report EG&G - 2565, EG&G Idaho Rept. NUREG/CR-5354, January 1990.
- [18] D. A. Petti, Z. R. Martinson, R. R. Hobbins, C. M. Allison, D. L. Carlson, D. L. Hagrman, T. C. Cheng, J. K. Hartwell, K. Vinjamuri, and L. J. Siefken. PBF

severe fuel damage scoping test 1-4 test results report. Technical Report EG&G - 2542, EG&G Idaho Rept. NUREG/CR-5163, February 1989.

- [19] D. J. Osetek. Results of the four PBF sever fuel damage tests. *Transactions of the Fifteenth Water Reactor Safety Information Meeting*, (Rept. NUREG/CP-0090), 1987.
- [20] R. R. Hobbins, D. J. Osetek, D. A. Petti, and D. L. Hagrman. The influence of the chemistry on severe accident phenomena in integral tests. *Proceedings of the Second Symposium on Nuclear Reactor Severe Accident Chemistry*, (Rept. NUREG/CP-0090), June 1988.
- [21] R. R. Hobbins, D. J. Osetek, D. A. Petti, and D. L. Hagrman. The influence of core degradation phenomena on in-vessel fission product behavior during severe accidents. *Proceedings of the International ANS/ENS Conference on Thermal Reactor Safety*, October 2-7 1988.
- [22] R. R. Hobbins, M.L. Russell, C.S. Olsen, and R. K. McCardell. Molten materials behavior in the Three Mile Island unit 2 accident. *Nuclear Technology*, (87), December 1989.
- [23] R. A. Lorenz, E.C. Beahm, and R.P. Wichner. Review of tellurium release rates from LWR fuel elements under accident conditions. *Proceedings of the International Meeting on Light Water Reactor Severe Accident Evaluation*, 1(ANS publication number 700085), 1983.
- [24] R. R. Hobbins, D. J. Osetek, D. A. Petti, and D. L. Hagrman. The influence of the chemistry on severe accident phenomena in integral tests. *Proceedings of the Second Symposium on Nuclear Reactor Severe Accident Chemistry*, (Rept. NUREG/CP-0090), June 1988.
- [25] F. J. Rahn, J. Collen, and A. L. Wright. Aerosol behavior experiments on light water reactor primary systems. *Nuclear Technology*, 81, May 1988.

- [26] D. R. Dickson and et al. Aerosol behavior in LWR containment bypass piping - results of LACE test LA3. *LACE-TR-011*, July 1987.
- [27] The marviken aerosol transport tests. Joint Reactor Safety Experiments in The Marviken Power Station Results from Test 1, MX5-59, February 1984.
- [28] M.L. Carbonneau and et al. Experiment analysis and summary report for OECD LOFT project fission product experiment LP-FP-2. Technical Report OECD LOFT-T-3806, June 1989.
- [29] R. S. Denning and et al. Radionulide release calculations for selected severe accident scenery. Technical Report NUREG/CR-4624, BMI-2139, Battelle Columbus Laboratories, July 1986.
- [30] J. Gosnell. Modification of pressure relief system. Technical report.
- [31] Atmospheric dispersion models for potential accident consequence assessments at nuclear power plants. *U.S. NRC regulatory Guide 1.145*, November 1982.
- [32] F. A. Gifford. An outline of theories of diffusion in the lower layers of the atmosphere. *Meteorology and Atomic Energy*, July 1968.
- [33] John R. Lamarsh. *Introduction to Nuclear Engineering*. Addison-Wesley Publishing Company, 1983.
- [34] Report of committee II on permissible dose for internal radiation (1959). *International Commission on Radiation protection*, October 1960. ICRP Publication 2.
- [35] T. Rockwell. Reactor shielding design manual. *TID-7004*, 1956.
- [36] Thomas Jaeger. *Principles of Radiation Protection Engineering*. McGraw-Hill Book Company, Inc., 1965. Oak Ridge National Laboratory.
- [37] R. G. Jaeger. Shielding fundamentals and methods. *Engineering Compendium on radiation Shielding*, 1968.

Appendix A

Tables

Table A.1: Total Core Fission Product Inventory

Isotope	Half-life	$\lambda_i(\text{sec}^{-1})$	$Y_i (\%)$	Q_s^1 ($\times 10^5$ Ci)						
				5MW	6MW	7MW	8MW	9MW	10MW	
Kr	85m	4.36h	4.41E-5	1.5	0.6490	0.7788	0.9086	1.0384	1.1682	1.3000
	87	78m	1.48E-4	2.7	1.1700	1.4040	1.6380	1.8720	2.1060	2.3400
	88	2.77h	6.95E-5	3.7	1.6000	1.9200	2.2400	2.5600	2.8800	3.2000
Xe	131m	12.0d	6.68E-7	0.03	0.0130	0.0156	0.0182	0.0208	0.0234	0.0260
	133m	2.3d	3.49E-6	0.16	0.0692	0.0830	0.0969	0.1107	0.1246	0.1380
	133	5.27d	1.52E-6	6.5	2.8100	3.3720	3.9340	4.4960	5.0580	5.6200
	135m	15.6m	7.40E-4	1.8	0.7780	0.9336	1.0892	1.2448	1.4004	1.5600
	135	9.13h	2.11E-5	6.2	0.4130	0.4956	0.5782	0.6608	0.7434	0.8260
	138	17m	6.79E-4	5.5	2.3800	2.8560	3.3320	3.8080	4.2840	4.7600
	138	17m	6.79E-4	5.5	2.3800	2.8560	3.3320	3.8080	4.2840	4.7600
I	131	8.05d	9.96E-7	2.9	1.2500	1.5000	1.7500	2.0000	2.2500	2.5100
	132	2.4h	8.02E-5	4.4	1.9000	2.2800	2.6600	3.0400	3.4200	3.8100
	133	20.8h	9.25E-6	6.5	2.8100	3.3720	3.9340	4.4960	5.0580	5.6200
	134	52.5m	2.20E-5	7.6	3.2900	3.9480	4.6060	5.2640	5.9220	6.5700
	135	6.68h	2.89E-5	5.9	2.5500	3.0600	3.5700	4.0800	4.5900	5.1000
Br	83	2.4h	8.02E-5	0.48	0.2080	0.2496	0.2912	0.3328	0.3744	0.4150
	84	30m	3.85E-4	1.1	0.4760	0.5712	0.6664	0.7616	0.8568	0.9510
Cs	134	2.0y	1.10E-8	0.0*	2.8600	3.4320	4.0040	4.5760	5.1480	5.7200
	136	13d	6.17E-7	0.006*	0.4140	0.4968	0.5796	0.6624	0.7452	0.8280
	137	26.6y	8.27E-10	5.9	2.3100	2.7720	3.2340	3.6960	4.1580	4.6200
Rb	86	19.5d	4.11E-7	2.8E-5*	0.6120	0.7344	0.8568	0.9792	1.1016	1.2200
Te	127m	90d	8.82E-8	0.056	0.0242	0.0290	0.0339	0.0387	0.0436	0.0484
	127	9.3h	2.07E-5	0.25	0.1080	0.1296	0.1512	0.1728	0.1944	0.2160
	129m	33d	2.43E-7	0.34	0.1470	0.1764	0.2058	0.2352	0.2646	0.2940
	129	72m	1.60E-4	1.0	0.4320	0.5184	0.6048	0.6912	0.7776	0.8650
	131m	30h	6.42E-5	0.44	0.1900	0.2280	0.2660	0.3040	0.3420	0.3810
	131	24.8m	4.66E-4	2.9	1.2500	1.5000	1.7500	2.0000	2.2500	2.5100
	132	77h	2.50E-6	4.4	1.9000	2.2800	2.6600	3.0400	3.4200	3.8100
	133m	63m	1.83E-4	4.6	1.9900	2.3880	2.7860	3.1840	3.5820	3.9800
	134	44m	2.63E-4	6.7	2.9000	3.4800	4.0600	4.6400	5.2200	5.8000

Table A.1: Total Core Fission Product Inventory

Isotope		Half-life	$\lambda_i(\text{sec}^{-1})$	Y_i (%)	Q_s^i ($\times 10^5$ Ci)					
					5MW	6MW	7MW	8MW	9MW	10MW
Sr	91	97h	1.99e-5	5.9	2.5500	3.0600	3.5700	4.0800	4.5900	5.1000
Ba	140	12.8d	6.27E-7	6.3	2.7200	3.2640	3.8080	4.3520	4.8960	5.4500
Ru	103	41d	1.96E-7	2.9	1.2500	1.5000	1.7500	2.0000	2.2500	2.5100
	105	4.5h	4.28E-5	0.9	0.3890	0.4668	0.5446	0.6224	0.7002	0.7790
	106	1.0y	2.20E-8	0.38	0.1640	0.1968	0.2296	0.2624	0.2952	0.3290
Rh	103	36.5h	5.27E-6	0.9	0.3890	0.4668	0.5446	0.6224	0.7002	0.7790
Tc	99m	6.04h	3.19E-5	0.6	0.2590	0.3108	0.3626	0.4144	0.4662	0.5190
Mo	99	67h	2.88E-6	6.1	2.6400	3.1680	3.6960	4.2240	4.7520	5.2800
Sb	127	93h	2.07E-6	0.25	0.1080	0.1296	0.1512	0.1728	0.1944	0.2160
	129	4.6h	4.32E-5	1.0	4.3200	5.1840	6.0480	6.9120	7.7760	8.6500
Nd	147	11.3d	7.10E-7	2.6	1.1200	1.3440	1.5680	1.7920	2.0160	2.2500
La	140	40.2h	4.79E-6	6.3	2.7200	3.2640	3.8080	4.3520	4.8960	5.4500
Ce	141	32d	2.51E-7	6.0	2.5900	3.1080	3.6260	4.1440	4.6620	5.1900
	143	32h	6.01E-6	6.2	2.6800	3.2160	3.7520	4.2880	4.8240	5.3600
	144	290d	2.76E-8	6.1	2.6400	3.1680	3.6960	4.2240	4.7520	5.2800
Zr	95	63d	1.27E-7	6.4	2.7700	3.3240	3.8780	4.4320	4.9860	5.5400
	97	17h	1.13E-5	6.2	2.6800	3.2160	3.7520	4.2880	4.8240	5.3600
Nb	95	35d	2.29E-7	6.4	2.7700	3.3240	3.8780	4.4320	4.9860	5.5400

71.64

Table A.2: Values of N_s^i/N_{235}^0 for Neutron-Capture Influenced Isotopes at $\phi_T = 4 \times 10^{13}$

Isotope	N_s^i/N_{235}^0
Xe 135	1.05×10^{-5}
Cs 134	1.4×10^{-1}
Cs 136	3.6×10^{-4}
Cs 137	1.5×10^0
Rb 86	8.0×10^{-4}

Table A.3: Parameters for Calculating Atmospheric Doses by Isotope

Isotope		E_{β}^i (Mev/dis)	E_{γ}^i (Mev/dis)	C_{γ}^i (rem/ $\frac{Ci-s}{m^3}$)	C_T^i (rem/Ci inhaled)
Kr	85m	2.7E-01	—	3.64E-02	2.0E-01
	87	1.3E00	—	1.81E-01	9.7E-01
	88	9.3E-01	—	4.67E-01	2.0E00
Xe	131m	—	16.4E-01	—	—
	133m	—	2.33E-01	—	—
	133	1.15E-01	—	9.06E-03	3.9E-01
	135m	—	5.27E-01	—	—
	135	3.1E-01	—	5.67E-02	9.1E-01
	138	8.0E-01	9.4E-01	—	—
	138	8.0E-01	9.4E-01	—	—
I	131	1.9E-01	—	8.72E-02	1.3E05
	132	7.70E-01	—	5.11E-01	6.6E03
	133	4.23E-01	—	1.54E-01	1.2E05
	134	8.10E-01	—	5.33E-01	1.1E03
	135	4.7E-01	—	4.19E-01	4.3E04
Br	83	1.18E-02	5.30E-01	—	—
	84	1.56E00	1.52E00	—	—
Cs	134	2.21E-01	—	3.50E-01	5.8E02
	136	1.14E-01	—	4.78E-01	6.9E02
	137	1.71E-01	—	1.22E-01	3.6E02
Rb	86	5.93E-01	—	2.07E-02	5.0E02
Te	127m	2.43E-01	—	1.10E-03	1.6E-01
	127	2.33E-01	—	9.36E-04	2.9E00
	129m	5.33E-01	—	7.83E-03	4.3E01
	129	4.83E-01	—	1.47E-02	8.1E-01
	131m	3.0E-01	—	3.14E-01	4.5E03
	131	7.13E-01	3.4E-01	—	—
	132	7.3E-02	—	4.75E-02	4.8E04
	133m	8.0E-01	6.5E-01	—	—
	133m	8.0E-01	6.5E-01	—	—

Table A.3: Parameters for Calculating Atmospheric Doses by Isotope

	Isotope	E_{β}^i (Mev/dis)	E_{γ}^i (Mev/dis)	C_{γ}^i (Rem/ $\frac{Ci-s}{m^3}$)	C_T^i (Rem per Ci inhaled)
Sr	91	8.9E-01	—	1.69E-01	1.3E02
Ba	140	3.4E-01	—	4.44E-02	2.2E02
Ru	103	7.0E-02	—	1.11E-01	5.2E01
	105	3.88E-01	—	1.79E-01	1.4E01
	106	1.3E-02	—	4.31E-02	4.8E01
Rh	103	1.89E-01	—	1.82E-02	6.4E00
Tc	99m	—	—	3.06E-02	4.6E01
Mo	99	4.1E-01	—	3.64E-02	9.4E01
Sb	127	5.0E-01	—	1.51E-01	1.0E02
	129	6.23E-01	—	2.68E-01	3.7E01
Nd	147	2.7E-01	—	3.14E-02	1.2E01
La	140	4.53E-01	—	5.67E-01	1.5E02
Ce	141	1.94E-01	—	1.38E-02	6.0E00
	143	4.63E-01	—	6.81E-02	1.8E01
	144	1.03E-01	—	4.31E-03	5.1E00
Zr	95	1.32E-01	—	1.62E-01	7.9E01
	97	6.37E-01	—	4.22E-02	7.7E01
Nb	95	5.33E-01	—	1.66E-01	8.1E01

Table A.4: Gamma Emission Energies by Isotope

Isotope	Photon Energy (Mev) and Distribution (%)
Kr 85m	0.15 (78), 0.3 (14)
87	0.4 (50), 0.8(8), 3.0(14)
88	0.03 (2), 0.15 (7), 0.2(35), 0.4(5), 0.8 (23), 1.5 (14), 2.0 (53)
Xe 131m	0.15 (2)
133m	0.2 (10)
133	0.08 (37)
135m	0.5 (81)
135	0.3 (91), 0.6 (3)
138	0.15 (10), 0.3 (30), 0.4 (12), 0.5 (3), 2.0 (37)
I 131	0.08 (3), 0.3 (5), 0.4 (82), 0.6 (7), 0.8 (2)
132	0.5 (20), 0.6 (99), 0.8 (85), 1.0 (22), 1.5 (8), 2.0 (2)
133	0.5 (86)
134	0.15 (3), 0.4 (8), 0.5 (8), 0.6 (18), 0.8 (160), 1.0 (11), 1.5 (9), 2.0 (5)
135	0.4 (6), 0.8 (8), 1.0 (38), 1.5 (46), 2.0 (10)
Br 83	0.5 (1.4)
84	0.6 (1), 0.8 (48), 1.0 (8), 2.0 (25), 4.0 (7)
Cs 134	0.5 (1), 0.6 (121), 0.8 (95), 1.0 (3), 1.5 (3)
136	0.06 (11), 0.08 (6), 0.15 (36), 0.3 (71), 0.8 (100), 1.0 (82), 1.5 (20)
137	0.6 (85)
Rb 86	1.0 (9)
Te 127m	0.06 (1)
127	0.4 (1)
129m	0.6 (3)
129	0.03 (17), 0.5 (7), 1.0 (1)
131m	0.08 (2), 0.10 (5), 0.2 (16), 0.3 (9), 0.8 (91), 1.0 (24), 1.5 (3), 2.0 (3)
131	0.15 (68), 0.5 (21), 0.6 (4), 1.0 (13)
132	0.05 (14), 0.2 (88)
133m	0.3 (11), 0.4 (1), 0.6 (23), 0.8 (8), 1.0 (89)
134	0.08 (21), 0.2 (48), 0.3 (21), 0.4 (19), 0.5 (35), 0.8 (45)

Table A.4: Gamma Emission Energies by Isotope

Isotope		Photon Energy (Mev) and Distribution (%)
Sr	91	0.6 (15), 0.8 (27), 1.0 (33), 1.5 (5)
Ba	140	0.03 (11), 0.15 (6), 0.3 (6), 0.4 (5), 0.5 (34)
Ru	103	0.5 (88), 0.6 (6)
	105	0.3 (17), 0.4 (6), 0.5 (20), 0.6 (16), 0.8 (48)
	106	—
Rh	103	0.3 (24)
Tc	99m	0.15 (90)
Mo	99	0.04 (2), 0.2 (7), 0.4 (1), 0.8 (16)
Sb	127	0.06 (1), 0.3 (3), 0.4 (9), 0.5 (29), 0.6 (45), 0.8 (17)
	129	0.4 (5), 0.5 (21), 0.6 (12), 0.8 (58), 1.0 (46)
Nd	147	0.10 (28), 0.3 (3), 0.4 (4), 0.5 (13)
La	140	0.3 (20), 0.5 (40), 0.8 (19), 1.0 (10), 1.5 (96), 3.0 (3)
Ce	141	0.15 (48)
	143	0.06 (11), 0.3 (46), 0.5 (3), 0.6 (7), 0.8 (10), 1.0 (1)
	144	0.08 (2), 0.15 (11)
Zr	95	0.8 (98)
	97	0.6 (92)
Nb	95	0.6 (100)

Table A.5: Attenuation and Absorption Coefficients

Gamma Energy E(MeV)	μ_c (cm ⁻¹)	μ_{ST} (cm ⁻¹)	μ_a (cm ² /g)	E'_{min} (MeV)	$\bar{\mu}_a$ (cm ² /g)
0.03	2.63	59.9	0.148	0.027	0.148
0.04	1.31	26.3	0.0668	0.035	0.0668
0.05	0.848	14.0	0.0406	0.042	0.0668
0.06	0.642	8.60	0.0305	0.049	0.0406
0.08	0.470	4.19	0.0243	0.061	0.0305
0.10	0.402	2.61	0.0234	0.072	0.0243
0.15	0.329	1.41	0.0250	0.095	0.0250
0.20	0.294	1.07	0.0268	0.112	0.0268
0.30	0.251	0.821	0.0287	0.138	0.0287
0.40	0.225	0.707	0.0295	0.156	0.0295
0.50	0.205	0.636	0.0297	0.169	0.0297
0.60	0.190	0.584	0.0296	0.179	0.0297
0.80	0.166	0.510	0.0289	0.194	0.0297
1.0	0.150	0.460	0.0280	0.204	0.0297
1.5	0.123	0.373	0.0256	0.218	0.0297
2.0	0.105	0.326	0.0237	0.227	0.0297
3.0	0.0858	0.276	0.0211	0.235	0.0297
4.0	0.0750	0.254	0.0195	0.240	0.0297

Table A.6: Shield Thicknesses in Mean Free Paths

Gamma Energy E(Mev)	Concrete (b)	Steel (b ₁)	Total (b ₂)
0.03	160.4	56.9	217.3
0.04	79.9	25.0	104.9
0.05	51.7	13.3	65.0
0.06	39.2	8.17	47.4
0.08	28.7	3.98	32.7
0.10	24.5	2.48	27.0
0.15	20.1	1.34	21.4
0.20	17.9	1.02	18.9
0.30	15.3	0.780	16.1
0.40	13.7	0.672	14.4
0.50	12.5	0.604	13.1
0.60	11.6	0.555	12.2
0.80	10.1	0.485	10.6
1.0	9.15	0.437	9.57
1.5	7.50	0.354	7.85
2.0	6.41	0.310	6.72
3.0	5.23	0.262	5.49
4.0	4.85	0.241	4.82

Table A.7: Point Isotopic Source Exposure Build-Up Factors for Iron (Steel)

Gamma Energy E (Mev)	b (μ T)		
	1	2	3
0.10	1.5	2.2	3.1
0.15	1.75	2.65	4.2
0.20	2.0	3.1	5.3
0.30	2.05	3.15	5.8
0.40	2.1	3.3	6.0
0.50	1.98	3.09	5.98
0.60	1.96	3.02	5.90
0.80	1.91	2.95	5.62
1.0	1.87	2.89	5.39
1.5	1.82	2.66	4.76
2.0	1.76	2.43	4.13
3.0	1.55	2.15	3.51
4.0	1.45	1.94	3.03

Table A.8: Coefficients of the Taylor Exposure Build-up Factor Formula

Gamma Energy E (Mev)	Concrete			Steel		
	A	α_1	α_2	A	α_1	α_2
0.10	139.5813	-0.04127	-0.02927	-	-	-
0.15	97.7220	-0.08301	-0.06400	-	-	-
0.20	87.8408	-0.10004	-0.07912	-	-	-
0.30	80.5000	-0.10500	-0.08400	-	-	-
0.40	46.6038	-0.10489	-0.07132	-	-	-
0.50	67.3716	-0.09198	-0.07061	31.379	-0.06842	-0.03742
0.60	70.0000	-0.08400	-0.06500	30.095	-0.06694	-0.03486
0.80	65.7882	-0.07061	-0.05247	27.526	-0.06390	-0.02975
1.0	77.7911	-0.05818	-0.04420	24.957	-0.06086	-0.02463
1.5	15.1893	-0.06012	0.00252	21.290	-0.05357	-0.01495
2.0	17.1222	-0.04488	0.00448	17.622	-0.04627	-0.00526
3.0	13.7579	-0.02849	0.02761	13.218	-0.04431	-0.00087
4.0	14.2241	-0.02223	0.02316	9.624	-0.04698	0.00175

Table A.9: Values of the Functions $G(1,p,0,b'_2)$ and $G(1,p,0,b''_2)$

Gamma Energy E (Mev)	b'_2	b''_2	$G(b'_2)$	$G(b''_2)$	$G(b'_2)$	$G(b''_2)$
			p=1.75	p=1.75	p=2.90	p=2.90
0.10	25.9	26.2	5.4×10^{-13}	3.85×10^{-13}	4.5×10^{-13}	3.6×10^{-13}
0.15	19.6	20.0	3.9×10^{-10}	2.62×10^{-10}	3.05×10^{-10}	2.07×10^{-10}
0.20	17.0	17.4	6.0×10^{-9}	3.9×10^{-9}	4.6×10^{-9}	3.0×10^{-9}
0.30	14.4	14.7	9.4×10^{-8}	6.8×10^{-8}	6.9×10^{-8}	5.0×10^{-8}
0.40	12.9	13.4	4.4×10^{-7}	2.6×10^{-7}	3.2×10^{-7}	1.9×10^{-7}
0.50	11.9	12.2	1.25×10^{-6}	9.2×10^{-6}	8.8×10^{-6}	6.4×10^{-6}
0.60	11.2	11.4	2.7×10^{-6}	2.2×10^{-6}	1.8×10^{-6}	1.5×10^{-6}
0.80	9.85	10.0	1.15×10^{-5}	9.84×10^{-6}	7.4×10^{-6}	6.23×10^{-6}
1.0	9.03	9.17	2.8×10^{-5}	2.4×10^{-5}	1.7×10^{-5}	1.55×10^{-5}
1.5	7.38	7.87	1.7×10^{-4}	9.6×10^{-4}	9.2×10^{-5}	5.6×10^{-5}
2.0	6.42	6.75	4.5×10^{-4}	3.2×10^{-4}	2.45×10^{-4}	1.8×10^{-4}
3.0	5.33	5.64	1.55×10^{-3}	1.05×10^{-3}	7.8×10^{-4}	5.6×10^{-4}
4.0	4.74	4.93	2.95×10^{-3}	2.45×10^{-3}	1.45×10^{-3}	1.15×10^{-3}

Table A.10: Air Scattering Input Parameters

Source Point	ψ_0 (Radians)	ϕ_0 (Radians)	φ_0 (Radians)	$x(\times 10^3 \text{cm})$	$h'(\text{m})$	$R'(\text{m})$
8m:						
Upper	0.349	0.314	—	2.27	—	—
Point 1	0.544	0.486	0.395	2.08	1.60	10.8
Point 2	0.668	0.636	0.245	1.98	4.80	11.7
Point 3	0.730	0.794	0.086	1.93	8.00	13.3
21m:						
Upper	0.138	0.070	—	3.43	—	—
Point 1	0.399	0.184	0.250	3.30	1.60	10.8
Point 2	0.572	0.285	0.194	3.24	4.80	11.7
Point 3	0.694	0.384	0.050	3.20	8.00	13.3

Table A.11: Steel Scattering Input Parameters

Source Point	ψ_1 (Radians)	ψ_2 (Radians)	ϕ_1 (Radians)	ϕ_2 (Radians)	$r_1(\times 10^3 \text{cm})$	$r_2(\times 10^3 \text{cm})$
8m:						
Upper	0.349	0.679	0.314	0.390	1.13	1.61
Point 1	0.544	0.950	0.486	0.563	1.19	1.70
Point 2	0.668	1.035	0.636	0.713	1.34	1.71
Point 3	0.730	1.066	0.794	0.872	1.51	1.74
21m:						
Upper	0.138	1.941	0.070	0.132	0.70	3.60
Point 1	0.399	1.821	0.184	0.248	0.97	3.60
Point 2	0.572	1.720	0.285	0.349	1.23	3.60
Point 3	0.694	1.621	0.384	0.448	1.46	3.60

Appendix B

Figures

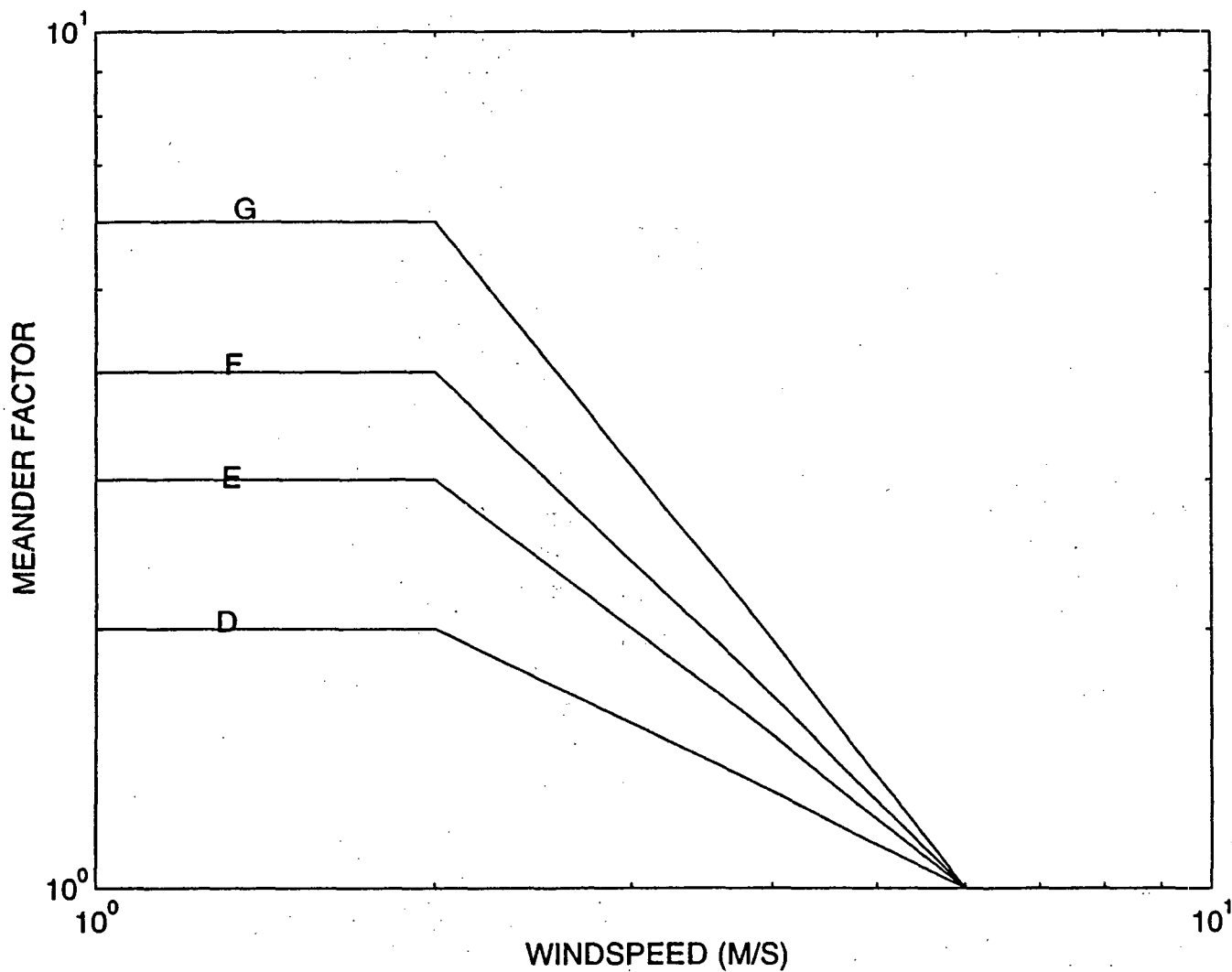


Figure B-1: Meander factors for correction of Pasquill-Gifford sigma y values by atmospheric stability class. D, E, F, and G are the stability classes.

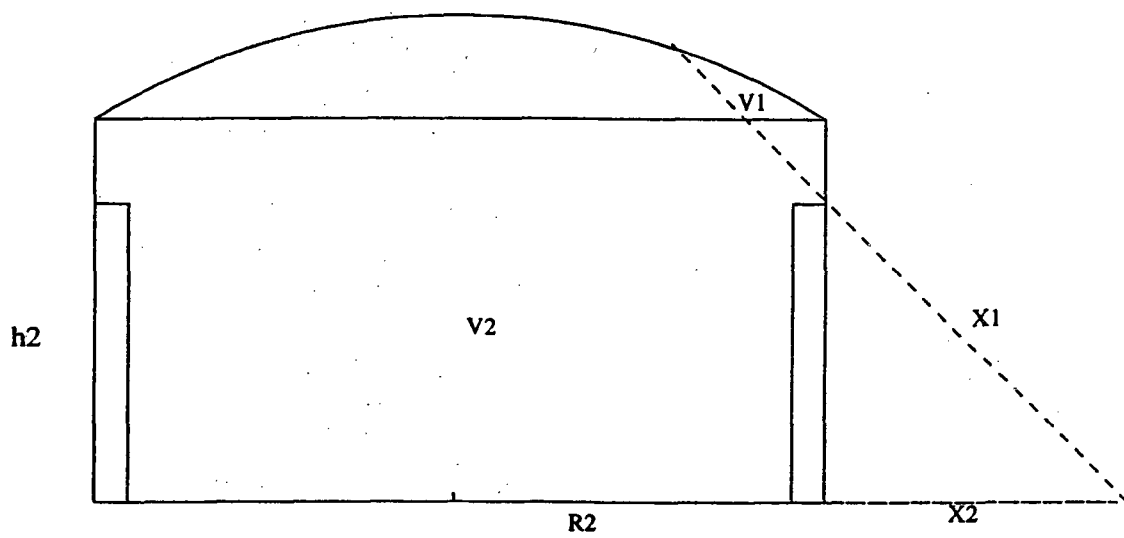


Figure B-2: Direct dose containment volume transformations

0.3% (non-volatile Fe)

Reactor Power (MW)	5	5	6	6	7	7	8	8	9	9	10	10
Site (Meter)	8	21	8	21	8	21	8	21	8	21	8	21
Whole Body (Rem):												
Containment Leakage Beta	4.29E-03	4.27E-03	5.15E-03	5.12E-03	6.01E-03	5.98E-03	6.87E-03	6.83E-03	7.72E-03	7.69E-03	8.58E-03	8.54E-03
Containment Leakage Gamma	5.60E-03	5.57E-03	6.72E-03	6.69E-03	7.84E-03	7.80E-03	8.96E-03	8.92E-03	1.01E-02	1.00E-02	1.12E-02	1.11E-02
Containment Leakage Total	9.89E-03	9.84E-03	1.19E-02	1.18E-02	1.39E-02	1.38E-02	1.58E-02	1.58E-02	1.78E-02	1.77E-02	1.98E-02	1.96E-02
Steel Dome Penetration	2.32E-03	1.79E-02	2.73E-03	2.11E-02	3.15E-03	2.43E-02	3.56E-03	2.75E-02	3.97E-03	3.07E-02	4.39E-03	3.39E-02
Shadow Shield Penetration	3.58E-02	1.73E-02	4.30E-02	2.07E-02	5.01E-02	2.42E-02	5.73E-02	2.77E-02	6.44E-02	3.11E-02	7.16E-02	3.46E-02
Air Scattering	4.20E-02	5.51E-02	4.84E-02	6.38E-02	5.48E-02	7.25E-02	6.12E-02	8.13E-02	6.77E-02	9.00E-02	7.41E-02	9.87E-02
Steel Scattering	1.16E-01	1.81E-01	1.34E-01	2.10E-01	1.54E-01	2.41E-01	1.72E-01	2.70E-01	1.91E-01	3.00E-01	2.09E-01	3.30E-01
Total	2.06E-01	2.81E-01	2.40E-01	3.28E-01	2.76E-01	3.76E-01	3.09E-01	4.23E-01	3.45E-01	4.69E-01	3.79E-01	5.17E-01
Thyroid (Rem):												
Containment Leakage	1.13E-03	1.13E-03	1.36E-03	1.35E-03	1.58E-03	1.58E-03	1.81E-03	1.80E-03	2.04E-03	2.03E-03	2.27E-03	2.25E-03

3% (non-volatile Fe)

Reactor Power (MW)	5	5	6	6	7	7	8	8	9	9	10	10
Site (Meter)	8	21	8	21	8	21	8	21	8	21	8	21
Whole Body (Rem):												
Containment Leakage Beta	4.39E-03	4.37E-03	5.27E-03	5.25E-03	6.15E-03	6.12E-03	7.03E-03	7.00E-03	7.91E-03	7.87E-03	8.79E-03	8.75E-03
Containment Leakage Gamma	5.86E-03	5.83E-03	7.03E-03	6.99E-03	8.20E-03	8.16E-03	9.37E-03	9.32E-03	1.05E-02	1.05E-02	1.17E-02	1.17E-02
Containment Leakage Total	1.03E-02	1.02E-02	1.23E-02	1.22E-02	1.44E-02	1.43E-02	1.64E-02	1.63E-02	1.84E-02	1.84E-02	2.05E-02	2.05E-02
Steel Dome Penetration	2.09E-02	1.79E-02	3.20E-03	2.47E-02	3.69E-03	2.85E-02	4.18E-03	3.23E-02	4.67E-03	3.61E-02	5.17E-03	3.98E-02
Shadow Shield Penetration	3.69E-02	1.79E-02	4.43E-02	2.14E-02	5.17E-02	2.50E-02	5.91E-02	2.86E-02	6.64E-02	3.21E-02	7.38E-02	3.57E-02
Air Scattering	4.91E-02	6.45E-02	5.70E-02	7.51E-02	6.48E-02	8.57E-02	7.27E-02	9.63E-02	8.05E-02	1.07E-01	8.84E-02	1.17E-01
Steel Scattering	1.37E-01	2.11E-01	1.60E-01	2.48E-01	1.82E-01	2.85E-01	2.05E-01	3.20E-01	2.28E-01	3.57E-01	2.51E-01	3.93E-01
Total	2.54E-01	3.22E-01	2.76E-01	3.81E-01	3.17E-01	4.38E-01	3.58E-01	4.94E-01	3.98E-01	5.51E-01	4.39E-01	6.06E-01
Thyroid (Rem):												
Containment Leakage	1.12E-02	1.12E-02	1.35E-02	1.34E-02	1.57E-02	1.56E-02	1.80E-02	1.79E-02	2.02E-02	2.01E-02	2.25E-02	2.24E-02